Front cover: *Historical remarks to the Institute for Chemical Research (ICR)*

The chemical structure shown on the front cover represents the general formula of pyrethrins.

The insecticidal constituent of pyrethrum flower, *Chrysanthemum cinerariaefolium*, is a mixture of cyclic keto-esters, referred to as "pyrethrins". The insecticidal activity of pyrethrins is so specific in respects of its quick knockdown effect, of the nontoxicity against mammals and of producing no resistance in insects.

For these reasons, remarkable advances have been made in the field of pyrethrum chemistry during the past half century, and almost all important structural and synthetic problems relating to naturally occurring pyrethrins have successively been dissolved by many workers before 1960. In consequence, it was determined that the natural pyrethrins consist of a mixture of four compounds, pyrethrin-I, pyrethrin-II, cinerin-I and cinerin-II, represented by following structure.

As can be seen from the structures, these compounds are formed by combination of cyclic keto-alcohol components, cinerolone or pyrethrolone, with the acid components, chrysanthemic acid or pyrethric acid. Among these four components, Yuzo Inouye and his collaborators under the supervision of the late professor Sankichi Takei succeeded in synthesis of pyrethric acid, monomethyl ester of chrysanthemum dicarboxylic acid, free acid itself, and their geometrical isomers. This work enabled the total synthesis of cinerin-II and pyrethrin-II for the first time. In addition, they established the absolute configuration of naturally occurring chrysanthemum diacid and pyrethrolone and cinerolone.

These studies contributed significantly not only to the advance of pyrethrum chemistry, but also to the elucidation between structure and bioactivity, and the development of an effective synthetic derivatives as insecticides.

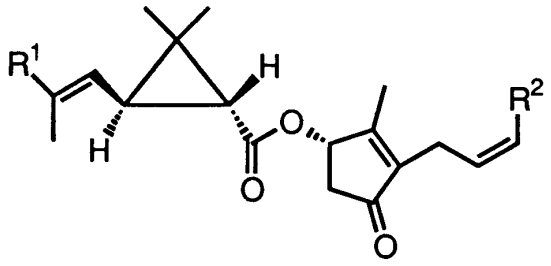

	R^1	R^2
Pyrethrin-I	CH_3	$CH=CH_2$
Pyrethrin-II	$COOCH_3$	$CH=CH_2$
Cinerin-I	CH_3	CH_3
Cinerin-II	$COOCH_3$	CH_3

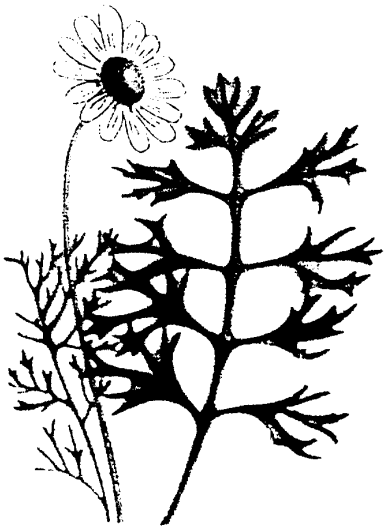

Pyrethrum Flower

CONTENTS

Preface

This is the 1996 edition of the ICR Annual Report and the 3rd volume of the new report series, which includes the summaries of the scientific works by 27 laboratories in 1996, and the list of publications of the research staffs. It is recognized that the activities of the ICR cover very extensive fields.

Currently, besides 27 full professors, 25 associate professors and 47 instructors are working in the ICR. About 200 graduate students are belonging to the ICR. In 1996, there were not many changes in staff. At the end of March, Professor K. Soda of the Molecular Microbial Science Laboratory has retired and Dr. N. Esaki was promoted to the full professor of the Laboratory. The 2 year term of Director for Professor T. Miyamoto has been finished in March. Since April, I am serving as the Director of the ICR, as the successor of Professor Miyamoto. 1996 was a memorial year for the ICR. Just 70 years has passed since the establishment of the Institute and therefore the following events were organized to celebrate the 70th anniversary. An international symposium was held in November 7 to 8 on the subject of "Controlled Organization and Molecular Dynamics of Polymers." This symposium was supported by Monbusho and 7 distinguished foreigner guests were invited. The total number of participants was almost 200, who were coming not only from Kyoto University, but also from many other universities and some industrial laboratories. The symposium was very successful to enhance the international communications and let our activities be known widely. This was the first symposium organized by the ICR. Actually 6 laboratories relating to polymer science were involved in the program committee. It is expected that laboratories in other divisions will organize similar events on some other subjects in forthcoming years.

The ceremony for the 70th anniversary of the ICR was held on November 29 at Miyako Hotel in Kyoto. Congratulatory addresses were presented by the Minister of Monbusho, Mr. T. Kosugi, the President of Kyoto University, Dr. H. Imura, the Chair of the Congress of the Research Institutes' Directors in National Universities, Professor S. Iwasaki, and by the Dean of the Faculty of Technology, Kyoto University, Professor N. Soga, respectively. Before the ceremony, recent results of each laboratories were exhibited as poster presentations, which were appreciated to be very effective to survey the activities of the ICR. After the ceremony, a party was held with more than 400 attendance. Speeches were given by the former president, Dr. K. Nishijima, the Director of Institute for Research in Humanities, Professor T. Sakagami and finally by Professor-emeritus M. Horio.

The history of ICR is 70 years long. However, concerning the potential for research, it is still in a growing period. 1997 should be a year to prepare for further developments. Two Research Projects on Priority Areas sponsored by Monbusho will start in 1997, of which leaders are professors in the ICR, K. Tamao and T. Shinjo. Several interdisciplinary researches have been initiated by the collaborations of ICR staffs and fruitful results are expected in near future. I hope this Annual Report will serve to inform you the progresses of the ICR year by year.

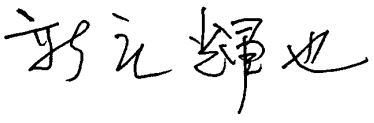

Teruya Shinjo
DIRECTOR

TOPIC AND INTRODUCTORY COLUMNS OF LABORATORIES

Cr-Kβ X-ray Emission Spectra in Several Chromium Compounds

Tatsunori Tochio, A.M.Vlaicu, Takashi Ishizuka, Daisuke Osawa, Yoshiaki Ito and Takeshi Mukoyama

Cr- Kβ x-ray emission spectra in chromium metal and five chromium compounds were measured by using a double crystal spectrometer with high resolution. Differences in the appearance of Kβ' and Kβ'' satellite lines are confirmed in the spectra of the compounds. The origin of Kβ' and Kβ'' satellite lines is discussed due to both the number of unpaired electrons and the symmetry of ligands around the chromium atom.

Keywords: Kβ' and Kβ" satellite lines/ exchange interaction/ number of unpaired electrons/symmetry of ligands/ molecular orbital

The K x-ray emission spectra of 3d transition elements have been with great interests for a long time because of their asymmetric shapes or the existence of satellite lines. These features indicate that some processes or interactions play an important role besides single electron transition between the levels of the diagram lines. Although multielectron excitations or multiplet splitting, etc. may be considered as origins of satellite lines, the origins of many satellite lines remain not clarified. Therefore, in order to elucidate the mechanism of their origins (especially of Kβ' and Kβ'' satellite lines) the K x-ray emission spectra of chromium in Cr metal, Cr_2O_3, $CoCr_2O_4$, $FeCr_2O_4$, K_2CrO_4 and $K_2Cr_2O_7$ were measured using a double crystal spectrometer with high resolution.

The Kβ' satellite line appears on the low energy side of the K$\beta_{1,3}$ lines which are originated from the single electron transition of 3p→1s. As can be seen from Figure1, the relative intensity of the Kβ' satellite line to the K$\beta_{1,3}$ lines for compound with octahedral symmetry is larger than that for compound with tetrahedral symmetry. Tsutsumi suggested that the Kβ' satellite line might be attributed to the exchange interaction between the total spin of 3p electrons s and that of 3d electrons S [1]. The Hamiltonian of this exchange interaction is given by

$$-(J/2)(1+4S\cdot s),$$

where J is the exchange integral. When one electron in the filled 3p shell moves into the vacancy in the 1s shell, this exchange interaction causes the energy splitting of the final states by the energy of DE which is given by

$$\Delta E=J(2S+1),$$

where S is the magnitude of S. The value of ΔE derived from this theory agrees well with the energy difference between the K$\beta_{1,3}$ lines and the Kβ' satellite line in observed

STATES AND STRUCTURES —Atomic and Molecular Physics—

Scope of research

In order to obtain fundamental information on property and the structure of materials, the electronic states of atoms and molecules are investigated in detail using X-ray, synchrotron radiation, ion beam from accelerator and nuclear radiation from radioisotopes. Theoretical analysis of the electronic states and development of new radiation detectors are also performed.

Prof
MUKOYAMA,
Takeshi (D Eng)

Instr
KATANO,
Rintaro (D Eng)

Instr
ITO,
Yoshiaki (D Sc)

Instr
NAKAMATSU,
Hirohide (D Sc)

Guest Res Assoc
Turgut Bastug (D Sc)
Students
YAMAGUCHI,Koichiro (DC)
OSAWA, Daisuke (DC)
SHIGEMI, Akio (DC)
SUZUKI, Chikashi (DC)
TOCHIO, Tatsunori (DC)
MASAOKA, Sei (MC)
ISHIZUKA, Takashi (MC)
NAKANISHI, Yoshikazu (RF)
Vlaicu A. Mihai (RS)

spectra. According to this theory, the relative intensity of Kβ' satellite lines to the K$\beta_{1,3}$ line is given by S/(S+1). The number of unpaired electrons is formally three (S=3/2) in the compounds with octahedral symmetry, zero (S=0) in the compounds with tetrahedral symmetry. Then this theory can account for the larger intensity of the Kb' lines in the compounds with octahedral symmetry. But it cannot explain the Kβ' satellite line quantatively and needs some modifications. Some trials to get better agreement by some modifications such as consideration of the effect of spectator hole or plasmon were performed [2][3]. However, some other modifications are still needed to account for the origin of the Kβ' satellite line sufficiently.

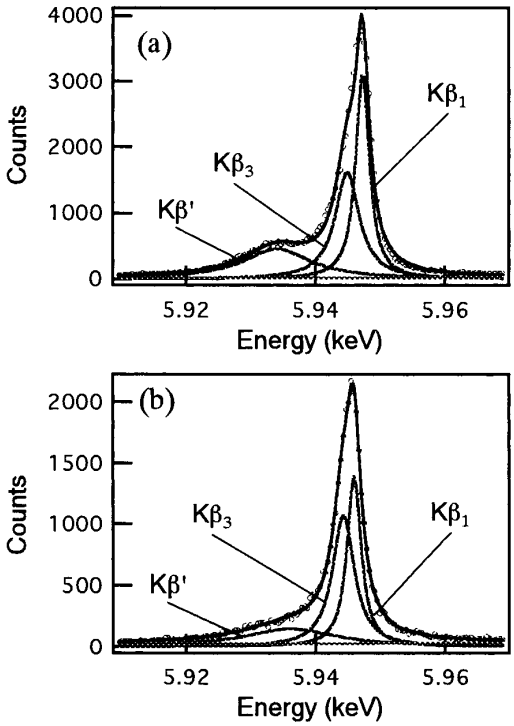

Figure 1. (a): The K$\beta_{1,3}$ and Kβ' spectra of $FeCr_2O_4$ (octahedral symmetry), (b): The K$\beta_{1,3}$ and Kβ' spectra of $K_2Cr_2O_7$ (tetrahedral symmetry)

The Kβ'' satellite lines with the K$\beta_{2,5}$ lines of chromium in $FeCr_2O_4$ (octahedral symmetry) and $K_2Cr_2O_7$ (tetrahedral symmetry) are shown in figure 2. The Kβ'' satellite line appears on the high energy side of the K$\beta_{2,5}$ lines. The Kβ_2 line and the Kβ_5 line are generated by the single electron transition of 4p→1s and 3d→1s respectively. It is easily seen that the relative intensity of Kβ'' satellite line to the K$\beta_{2,5}$ lines in $K_2Cr_2O_7$ (tetrahedral symmetry) is much larger than that in

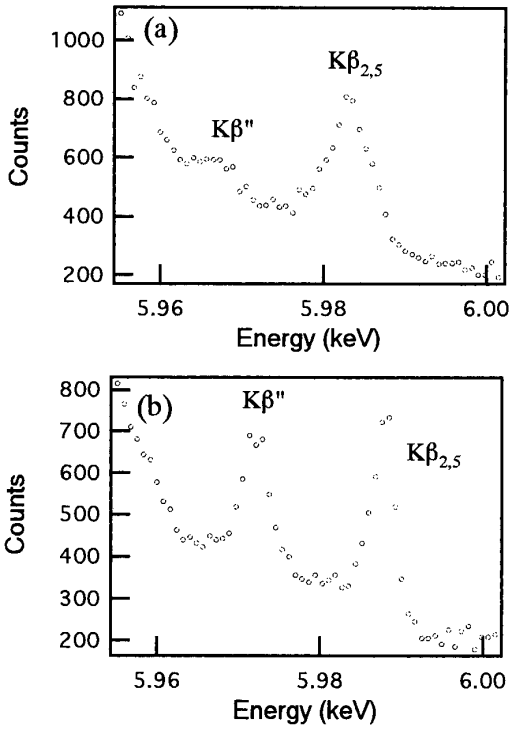

Figure 2. (a): The K$\beta_{2,5}$ and Kβ" spectra of $FeCr_2O_4$ (octahedral symmetry), (b): The K$\beta_{2,5}$ and Kβ" spectra of $K_2Cr_2O_7$ (tetrahedral symmetry)

$FeCr_2O_4$ (octahedral symmetry). This way of appearances of the Kβ'' satellite line is opposite to that of the Kβ' satellite line. It was reported that the origin of the Kβ'' satellite line might be ascribed to the molecular orbital [4]. To investigate these lines more precisely the spectra with high S/N are necessary though it is difficult to get because of the weakness of the K$\beta_{2,5}$ lines and Kβ'' satellite line.

Tuning the energy of the incident beam, by which we can controll the posssibility of occurrence of some special processes, gives us useful imformations about the effect of various processes on x-ray emission spectra. Recently the advent of synchrotron radiation facility made this kind of experiment possible. Such experiments will help us to solve many problems of x-ray emission spectra.

References

1. K. Tsutsumi, J. Phys. Soc. Jpn. **14**,1696 (1959)
2. M. Deutsch, G. Hözer, J. Hätwig, J. Wolf, M. Fritsch and E. Föster, Phys. Rev. A, **51**, 283 (1995)
3. K. S. Srivastava *et al*., Phys. Rev. A, **19**, 4336 (1979); **25**, 2838 (1982)
4. T. Mukoyama, K. Taniguchi, H. Adachi, Phys. Rev. B, **34**, 3710 (1986)

Chemical Mapping by Energy-filtering Transmission Electron Microscopy

Hiroki Kurata, Seiji Isoda and Takashi Kobayashi

We report a chemical map by using electrons with an energy-loss corresponding to a specific peak of near-edge fine structure by an energy-filtering transmission electron microscopy. The possibility of distinguishing elements in different chemical states is a prominent advantage of the chemical mapping compared to the ordinary elemental mapping.

Keywords : Energy-loss / EFTEM / ELNES / Elemental map / EELS

Electron energy-loss spectroscopy (EELS) is a powerful technique to analyze the elemental composition and electronic structure at local area of materials. In particular, the energy-loss near-edge structure (ELNES) appearing in a core-loss spectrum has useful information about the chemical bond around an excited atom. Such features in ELNES can be used for observation of energy-filtering image specific to a particular type of chemical bond, which is called chemical mapping.

There are two approaches to get a chemical map: one is done by combining the EELS with a scanning transmission electron microscopy (STEM). The other one is based on a recently developed energy-filtering transmission microscopy (EFTEM).[1] The first chemical map based on the EFTEM method has been reported by Krivanek who observed unstained polystyrene particles in a polyethylene matrix using the π^*-plasmon peak.[2] In the present work, we report the first map using core-loss intensity by the EFTEM method.

Energy-filtering images were observed by a high-voltage electron microscope (JEOL ARM-1000) equipped with an energy filter of Gatan (GIF) under the column of the microscope.[3] Specimen for observations was fine particles of lead chromium oxide ($PbCrO_4$) covered with a thin amorphous silicate (SiO_2). The size of fine particles were about 200nm and the thickness of amorphous SiO_2 film was about 10nm. Ordinary elemental map was observed using electrons lost energy corresponding to an O K-edge with an energy-selecting slit of 20eV width, which was set at 547±10eV.

For chemical mapping, the oxygen K-edge ELNES peak located at 529eV loss-energy, which is specific to the fine particles, was used. Because this peak was rather sharp, the width of energy-selecting slit was chosen to be 8eV. The magnification was 42,500 times on a slow-scan CCD camera with the pixel size of 24x24mm^2.

In the elemental distribution image, the image of O is

STATES AND STRUCTURES —Crystal Information Analysis—

Scope of research

Structures of materials and their structural transition associated with chemical reactions are studied through the direct observation of atomic or molecular imaging by high resolution microscopy. It aims to explore new methods for imaging with high resolution and for obtaining more detailed chemical information. The following subjects are studied: direct structure analysis of ultrafine crystallites and ultrathin films, crystal growth and adsorption states of organic materials, and development on high resolution electron microscopy as well as electron energy-loss spectroscopy.

Prof
KOBAYASHI,Takashi
(D Sc)

Assoc Prof
ISODA, Seiji
(D Sc)

Instr
OGAWA, Tetsuya
(D Sc)

Assoc Instr
MORIGUCHI, Sakumi

Guest Scholars
MAGONOV, Sergei (D Sc)
MILES, Mervyn (D Sc)

Students
HASHIMOTO, Syugo (DC)
IRIE, Satoshi (DC)
KUWAMOTO, Kiyoshi (DC)
KOSHINO, Masanori (DC)
YAJI, Toyonari (RS)
SUGA, Takeo (MC)
TSUJIMOTO, Masahiko (MC)
YOSHIDA, Kaname (MC)
FURUKAWA,Chieko (MC)

contributed from both regions because oxygen atoms are contained in the $PbCrO_4$ particles and also the SiO_2 films. The aim of chemical mapping is to visually discriminate both materials in the oxygen map by means of the difference of oxygen K-edge ELNES. Fig.1 shows the ELNES spectra of oxygen K-edge taken from each region of the fine particles or the amorphous SiO_2 films. These spectra were measured by the image mode with an entrance aperture of 1mm, so that the diameter of selected area was 40nm. The ELNES features are different from each other, which indicates that the chemical bonding around oxygen atoms is different between $PbCrO_4$ particles and amorphous SiO_2 films.

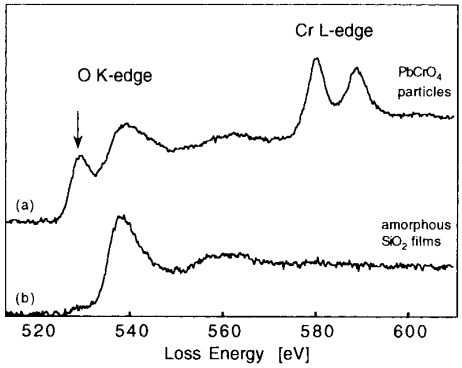

Figure 1 Energy-loss near-edge structure of oxygen K-edge measured from fine particles (a) and amorphous SiO2 films (b).

The most prominent difference is the appearance of the first peak at 529eV (indicated by the arrow) in the spectrum of particles. This peak is characteristic to the chromium oxide ion, $(CrO_4)^{2-}$, in which a six-valence chromium ion (Cr^{6+}) is tetrahedrally surrounded by four oxygen atoms. According to the electronic structure of the $(CrO_4)^{2-}$ cluster, the LUMO is a bound antibonding state which consists of 3d orbital of the chromium ion and some amount of 2p orbital of oxygen atoms. Such mixing of 2p orbital of oxygen allows the transition from 1s core level to the LUMO. Therefore, the first peak at 529eV can be attributed to the transition to the LUMO. The second broad peak centered at 538eV is due to the transition to the unoccupied antibonding states formed by the chromium 4s and 4p orbitals and oxygen 2p orbitals.

In contrast to the above, the first peak at 529eV was not observed in the spectrum of SiO_2 films. The $(SiO_4)^{4-}$ cluster has the same tetrahedral symmetry as the $(CrO4)^{2-}$ cluster. However, the energy gap between the HOMO and the LUMO of $(SiO_4)^{4-}$ cluster is about 10eV which is quite large compared to that of $(CrO_4)^{2-}$ cluster (3.3eV), so that the peak around 538eV in the spectrum of amorphous SiO_2 films is attributed to the transition to the LUMO.

The existence of the peak at 529eV clearly demonstrates the different properties of chemical bond around oxygen atoms in both materials; this peak relates to the existence of the Cr 3d orbital near the Fermi level. Such the difference can be used for the chemical mapping. Fig.2(a) shows the energy-filtering image formed by electrons with an energy-loss of 529±4eV. In this image only the $PbCrO_4$ particles are observed. Fig.2(b) shows the energy-filtering image formed by electrons with an energy-loss of 538±4eV, in which the particles and the amorphous SiO_2 films are both observed because of the equal contributions to this peak from both regions as shown in spectra of Fig.1.

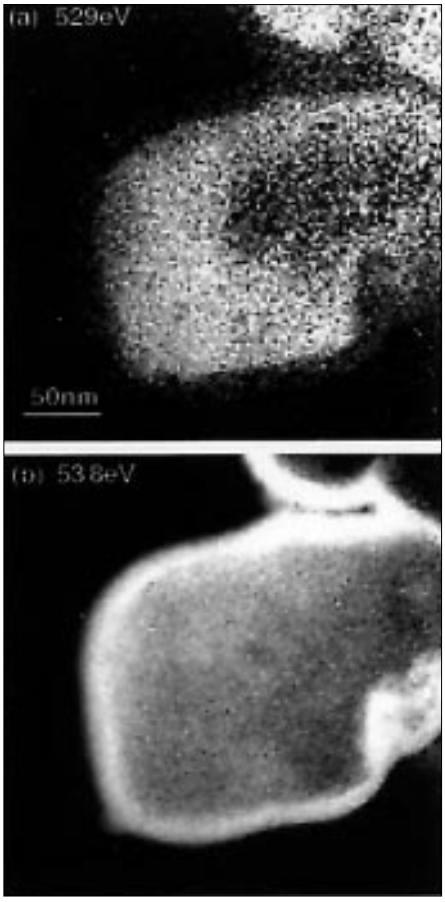

Figure 2 Chemical maps formed by electrons with the energy-loss of (a) 529±4eV and (b) 538±4eV.

The above results establish that the chemical mapping is useful to individualize the different chemical phase.[4] The present result proves that the chemical mapping at a resolution of several nanometer is available in practical way.

References

1. Reimer L.: Energy-filtering transmission electron microscopy. Berlin: Springer-Verlag, (1995).
2. Krivanek O. L.: *Proceedings of 2nd NIRIM International Symposium on Advanced Materials*, Tukuba: Bando Y., Kamo M., Haneda H., Aizawa T. eds: 33-38 (1995)
3. Kurata H., Moriguchi S., Isoda S., Kobayashi T.: *J. Electron Microsc.*, **45**: 78-83 (1996)
4. Kurata H., Isoda S. and Kobayashi T.: *J.Electron Microsc.*, **45**, 317-320 (1996)

Quantification of Stacking Faults in β-Form Single Crystals of Syndiotactic Polystyrene

Masatoshi Tosaka, Masaki Tsuji and Shinzo Kohjiya

The β-form single crystals of syndiotactic polystyrene, each of which inevitably contains the stacking faults, were grown isothermally from dilute solution at a crystallization temperature, *Tc*, ranging from 150 to 210°C. Theoretical treatment based on our structure model of the fault well explained the characteristic features of the electron diffraction patterns. Then the probability of presence of the fault was estimated for each *Tc* by measauring the mean half-breadth of the streaked reflections in the patterns. The probability thus estimated was in good agreement with that obtained from the number of the faults in a unit length: the number was counted directly in the high-resolution and/or the dark-field images taken by transmission electron microscopy.

Keywords: Syndiotactic polystyrene/ Single crystal/ Stacking fault/ Transmission electron microscopy/ TEM/ Electron diffraction/ Dark-field image/ High-resolution image/ Cryo-protection

In four polymorphs of syndiotactic polystyrene [s-PS] reported so far, the β-form (orthorhombic: *a*=2.87nm, *b*=0.88nm, *c*(chain axis)=0.51nm) always contains stacking faults. Existence of the stacking faults is readily deduced from the *hk*0 electron diffraction [ED] pattern of the β-form single crystal. The pattern is characterized by certain reflections (*h*+*k*=odd) streaked in the direction parallel to the a*-axis, while the other reflections (*h*+*k*=even) are spot-like. This feature is well explained by the following model (1). The regular structure of the β-form is composed of two kinds of motifs. Each motif is a bi-molecular layer, *i.e.*, it is composed of two mono-molecular layers extended parallel to the *bc*-plane (Fig.1). Thus the regular structure is defined as the alternating stack of two different motifs. A sequence of successive two motifs of the same type incorporated in the stack is regarded as the stacking fault. In this case, however, no change takes place in the *ac*- nor *bc*-projections. Therefore, *h*00 and 0*k*0 reflections are to remain spot-like. Theoretical formulation of the ED intensity distribution based on this model explains successfully the characteristic features observed in the real ED pattern. Accordingly, as the intensity distribution profile is directly related to the probability of presence of the stacking fault, *p*, then the faults can be quantified by measuring the ED intensity distribution (2). In this work, we propose a method to estimate *p* by analyzing the selected-area ED pattern from the s-PS single crystal. The *p* value thus estimated is compared with that obtained from the number of the faults in a unit length, which number was counted directly in the high-resolution images (1-3) and/or the dark-field [DF] images (2,3) taken by transmission electron microscopy [TEM]. The dependence of *p* on the

STATES AND STRUCTURES —Polymer Condensed States—

Scope of research

Attempts have been made to elucidate the molecular arrangement and the mechanism of structural formation/change in crystalline polymer solids, polymer gels and elastomers, polymer liquid crystals, and polymer composites, mainly by electron microscopy and/or X-ray diffraction/scattering. The major subjects are: synthesis and structural analysis of polymer composite materials, preparation and characterization of polymer gels and elastomeric materials, structural analysis of crystalline polymer solids by direct observation at molecular level resolution and in situ *studies on structural formation/change in crystalline polymer solids.*

Prof KOHJIYA, Shinzo (D Eng)

Assoc Prof TSUJI, Masaki (D Eng)

Instr URAYAMA, Kenji (D Eng)

Instr TOSAKA, Masatoshi

Assoc Instr MURAKAMI, Syozo (D Eng)

Students

HIRATA, Yoshitaka (DC)
SHIMIZU, Toshiki (DC)
TSUJIMOTO, Jun-ichi (MC)
FUJITA, Masahiro (MC)
KAWAMURA, Takanobu (MC)
KAMIJO, Takashi (UG)
KASAI, Yutaka (UG)
TERAKAWA, Katsumi (RF)
LUO, Zhaohui (RS)
NOVILLO, Fernando A. (RS)

crystallization temperature, *Tc*, will be then discussed on the basis of growth theory (4) of folded-chain polymer crystals.

The s-PS sample (Mw=7×10⁴) was supplied by Idemitsu Petrochemical Co., Ltd. A mixture of *n*-tetradecane /decahydronaphthalene (2:1 v/v) was used as the solvent. Single crystals of s-PS were isothermally grown on the newly cleaved NaCl surface from an 0.01wt% solution at a desired *Tc* ranging from 150 to 225°C. Some of the crystals grown at 165°C were annealed in air before removal of NaCl at a given temperature, *Ta*, ranging from 170 to 260°C (melting point: *ca*. 270°C). The specimens were morphologically investigated at room temperature by TEM with a JEOL JEM-200CS operated at 200kV. The intensity distribution in the ED pattern was measured by several methods (2). High-resolution TEM [HRTEM] was carried out with a cryogenic microscope (JEOL JEM-4000SFX operated at 400kV). In this case, specimens were cooled down to 4.2K to minimize their radiation damage. The moiré technique (3) was introduced to detect the position of the stacking fault in the HRTEM images, as a shift of (210) lattice fringes (see Fig.1).

Single crystals with a fairly large monolayered area were obtained below 210°C by isothermal crystallization for two hours. ED patterns were obtained from monolayered areas. In every ED pattern, the mean half-breadth of streaked reflections with $h+k$=odd was calculated, and then was corrected for "instrumental broadening" by using that of spot-like reflections with $h+k$=even as a reference. In this case, the structure factor of each motif is assumed to be constant in the range assigned to one reciprocal lattice point. The probability p was estimated with the following equation from this corrected mean half-breadth H of the streaked reflections:

$$p = [\cos\pi H - 1 + \{ (\cos\pi H - 2)^2 - 1 \}^{1/2}] /2$$

Figure 2 shows the weak dependence of p on *Tc*, and predicts that it is fairly difficult to grow a fault-free single crystal of the β-form. If p is determined only by the growth rates of the regular and the faulted structures, it might be expressed as (5):

$$p = G_F / (G_R + G_F)$$

Here G_R and G_F are the growth rates of the regular and the faulted structures, respectively. By introducing an energy difference ΔE between the regular and the faulted structures, p is expressed as a function of *Tc*. This calculation, however, showed much stronger dependence of p on *Tc* than that obtained experimentally, when ΔE was taken to be constant, namely independent of *Tc*. This discrepancy between the experimental and the theoretical *Tc*-dependence of p seems to come mainly from the *Tc*-dependence of ΔE. Assuming, therefore, that ΔE depends on *Tc*, we calculated $\xi(=\Delta E/\Delta h_f)$ by using the experimentally obtained *Tc*-dependence of p, where Δh_f is the heat of fusion for the regular structure.

The plot of ξ against *Tc* showed excellent linear relationship (5) for both of the growth regimes I and II (4), and this linearity well evidenced the validity of our treatment. It was, consequently, expected that the faulted structure becomes more stable (*i.e*., has lower free energy) than the regular one at temperatures higher than a certain critical temperature (*ca*. 223°C). This result thus means that in crystallization above the critical temperature, the faulted structure will become dominant (p>0.5). In addition, the above-mentioned theoretical formulation for the ED intensity distribution predicts that when p>0.5, the reflections with $h+k$=odd will disappear and each of the spot-like reflections with $h+k$=even is overlapped by a streak. This prediction suggests that a new crystal lattice will be formed when p>0.5 and is to correspond to the β'-form (6).

Isothermal annealing of the β-form single crystals prepared at *Tc*=165°C, which give the maximum value of p as seen in Fig.2, resulted in only a small decrease in the amount of the faults with an increase in *T*a up to 260°C (2). This result illustrates that once the faults are incorporated in the crystal, it might be very difficult to eliminate them only by annealing.

References

1. Tsuji M, Okihara T, Tosaka M, Kawaguchi A and Katayama K, *MSA Bulletin*, **23**, 57 (1993).
2. Hamada N *et al*., in preparation to be submitted to *Macromolecules*.
3. Tosaka M *et al*., submitted to *Macromolecules*.
4. Hoffman J D, Davis G T and Lauritzen,Jr. J I, in "Treatise on Solid State Chemistry", vol. 3, ed. by Hannay NB, Plenum Press, New York, chapt. 7, pp. 497-614 (1979).
5. Tosaka M *et al*., in preparation.
6. De Rosa C, Rapacciuolo M, Guerra G, PetracconeV and Corradini P, *Polymer*, **33**, 1423 (1992).

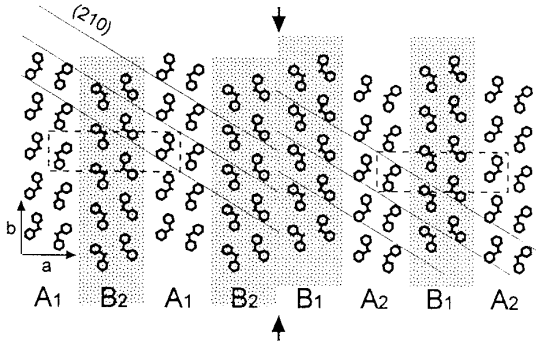

Figure 1. Definition of two types of motifs (1, 3).
A rectangle drawn with broken lines illustrates the unit cell of the regular structure. A pair of arrows indicate the position of the stacking fault. Oblique straight lines illustrate the (210) lattice planes in both sides of the fault.

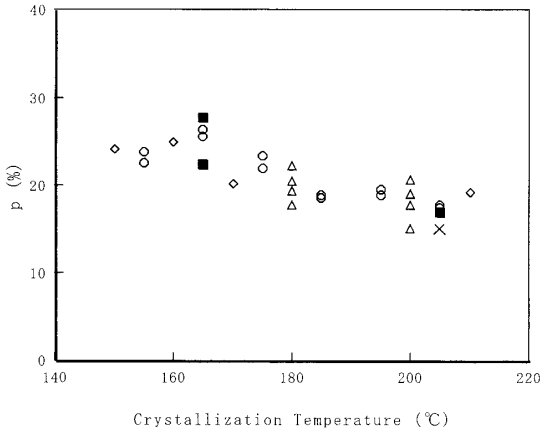

Figure 2. Dependence of p on the crystallization temperature, *T*c (2).
O, Δ and open square : ED, Closed square: DF, × : HRTEM.

NMR Study of Water Structure in Supercritical States

Masaru Nakahara, Nobuyuki Matubayasi, and Chihiro Wakai

The proton chemical shift of water is measured at temperatures up to 400°C and densities of 0.19, 0.41, 0.49, and 0.60 g/cm^3. The magnetic susceptibility correction is made in order to express the chemical shift relative to an isolated water molecule in the gas phase. Comparison of the observed chemical shift to that of a solitary water molecule in an organic solvent shows that the hydrogen bonding persists in the supercritical water. At each density, the strength of the hydrogen bonding is found to reach a plateau value at high temperatures.

Keywords : Supercritical/ Water/ Hydrogen bonding/ NMR/ Proton chemical shift

Water, which is an unusual solvent in ambient conditions, has recently been revealed to be a unique medium for chemical processes in super- and subcritical conditions. In these extreme conditions, water loses its characteristics in ambient conditions and the solvation properties change drastically. In order to understand and control the solvation properties on the molecular level, it is indispensable to characterize the microscopic structure of water in super- and subcritical conditions. Since the hydrogen bonding is the origin of the unique properties of liquid water at ambient conditions, it is desirable to study supercritical water with an experimental method which sensitively probes the hydrogen bonding of water. In this work, we study water in super- and subcritical conditions using high-resolution NMR spectroscopy combined with the capillary method. The proton chemical shift is known to be sensitive to the hydrogen bonding of the observed proton with its environment, and we measure the proton chemical shifts of water up to a supercritical temperature 400°C.

In the capillary method, a capillary is placed in an NMR sample tube, standing up parallel to the external magnetic field. The content of water in the capillary uniquely determines the transition temperature T_t at which the distinction between the liquid and gas phases disappears, and the density of water remains constant when the temperature is raised beyond T_t. At a temperature above T_t, the temperature and density can be controlled as independent variables in the capillary method. At a temperature below T_t, on the other hand, since the water in the capillary is in the two-phase region, only the temperature can be controlled as an independent variable and the densities of the liquid and gas phases are given by the saturation curve. The water contents examined in this work are x = 0.19, 0.41, 0.49, and 0.60, where x is the ratio of the water volume in the capillary to the total volume of the capillary at room temperature.

When the chemical shift is to be determined, a reference

INTERFACE SCIENCE —Solution and Interfaces—

Scope of research

Structure and dynamics of a variety of ionic and nonionic solutions of physical, chemical, and biological interests are systematically studied by NMR under extreme conditions. High pressures and high temperatures are employed to shed light on microscopic controlling factors for the structure and dynamics of solutions. Vibrational spectroscopic studies are carried out to elucidate structure and orientations of organic and water molecules in ultra-thin filns. Crystallization of protein monolayers, advanced dispersion systems at liquid-liquid interfaces, and biomembranes are also investigated.

Prof
NAKAHARA, Masaru
(D Sc)

Assoc Pro
UMEMURA, Junzo
(D Sc)

Instr
MATSUMOTO, Mutsuo
(D Sc)

Instr
KIMURA, Noriyuki
(D Sc)

Instr
MATUBAYASI, Nobuyuki
(Ph D)

Assoc Instr
OKAMURA, Emiko
(D Ph)

Guest Research Associate
SCHROEDER, Petra (D Sc)

Students
WAKAI, Chihiro (DC)
TANO, Takanori (DC)
SAKAI, Hiroshi (DC)
BOSSEV, Dobrin (DC)
YOSHIMOTO, Yoshitaka (MC)
KONISHI, Hirofumi (MC)
TOYA, Hiroshi (MC)
AKIYAMA, Hisashi (MC)

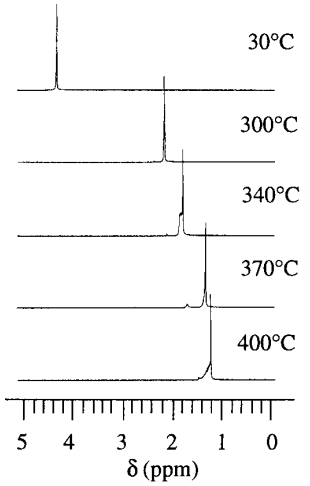

Figure 1. Proton spectra of water from the capillary with the water content $x = 0.41$.

material needs to be chosen. In this work, we do not employ any reference material by directly correcting the effect of the bulk magnetic susceptibility on the magnetic field exerted on a water proton. The magnetic field exerted on a proton differs from the applied magnetic field by a factor determined by the bulk magnetic susceptibility of the fluid. It is thus possible to correct the effect of the bulk magnetic susceptibility from the knowledge of the susceptibility as a function of the temperature and density. The chemical shift of water in the fliud relative to an isolated water molecule in the gas phase can then be obtained from the resonance frequency.

The proton spectra for the water content $x = 0.41$ are shown in Fig. 1 as a function of the temperature T. While the peak shifts upfield as the temperature is raised, the chemical shift δ does not drop to 0 ppm even at 400°C. In Fig. 2(a), we show the chemical shift δ as a function of the temperature T for each capillary with the water content x. Below the critical temperature (374°C), the curve with the lower-field values of δ represents the chemical shift of water in the liquid phase and the curve with the higher-field values represents the chemical shift of water in the gas phase. When the temperature is above T_t , where water is in the one-phase region, the chemical shift is a function of both the temperature T and the density x. The chemical shift δ in the super- and subcritical region is shown in Fig. 2(b). As expected, it is shown in Fig. 2(b) that the chemical shift increases with the density at each temperature above the critical temperature. It is striking in Fig. 2(b), on the other hand, that the chemical shift at a temperature above T_t is constant within the error bars at each density. In other words, δ reaches a plateau value beyond the transition

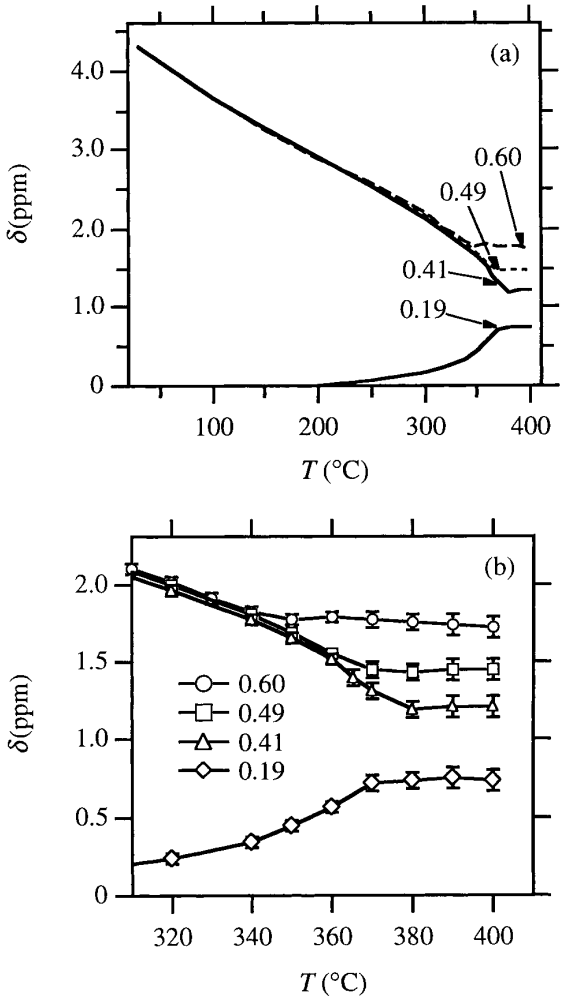

Figure 2. (a) The chemical shifts δ as functions of the temperature T. (b) A magnification of (a) in the super- and subcritical region.

temperature.

Since the chemical shift of a solitary water molecule in weakly hydrogen bonding chloroform solvent was found to be 1.2 ppm relative to an isolated water molecule in the gas phase, Fig. 2 shows that the hydrogen bonding of water persists in the supercritical region at the densities $x = 0.41$, 0.49, and 0.60 g/cm^3. A simple two-state model provides a semi-quantitative estimate of the lower bound of the probability of formation of the hydrogen bonding in a pair of water molecules. The probability at 400°C is larger than 0.7 at a density of 0.60 g/cm^3, it is larger than 0.4 at 0.49 g/cm^3, and it is larger than 0.1 at 0.40 g/cm^3. These estimates agree well with those from computer simulations.

Valence Electronic Structure at the Interface of an Organic Double-Layered Thin Film

Naoki Sato

Valence electronic levels at the interfaces of a photovoltaic double-layered organic thin film prepared from *N,N'*-dimethylperylene-3,4,9,10-bis(dicarboximide) (DM-PBDCI) and chloroaluminum phthalocyanine (ClAlPc) have been examined using ultraviolet photoelectron spectroscopy (UPS). The electronic structure of a DM-PBDCI film at the interface with a substrate demonstrates notable difference between ZnO and Cu. An energetic scheme for the interface of a ClAlPc/DM-PBDCI film is proposed on the basis of the obtained results.

Keywords: Electronic structure/ Interface/ Photovoltaic cell/ Phthalocyanine / Organic double-layered thin film/

To examine if the electronic structure at the interface of a p-n junction prepared from organic semiconductors could be understood on the same basis as that from inorganic semiconductors, direct observations have been tried for the valence electronic structure in an evaporated thin film of an organic semiconductor at the interface with a conducting substrate (Cu, Au, ZnO or indium tin oxide (ITO) glass) or another organic film, using UV photoelectron spectroscopy (UPS) [1]. The system examined was a double-layered organic thin film, which has already been confirmed to show a notable photovoltaic effect [2], fabricated from *N,N'*-dimethylperylene-3,4,9,10-bis(dicarboximide) (DM-PBDCI) and chloroaluminum phthalocyanine (ClAlPc).

The UPS apparatus applied in this work was equipped with an H_2 discharge lamp attached to a VUV monochromator, used in the photon energy region from 6 to 10 eV, and also with a spherical retarding-field analyzer. Such an apparatus was useful to determine absolute energy values including work functions.

The principal experimental procedure was initial UPS measurement of a particular substrate and the cycle of the following evaporation of an organic material by several tenths-to-several nm in thickness on it with in-situ UPS measurement.

First, work functions of Cu, Au, ITO and a ZnO overlayer on ITO were determined as 4.8_2, 4.7_5, 4.1 and 3.7_4 eV, respectively. The features of UP spectra of DM-PBDCI evaporated 10 nm-thick films measured with the same excitation photon energy are almost the same for the films on Cu, Au and ZnO substrates, whereas the film on an ITO plate shows a spectrum different from the spectra of the other films. However, work functions and the threshold ionization energies observed for the films support the n-type nature of DM-PBDCI, when assumed that the energy gap of a DM-PBDCI film coincides with the energy of optical absorption edge, 2.14 eV.

While UP spectra of DM-PBDCI thin films on Cu and ZnO

INTERFACE SCIENCE —Molecular Aggregates—

Scope of research

The research at this subdivision is devoted to correlation studies on structures and properties of both natural and artificial molecular aggregates from two main standpoints: photoelectric and dielectric behaviors. The electronic structure of molecular and/or polymeric thin films is studied using photoelectron spectroscopies in connection with the former, and its results are applied to create novel molecular systems with characteristic electronic functions. The latter is concerned with heterogeneous structures in microcapsules, biopolymers, biological membranes and biological cells, and the nonlinearity in their dielectric properties is also studied in relation to molecular motions.

Prof
SATO, Naoki
(D Sc)

Assoc Prof
ASAMI, Koji
(D Sc)

Instr
KITA, Yasuo
(D Sc)

Instr
YOSHIDA,Hiroyuki
(D Sc)

Students
ENDO, Sotaro (MC)
ODA, Masao (DC)
SAKUMA, Taro (MC)
YANO, Setsuko (MC)

substrates exhibited no significant thickness dependence in the thickness range from 7 to 22 nm, those of the film on a ZnO substrate demonstrated a notable thickness dependence in the range from 1.4 to 160 nm. The principal change in the UP spectra is their apparent rigid shifts with increasing thickness, in particular, in rather thin thickness region, which suggests that the work function of the DM-PBDCI film might change with its thickness. An additional change observed for films no thicker than 10 nm is related with a clear increase of the threshold ionization energy. These observations indicate that electronic energy levels in the DM-PBDCI film at the interface with ZnO suffer from modulation being similar to the band bending at the interface of inorganic semiconductors.

The threshold ionization energy of a ClAlPc film on a Cu substrate is determined to be 5.0_4 eV, while the value of its work function is scattered within 0.4 eV centering around 4.6 eV. Assuming again that the energy gap of the ClAlPc film also coincides with the energy of optical absorption edge, 1.4 eV, the p-type nature of ClAlPc could be supported.

A ClAlPc film overlayed on a DM-PBDCI one (deposited on a Cu substrate) in the thickness of 11 nm showed the following UP spectral change: Although a small contribution from the underlayer DM-PBDCI film was observed in the spectra of ClAlPc films in the thickness less than 3 nm, the spectra of the films in the thickness range from 3 to 7 nm indicated an energy shift of the vacuum level smaller than that of the hole conduction level, and the spectra obtained for thicker (up to ~70 nm) films were almost the same as one another.

By examining the experimental results above, a schematic of energy diagram at the interface of a ClAlPc/DM-PBDCI double-layered thin film is proposed, although energy levels in the DM-PBDCI underlayer are supposed to match with those in the ClAlPc overlayer. The behaviors of the electron and hole conduction levels as well as the vacuum level in the diagram appear to be in reasonable agreement with a conclusion to be obtained from the theory on a p-n heterojunction of inorganic semiconductors. This is identical with the conclusion of our previous UPS study on organic thin film/metal interfaces [3].

This work has been carried out in cooperation with Mr. Masao Yoshikawa at the Research and Development Center of RICOH Co., Ltd.

References

1. Sato N and Yoshikawa M, *J. Elect. Spectrosc. Relat. Phenom.*, **78**, 387 (1996).
2. Yoshikawa M, et al., unpublished results.
3. Yoshida S, Kozawa K, Sato N and Uchida T, *Bull. Chem. Soc. Jpn.*, **67** 2017 (1994).

Dielectric Monitoring of Biological Cell Growth Using an Inductive Probe

Koji Asami, Takeshi Yonezawa, Hideki Wakamatsu, and Naohiko Koyanagi

A new measurement technique with an inductive probe has been developed for monitoring dielectric behavior of biological cells in fermentation, which is superior to conventional methods with regard to being free from the interference due to electrode polarization and bubble formation on electrodes.

Keywords: Dielectric measurement technique/ Biological cell suspension/ Electrode-less method/ Estimation of microbial biomass

Application of dielectric spectroscopy to the estimation of microbial biomass during fermentation was first made by Harris et al. [1]. Excellent linear relationships between the permittivity and the cell concentration (or cell mass) of cell suspensions were obtained for various cells [1,2]. In the dielectric measurements, however, we have some problems as follows: (1) The permittivity change of the fermenting broth is very small within a few hundreds in permittivity unit. Hence, we need a high precision instrument for the measurements. (2) With culture media containing electrolytes, electrode polarization causes serious errors. (3) Bubble formation at electrode surfaces interferes with the measurements. To solve these problems we have lately developed an electrode-less method [3] that is free from the electrode polarization effect and from the interference of the bubble formation on electrode surfaces. The method that is based on electromagnetic induction does not require metal electrodes but a probe that consists of two coaxial toroidal coils covered with epoxy resin (E-5050 Colloid Dielectric Probe, Hewlett-Packard). For measurements the probe is just immersed in a sample liquid, and its relative permittivity and conductivity are automatically obtained with a computer controlled Precision LCR Meter (Hewlett-Packard) over a frequency range of 100 kHz to 30 MHz. The performance of the method has been tested for beer and whisky fermentation [3]. The results demonstrated that the electrode-less method with the inductive probe provides a powerful and versatile technique for in situ and real time monitoring of cell growth in laboratory and industrial fermentation.

References

1. Harris C M, Todd R W, Bungard S J , Lovitt R W, Morris G and Kell D B, *Enzyme Microb. Technol.*, **9**, 181 (1987).
2. Mishima K, Mimura A, Takahara Y, Asami K and Hanai T, *J. Ferment. Bioeng.*, **72**, 291 (1991).
3. Asami K, Yonezawa T, Wakamatsu H and Koyanagi N, *Bioelectrochem. Bioenerget.*, **40**, 141 (1996).

Molecular Design of Chelating Ligands with Highly Selective Recognition and Separation Functions for Group 13 Metal Ions

Shigeo Umetani, Quyen T. H. Le and Masakazu Matsui

Highly selective ligands for group 13 metal ions (Al^{3+}, Ga^{3+} and In^{3+}) have been successfully designed taking into consideration the bite size (O-O distance in the chelate ring) and the interligand contact in the complex. The complexation of Al^{3+} was found to be under the effect of the interligand contact and that of In^{3+} the bite size. The appropriate substituents were introduced to β-diketone type ligands to control the bite size and the volume of the ligand.

Keywords: Solvent extraction / β-Diketone / Acylpyrazolone / Molecular recognition / Substituent effect / Bite size / Interligand contact

Studies on the solvent extraction with modified β-diketones such as α-phenylacetylacetone (PhAA) or α-phenybenzoylacetone (PhBA) revealed that the complexations of group 13 metal ions are strongly affected by the bite size (O-O distance in the chelate ring) and the interligand contact in the complex [1]. Al^{3+} and In^{3+} are readily extracted into the benzene phase with AA and BA in the order, $Al^{3+} > In^{3+}$. On the other hand, In^{3+} was totally unextractable with PhAA and PhBA. Considering that the phenyl group is introduced at the α-position, which is the opposite side of the complexation site, those extraction behaviors are surprising. The X-ray crystallographic studies on the structures of In β-diketonates show that the bite size in the In complex is one of the longest among the metal β-diketonates and the complexation of In^{3+} is disturbed by the substituent at the α-position of β-diketone, which prevents the O-O distance from widening to fit the structure of the complex. In addition, the complexation of Al^{3+} was found to be under the great influence of the interligand contact due to its remarkably small ionic radius. Al^{3+} is usually extracted better than In^{3+} owing to the smaller ionic radius, however, the opposite extraction order is seen for the extractants having bulk terminal substituents such as

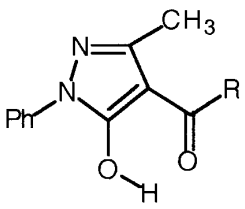

		R
HPMAP	(□)	-CH_3
HPMBP	(○)	-Ph
HPM1NP	(▽)	-1-Naph
HPM2NP	(△)	-2-Naph
HPMPiP	(◇)	-$C(CH_3)_3$

INTERFACE SCIENCE —Separation Chemistry—

Scope of research

Our research activities are concerned in selective complex formation systems (molecular recognition). Major subjects of the research are followings: (1) Design and synthesis of the selective complex formation systems. Ligands (host molecules) that have novel functions in separation of metal ions and guest molecules are designed and synthesized. Their functions are analyzed basing on structures of the ligands and complexes. (2) Biogeochemistry of trace elements in the hydrosphere. Novel analytical methods for trace elements are developed. The behavior of trace elements in the hydrosphere is explored.

Prof
MATSUI, Masakazu
(D Sc)

Assoc Prof
UMETANI, Shigeo
(D Sc)

Inst
Sasaki, Yoshihiro
(D Sc)

Techn
SUZUKI, Mitsuko
(D Sc)

Lect (pt):
KAWASHIMA, Munetsugu (D Sc)

Students:
OBATA, Hajime (DC),
SASAKI, Takayuki (DC),
YOSHIDA Yumi (DC),
LE, T H Quyen (DC),
MITO, Saeko (MC),
AKIYAMA, Shoji (MC),
MORI, Koji (MC),
TOKUTOME, Chikako (MC),
IDO, Hidekazu (RF)

dibenzoylmethane and thenoyltrifluoroacetone. Thus, the extraction of Al^{3+} is expected to be lowered by the bulky terminal substituents. Highly selective ligands for group 13 metals (Al^{3+}, Ga^{3+}, In^{3+}) have been successfully designed taking the two factors into consideration.

Five acylpyrazolone derivatives have been prepared as seen in the scheme. They are 1-phenyl-3-methyl-4-acetyl (HPMAP), -benzoyl (HPMBP), -(1-naphthoyl) (HPM1NP), -(2-naphthoyl) (HPM2NP), and -pivaloyl (HPMPiP) -pyrazolones. The O-O distances were estimated by the MNDO/H calculation, which is MNDO that takes into consideration the hydrogen bonding and has been found to be most suitable among the semi-empirical molecular orbital calculations to evaluate the structures of β-diketone type organic ligands [2]. The O-O distances of the acylpyrazolones except for HPMPiP are 2.60 - 2.65 Å, while that of HPMPiP is 2.46 Å. The ^{1}H-NMR spectra show the evidence for the hydrogen bond strength. The signal assigned to the hydroxyl proton of HPMPiP appeared at δ 14.9; whereas those for the other acylpyrazolones are too broad to observe at δ 10-20. This signal did not move through changing the concentration (0.01 - 0.1 mol dm^{-3}) and was found to disappear after adding D_2O. It was reported that the hydrogen bonded enolic proton signal appears at that low magnetic field.

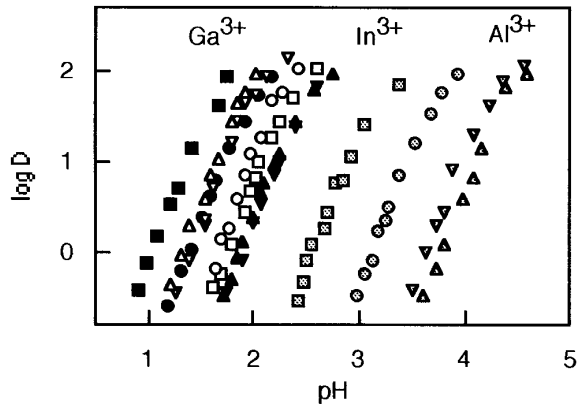

Figure 1 Extraction of Al^{3+} (gray symbols), Ga^{3+} (solid symbols) and In^{3+} (blank symbols) into benzene with acylpyrazolones. $[acylpyrazolone]_o = 5x10^{-3}$ mol dm^{-3} in benzene. $[NaClO_4] = 0.1$ mol dm^{-3}.

The extractions of Al^{3+}, In^{3+} and Ga^{3+} into benzene are shown in Fig.1 plotting the logarithmic value of the distribution ratio of metal ions (D) against pH. Being derived from the five membered heterocyclic 4-pyrazolone, the O-O distances of the present acylpyrazolone derivatives except for HPMPiP are longer than those of the conventional β-diketones. Owing to their long O-O distances, the extraction of In^{3+} was not disturbed and was made at pH 1-2. The extraction of Al^{3+} was seen in the higher pH region, although

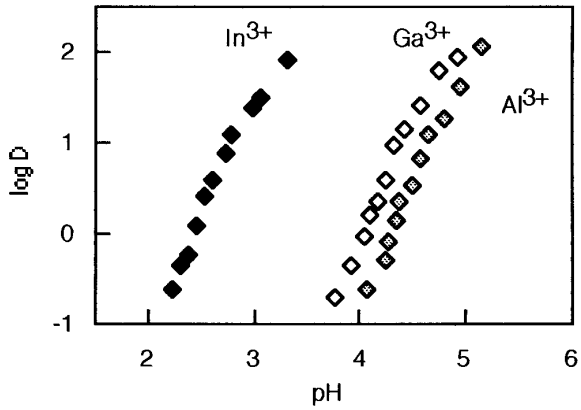

Figure 2 Extraction with HPMPiP. $[HPMPiP]o = 5x10^{-3}$ mol dm^{-3} in benzene. $[NaClO_4] = 0.1$ mol dm^{-3}.

the ionic radius of Al^{3+} is much smaller than that of In^{3+}. Considering that the acylpyrazolones themselves are bulky ligands and their acidities are quite similar, it is clear that the extraction of Al^{3+} is under the effect of the interligand contact. It was found that the extraction reduces as the substituent at the 4-position becomes bulkier. The quantitative separation of Al^{3+} from In^{3+} can be readily achieved with the naphthoylpyrazolones. The extraction of In^{3+} does not depend on the size of the substituents. The effect of the interligand contact is also seen in the extraction of Ga^{3+}. While the ionic radius of Ga^{3+} is smaller than that of In^{3+}, their extractions were similar. In addition, the extractability decreases as the substituents becomes bulkier like the case of Al^{3+}. All of the acylpyrazolones examined are available to quantitatively separate Al^{3+} and Ga^{3+}. Owing to the steric repulsion between the 4-pivaloyl and 3-methyl groups, the O-O distance of HPMPiP is narrowed and the extraction of In^{3+} came close to that of Al^{3+} as seen in Fig. 2, resulting in a quantitative separation of Ga^{3+} from Al^{3+} and In^{3+}.

From our results so far, there are two factors governing the complexation of group 13 metal ions with β-diketones: the distance between the two donating oxygens and the interligand interaction, and their balance should decide the stability of each complex, that is, the extraction order, as well as the separation of Al^{3+} and In^{3+}. This observation may contribute to the basic knowledge on organic ligands, especially on the concepts of their complexation with metal ions, and confirms our suggestion for a perspective strategy for designing novel ligands of high selectivity from well-known typical ones [2].

References

1. Le T H Q, Umetani S, Suzuki M, Matsui M, *J. Chem. Soc., Chem. Commun*., 2271 (1995).
2. Le T H Q, Umetani S, Suzuki M, Matsui M, *J. Chem. Soc., Dalton Trans*., in press.

Magnetic Polarization of Au Layers in M/Au Metallic Multilayers (M=Fe, Co, Ni) Investigated by Mössbauer Probe Atoms

Nobuyoshi Hosoito, Takeshi Emoto, Sunao Hamada and Teruya Shinjo

Magnetic polarization of nonmagnetic Au layers in ferromagnetic/ nonmagnetic metallic multilayers was probed by ^{119}Sn and ^{57}Fe Mössbauer spectroscopy. The Mössbauer probe atoms located in the Au layer with various depths from the interface show depth-dependent large hyperfine field, indicating magnetic polarization in the Au layer. The depth profiles of the magnetic polarization are discussed in Fe/ Au, Co/ Au and Ni/ Au systems.

Keywords: Magnetic polarization/ Metallic multilayer/ Mössbauer spectroscopy

Recently much attention has been paid to the properties of multilayers consisting of alternating magnetic and nonmagnetic materials. Parkin et al.[1] reported long-period oscillations in the exchange coupling of two ferromagnetic layers separated by a nonmagnetic spacer layer as a function of the thickness of the nonmagnetic layer. Oscillatory coupling as a function of spacer layer thickness was found in Fe/Cr, Co/Cr, Co/Ru, Co/Cu, Fe/Cu and numerous other systems.[2-5] To understand the origin of the indirect exchange coupling through the nonmagnetic layer, it is important to investigate the magnetic properties of nonmagnetic spacer layers in the multilayers. Furthermore we stress that investigation of the magnetic properties of the nonmagnetic layers contacting with the ferromagnetic layers is of great importance irrespective of the oscillatory behavior, because the contact of the ferromagnetic layer to the nonmagnetic layer should change the electronic state of the nonmagnetic layer.

In this report, we will present the results of Mössbauer measurements on M/Au (M=Fe, Co and Ni) multilayers with ^{119}Sn and ^{57}Fe probes in the Au layers. The multilayers were prepared by alternate vacuum evaporation under ultra-high vacuum. The Mössbauer probe atoms, ^{119}Sn or ^{57}Fe, are inserted into the Au layer with changing their depth from the M/Au interface. The thicknesses of probe layers are 1.5 Å for Sn and 1 Å for Fe, which correspond to half a monolayer.

SOLID STATE CHEMISTRY —Artificial Lattice Alloys—

Scope of research

By using vacuum deposition method, artificial multilayers have been prepared by combining various metallic elements. The recent major subject is an interplay of magnetism and electric transport phenomena such as the giant magnetoresistance effect. Fundamental magnetic properties of metallic multilayers have been studied by various techniques including Mössbauer spectroscopy using Fe-57, Sn-119, Eu-151 and Au-197 as microprobes, and neutron diffraction. Preparation of microstructured films is attempted and novel magnetic and transport properties are investigated.

Prof
SHINJO, Teruya
(D Sc)

Assoc Prof
HOSOITO,Nobuyoshi
(D Sc)

Instr
MIBU, Ko
(D Sc)

Techni
KUSUDA,Toshiyuki

Students
EMOTO, Takeshi (DC)
NAGAHAMA, Taro (DC)
HAMADA, Sunao (DC)
ITO, Takahiro (MC)
SHIGETO, Kunji (MC)
NISHIDA, Keisuke (MC)

Research Fellow
ONO, Teruo

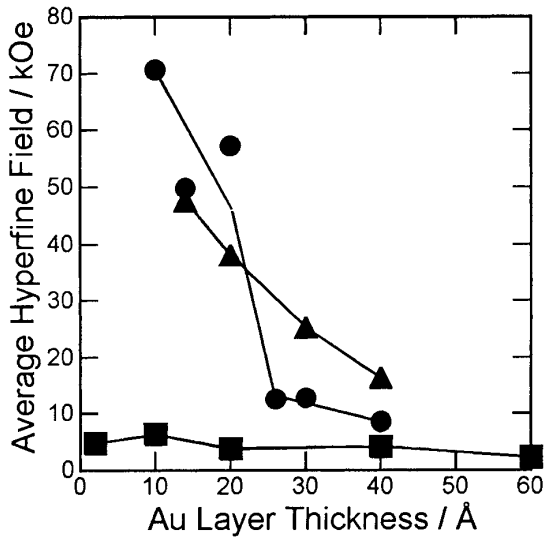

Figure 1. Au layer thickness dependence of Sn average hyperfine field in Fe/Au (triangle), Co/Au (circle) and Ni/Au (square) multilayers. The Sn probes are inserted in the center of the Au layer.

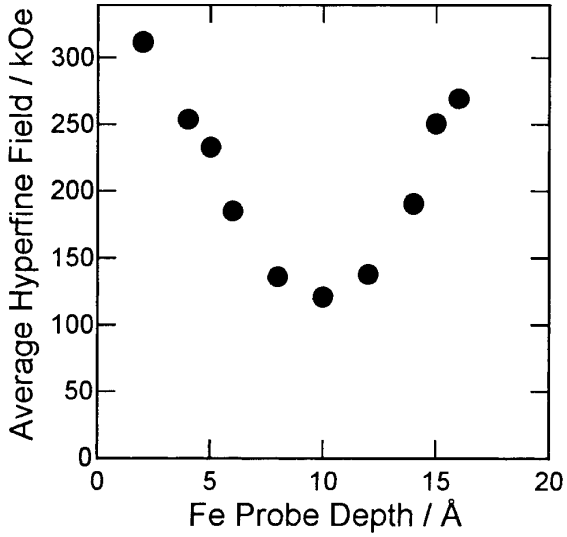

Figure 2. Fe probe depth dependence of average hyperfine field in the Co/Au multilayer.

Transmission Mössbauer spectra were measured with a conventional Mössbauer spectrometer with a velocity transducer, a multichannel analyzer and a proportional counter. Measuring temperature is varied between 4.2 K and room temperature. In this report, we will discuss the results at room temperature

Due to the depth-selective insertion of the Mössbauer probes, the Mössbauer spectra offer us very local information about the electronic state of the Au layer. However the Sn and Fe probes indicate somewhat different information on the magnetic polarization of the Au layer because the Sn atoms have no magnetic moment and the Fe atoms have magnetic moment. The Sn nuclei directly sense the magnetic polarization of the Au layer as a hyperfine field. On the other hand in the case of Fe probes, the magnetic polarization acts as an effective field on the Fe magnetic moments to slow down their thermal fluctuation rate. As a result, the Fe nuclei feel a hyperfine field if the magnetic polarization is strong enough. Therefore in both cases, the hyperfine field is thought to be a measure of the strength of the magnetic polarization in the Au layer though the detailed mechanism is different in both cases.

Among the comprehensive studies, a typical result for Sn obtained at room temperature is shown in Fig.1. A series of samples with the structures of …/M(20 Å)/ Au(*X*/2 Å)/ Sn(1.5 Å)/ Au(*X*/2 Å)/M(20 Å)/…, where M=Fe, Co and Ni, is prepared with varying the Au layer thickness *X*. The average hyperfine field at the central point of the Au layer (depth=*X*/2) is obtained from the fitting of the Sn Mössbauer spectrum. In the case of M=Fe (triangle in Fig.1), the average hyperfine field smoothly decreases with increase the depth of the Sn probe *X*/2. In contrast, the average hyperfine field for M=Co (circle) changes suddenly at around *X*/2=10. The average hyperfine field with *X*/2≤10 is very large, but the average hyperfine field with *X*/2>10 becomes small. In the case of M=Ni (square), the average hyperfine field is about 5 kOe. This value is, of course, very small. However, it is quite sure that the Sn probe atoms feel non-zero hyperfine field if we compare the peak widths of the Mössbauer spectra for the Ni/Au(Sn) multilayers with an Au(Sn) reference film. At present stage, these features including the temperature dependence cannot be explained with any simple model. Band calculations with a realistic approximation are desired.

Figure 2 shows an example using Fe probes. The sample structure is …/Co(20 Å)/ Au(20-*t* Å)/ Fe(1 Å)/ Au(*t* Å)/Co(20 Å)/… i.e. the Fe probe atoms are inserted into various depth *t* from the Co-Au interface of the Co(20 Å)/ Au(20Å) multilayer. The obtained average hyperfine field at room temperature is plotted against the Fe probe depth *t*. The result shown in Fig.2 is qualitatively consistent with that obtained with the Sn probes. The advantage in using Fe as a probe is higher resolution in the Mössbauer peak width than that of the Sn probe case. Indeed, layer-by-layer resolution is obtained in the profiles of the Mösbauer spectra.[6] The average hyperfine filed is indirectly related to the magnetic polarization through a thermal fluctuation phenomenon of the Fe magnetic moment. To obtain a quantitative estimation of the magnetic polarization of the Au layer from the obtained average hyperfine field, Mössbauer measurements in the applied filed are necessary and are under way.

References

1. S.S.P.Parkin, N.More and K.P.Roche: Phys. Rev. Lett. **64**(1990) 2304.
2. W.R.Bennett, W.Schwarzacher and W.F.Egelhoff, Jr.: Phys. Rev. Lett. **65**(1990) 3169.
3. D.H.Mosca, F.Petroff, A.Fert, P.A.Schroeder, W.P.Pratt Jr. and R.Laloee: J. Magn. Magn. Mater. **94**(1991) L1 .
4. S.S.P.Parkin, R.Bhadra and K.P.Roche: Phys. Rev. Lett. **66**(1991) 2152 .
5. S.S.P.Parkin: Phys. Rev. Lett. **67**(1991) 3598 .
6. S.Hanada, N.Hosoito and T.Shinjo: J. Phys. Soc. Jpn. **66** (1997) 30.

Electric Field Effects in Ultrathin $YBa_2Cu_3O_{7-\delta}$ Films

Yoshichika Bando and Takahito Terashima

Charging effects on transport properties of ultrathin $YBa_2Cu_3O_{7-\delta}$ (YBCO) films are measured using FET-like junctions of YBCO in thickness ranging from 1 to 10 unit cell thicknesses (UCT). An electric(E-) field experiment without magnetic field finds that the changes of Kosterlitz-Thouless transition temperature is observed as a function of applied E-field. The changes of superconducting properties are linearly correlated to those of the normal resistance, namely, the induced areal carrier densities.

Keywords: High-T_C superconductivity/ $YBa_2Cu_3O_{7-\delta}$/ Ultrathin film/ Electric field effect

Electric (E-) field effects in superconductors have attracted much attentions from the interest in fundamental physics as well as the device applications. By using an E-field effect junction, we could examine an effect of the carrier density on superconductivity without any reconstruction of sample structure. The change of superconducting transition temperature T_C by E-field have observed for the first time for the thin films of conventional superconductors of Sn and In. Recent works on the E-field effects are mainly devoted to high temperature superconductors (HTSC) since the effects on superconductivity are expected to be large because of the low carrier density n and the short coherence length of HTSC. Here we will report the E-field effects in ultrathin $YBa_2Cu_3O_{7-\delta}$ (YBCO) films [1,2].

Figure 1 depicts the top view of a 3-terminal junction used in the E-field effect experiment. *C*-axis-oriented YBCO films with thicknesses from 1 to 10 unit-cell-thickness (UCT) were prepared onto a (100) surface of $SrTiO_3$(STO) by using an activated-reactive evaporation technique. A buffer layer of several UCT nonsuperconducting $PrBa_2Cu_3O_{7-\delta}$(PBCO) was first prepared onto a STO (100) substrate heated up to 680 ˚C, and then a YBCO film was grown onto the buffer layer of PBCO. After deposition of a 3 nm capping layer of STO on YBCO film, the film was cooled down to room temperature in an oxygen atmosphere of 0.01 MPa. After exposure to air, a masking plate was set up to open a window wider than the sample area of YBCO for STO deposition. A thick dielectric STO film (120 nm) was deposited onto the capping STO layer at 690˚C. Finally a gate electrode of thin Pt film (40nm) was prepared in a separate evaporator with a lead wire attached. The distribution of applied E-field in the YBCO film was uniform over the sample. An areal charge density ΔN induced in the junction area S (0.51cm^2) of the YBCO film was evaluated by $\Delta N = CVg/eS$ from an applied gate voltage V_g and a capacitance C that was almost independent of temperature T within an error of 20% in the temperature range of this experiment between 4K and 100K, where S is the surface area of the capacitor and e is the unit charge. The

SOLID STATE CHEMISTRY —Artificial Lattice Compounds—

Scope of research

Syntheses of oxide thin films by reactive evaporation and ceramics by solid state reaction and their characterizations are studied. The main subjects are: preparation and characterization of ultrathin films of high-T_c superconductors: investigation of growth mechanism of thin films by in situ reflection high-energy electron diffraction: phase diagram of Bi_2O_3-SrO-CaO-CuO system: growth and characterization of single crystals of Bi-Sr-Ca-Cu-O system: preparation and observation of dielectric properties of ferroelectric thin films: preparation and characterization of metallic and ferromagnetic $SrRuO_3$ thin films: scanning tunneling microscope observation of surface structures and electronic states of metallic oxide thin films

Prof
Bando, Yoshichika
(D Sc)

Instructor
IKEDA, Yasunori

Instructor
TERASHIMA, Takahito
(D Sc)

Students:
IZUMI, Makoto (DC)
NIINAE, Toshinobu (DC)
NAKAZAWA, Kazuyuki (MC)
YAMADA, Takahiro (MC)
FURUBAYASHI, Yutaka (MC)
KAWANO, Katsuya

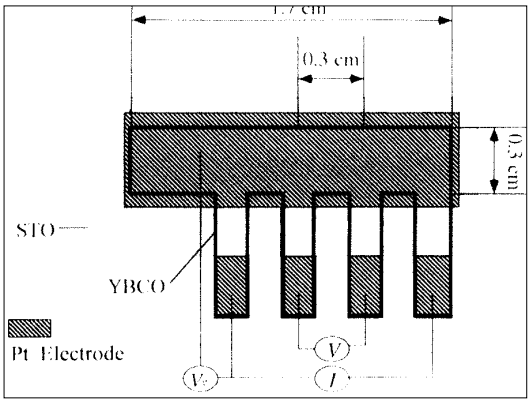

Figure 1. Top view of a FET-like junction.

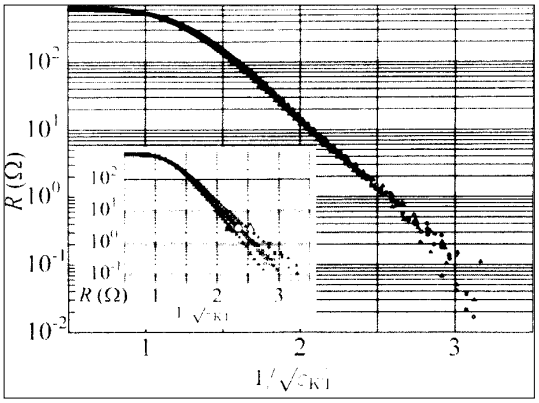

Figure 3. Temperature dependence of the resistance scaled in terms of ε_{KT} for a 2UCT YBCO film under zero magnetic field. The inset shows these in terms of ε_{KT0}. Symbols denote (O) V_g = 0, (Δ) V_g = 0.29V and (▲) V_g = -0.29V, respectively.

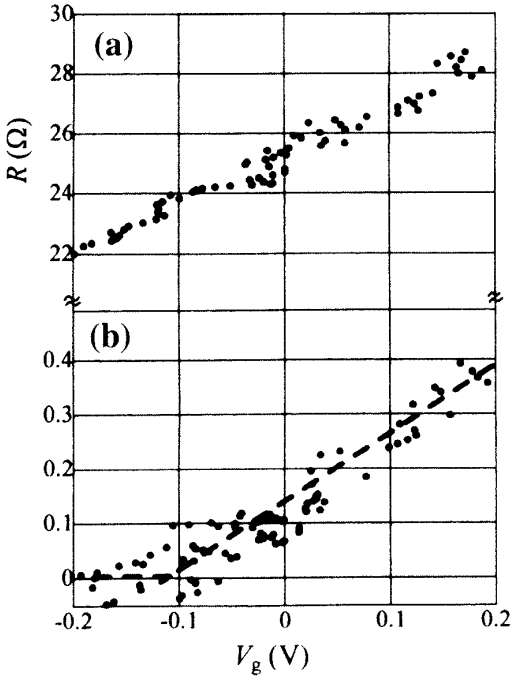

Figure 2. Change in R as a function of V_g for a 2UCT YBCO film at two representative fixed temperatures. (a) is for T = 45K and (b) for T = 35K, respectively.

dielectric constant of STO film was evaluated from the capacitance measurement as ε_e~2000 and the induced areal carrier density ΔN can be calculated via $\Delta N = \varepsilon_e\varepsilon_0 V_g/de$ = $9.22\times10^{13}V_g$(/cm^2) with d = 120nm, where ε_0 is the dielectric constant in vacuum.

E-field effects on resistance for 2 UCT (2.4nm)YBCO film are shown in Figs. 2(a) and (b) for representative fixed temperatures, that is, (a) is in the transition region of high resistance state at 45 K and (b) immediately above the onset temperature of R, respectively, where we applied a gate voltage to a Pt electrode. In Fig.2(a) , resistance R changes linearly with V_g across V_g = 0. For a negative V_g, R is lowered with decreasing V_g, and it is enhanced for an opposite polarization of V_g. On the other hand, in Fig. 2(b), R changes with V_g in a nonlinear fashion, that is, it approaches zero at a certain negative V_g and remains zero for a large negative V_g within an experimental error. This indicates that the onset temperature of zero resistance is altered by the applied E-field.

We analyzed the superconducting transition of ultrathin YBCO films by using the theory of Kosterlitz-Thouless (KT) transition. The superconducting part σ_S of the sheet conductance σ for the KT transition ig given by

$$\sigma_S = \sigma_N \exp\left(2(b\varepsilon_C/\varepsilon_{KT})^{1/2}\right) \qquad (1)$$

where σ_N and b are unknown parameters, $\varepsilon_C = (T_{mf}-T_{KT})/T_{KT}$, $\varepsilon_{KT} = (T-T_{KT})/T_{KT}$, T_{KT} is the transition tempertature of the KT transition, and T_{mf} is that of the mean-field transition, respectively. To evaluate T_{KT} we treated σ_N, $b\varepsilon_c$ and T_{KT} as fitting parameters and then the temperature was scaled to ε_{KT}. We obtain for T_{KT} 33.39K, 34.09K and 34.79K for V_g = +0.29V, 0V and -0.29V, respectively.

In Fig. 3, resistance curves under applied E-fields V_g = +0.29 V and V_g =0 are shown in respective scaling temperatures $1/(\varepsilon_{KT})^{1/2}$ based on eq. (1) where T_{KT} is chosen for each V_g. For scaling, R is shown against the scaling temperature $1/(\varepsilon_{KT0})^{1/2}$ for a fixed T_{KT} of V_g = 0 in the inset of Fig. 3. Here, the curves for V_g = +0.29V are separated by a straight line for V_g = 0 and deviate from each other at low temperatures. In contrast to this, they collapse into a unified function when scaling temperatures $1/(\varepsilon_{KT})^{1/2}$ are used for respective T_{KT}´s for each V_g.

We compare the E-field effects on T_{KT} with those on R_n and find that $\Delta T_{KT}/T_{KT}$ is proportional to $\Delta R/R_{n0}$ for various applied E fields. E-field effects study for other systems is in progress.

References

1. K. Kawahara, T. Suzuki, E. Komai, K. Nakazawa, T. Terashima and Y. Bando, Physica C, **266**, 149-156 (1996).
2. T. Kawahara, T. Suzuki, K. Shimura, T. Terashima and Y. Bando, Physica C, **235-240**, 3363-3364 (1994).

High Critical Current Density in the Heavily Pb-Doped $Bi_2Sr_2CaCu_2O_{6+\delta}$ Superconductor: Generation of Novel Pinning Centers

Zenji Hiroi and Mikio Takano

Critical current density (J_c) is a parameter of primary importance for potential applications of high temperature copper oxide superconductors (HTSCs). It is principally limited by the breakdown of zero-resistive current due to thermally activated flux flow at high temperatures and high magnetic fields. Here we report a dramatic increase in J_c in $Bi_2Sr_2CaCu_2O_{6+\delta}$ (Bi-2212) single crystals doped with a large amount of Pb.

Keywords: high temperature copper oxide superconductors/ Bi-2212 phase/ single crystals/Pb doping/ critical current density

HTSCs exhibit an unusual magnetic field - temperature (*H* - *T*) phase diagram which is quite different from that of conventional superconductors. The major origin is strongly two-dimensional (2D) characters of HTSCs, as well as short coherence lengths and elevated critical temperatures (T_c's), which dramatically change the vortex state in magnetic fields perpendicular to the CuO_2 layers; vortex lines become ill-defined and transform into pancake vortices confined within the CuO_2 layers which couple only weakly between the layers. Then, the role of thermal fluctuation on the dynamics of vortices is enormously enhanced, and flux flow occurs in a wide temperature range below T_c, resulting in a finite resistivity. A practically important boundary in the *H-T* phase diagram is called the irreversibility line (IL) which marks the boundary between the regions of reversible and irreversible magnetic behaviors. It is believed that the vortices are pinned by defects in crystals below the IL, while they can move in response to external forces above the IL, which means the vanishment of finite *Jc*. From the viewpoint of practical applications it is particularly important to expand this irreversible regime and, at the same time, to increase J_c.

A key to increase J_c is to generate efficient pinning centers in crystals. Recent studies using heavy ion irradiation have clearly exemplified that aligned columnar defects serve as flux pinning centers and the IL shifts upward. A similar improvement was recently reported for composites in which

SOLID STATE CHEMISTRY —Multicomponent Materials—

Scope of Research

Novel inorganic materials that have new, useful or exotic features such as superconductivity, ferromagnetism and quantum spin ground state are synthesized by novel methods. Particularly the search for spin ladder materials is intensively conducted by means of a high pressure synthesis at 3-8 GPa, where materials of high density unavailable under ambient pressure can be obtained

Prof
TAKANO, Mikio
(D Sc)

Assoc Prof
HIROI, Zenji
(D Sc)

Instr
AZUMA, Masaki
(D Sc)

Guest Scholar
CHEN, Teng-Ming (Prof, Ph D)
Students
CHONG, Ikse (DC)
KOBAYASHI, Naoya (DC)
YAMAURA, Kazunari (DC)
POULSEN, Jakob (DC)
KAWASAKI, Shuji (DC)
IZAKI, Takahito (MC)
KAIMORI, Shingo (MC)
FUJISHIRO, Yoshie (MC)
MATSUNAGA, Takanobu (MC)
IIDA, Mamoru (MC)
OKUMURA, Makoto (MC)
NABESHIMA, Yasuki (MC)

MgO nanorods of 20 nm in diameter were embedded in matrix Bi-2212 films. However, these methods are rather formidable and not useful in practical material processing.

We have studied the single crystal growth of Bi-2212 and found that the partial replacement of Bi by a large amount of Pb (0.6 per formula unit) surprisingly affects the magnetic properties of Bi-2212. Electron microscopy has revealed characteristic microstructures which is probably responsible for the observed enhancement in J_c: thin (≈ 10 nm) plate-like domains having a modulation-free structure appear with spacings of 50 - 100 nm along the b axis. This simple and ordinary chemical substitution would offer an alternative, technologically more promising method to prepare high-performance Bi-2212 wires which can be used at high temperatures and high magnetic fields.

Nonmagnetic Impurity Effects on a 2-Leg Quantum Spin Ladder Compound $SrCu_2O_3$

Masaki Azuma amd Mikio Takano

Nonmagnetic impurity effects on a 2-leg quantum spin ladder with a large spin gap of about 400K were investigated. Surprisingly, only a few % of impurity was found to drive the host gapeless and antiferromagnetically ordered at a composition dependent temperature below 10K

Keywords: Quantum spin ladder/ Spin gap/ Nonmagnetic impurity/ Magnetic susceptibility/ Specific heat/ NMR and NQR/ Inelastic neutron scattering

Quantum spin ladder is a newly found quasi-one dimensional (1D) system with an energy gap, "spin gap", between the singlet spin liquid ground state and the first triplet excitation state, as also seen in Haldane and spin-Peierls materials (see ICR Annual Report Vol. 2). $SrCu_2O_3$ is a high pressure phase discovered by us which comprises 2-leg ladders made of antiferromagnetic Cu-O-Cu linear bonds. These ladders are connected with each other spatially but are separated from each other magnetically because of the 90° Cu-O-Cu bond and spin frustration at the interface. This oxide is the very first even-leg spin ladder system for which the existence of such a spin gap (~ 400 K in width) has been confirmed experimentally through the measurements of the magnetic susceptibility, the nuclear spin relaxation time, T_1 and inerastic neutron scattering.

There are interests in exploring the possible onset of magnetic states induced by impurities in gapped 1D antiferromagnets and many theoretical and experimental works have been made on spin-Peierls and Haldane materials. We have studied effects of a nonmagnetic impurity introduced into $SrCu_2O_3$ and found that the impurity causes an unusual magnetic state.

Zn^{2+} was chosen as the nonmagnetic impurity because its ionic radius is similar to that of Cu^{2+}. Magnetic susceptibility, specific heat, NMR, NQR and inelastic neutron scattering studies were performed for $Sr(Cu_{1-x}Zn_x)_2O_3$ ($x \leq 0.08$). All these experimental results have given us the following picture quite consistently. It is wrong to assume that a Zn atom induces a free moment localized around it as naively expected from the gapped nature of the host. Instead, the original ground state is disturbed in a more extended way such that a finite density of states appears in the energy gap and grows without affecting the magnitude of the gap until the gap closes finally around x = 0.04. The system behaves as a gapless 1D antiferromagnet and experiences an antiferromagnetic ordering at a low temperature. The Néel temperature showed a systematic Zn concentration dependence with a broad maximum at around 4 % substitution (T_{Nmax} ~ 8K).

The Microscopic Basis of the Low-Frequency Excitations in B_2O_3 Glass

Takashi Uchino, Hong Lin, Hiromitsu Kozuka and Toshinobu Yoko

We have performed ab initio molecular orbital calculations on the clusters modeling the medium-range ordering (MRO) region of B_2O_3 glass at the Hartree-Fock (HF)/6-31G* levels. Their equilibrium geometries, harmonic vibrational frequencies, and Raman scattering intensities have been calculated. The calculations have reproduced the boson peak frequencies of vitreous B_2O_3 observed at 24 cm^{-1} and 137 cm^{-1}. The normal coordinates have demonstrated that these low-frequency vibrational modes are due to the wavelike motions of atoms within the region composed of one (for the mode at 137 cm^{-1}) or two (for the mode at 24 cm^{-1}) boroxol ring(s). The results suggest that the boson peak originates from the collective harmonic vibrations localized in the MRO region of glasses.

Keywords: *B_2O_3 glass*, Raman spectra, Low-frequency properties, Molecular orbital calculations, Localized vibrations

The low-frequency (< 200 cm^{-1}) relaxations and vibrations in amorphous systems have been the focus of numerous studies aimed at understanding the anomalous low temperature properties and glass transition phenomena observed in such systems. Although the relaxational part of the dynamics in supercooled liquids is well described by the mode coupling theory (MCT) [1], the vibrational excitations generally called the "boson peak" cannot be explained with MCT, and the origin of the boson peak is still unsettled. Thus, the understanding of the boson peak near the glass transition temperature T_g remains an important goal in solid-state physics today. It has recently been suggested that the atomic motions in a medium range scale of the order of ~10 Å in amorphous solids have a close relation to the boson peak [2]. This strongly suggests that the normal-mode analysis of molecules modeling a medium range order (MRO) in a particular glass will shed new light on the physical origin of the boson peak.

B_2O_3 glass has been widely used to study its low-frequency vibrational properties [3]. The low-frequency Raman scattering spectra of B_2O_3 glass are characterized by a nonsymmetric boson peak with a broad maximum around 25 cm^{-1}; the peak shifts slightly to higher frequencies with decreasing temperature. In this work, ab initio molecular

SOLID STATE CHEMISTRY —Amorphous Materials—

Scope of research

Inorganic amorphous materials with various functions are the targets of research in this laboratory. (1) To obtain a clear view of "what is glass" and the bases for designing functional glasses, we investigate the structure of glasses using X-ray and neutron diffraction analysis, high resolution MAS-NMR, and ab initio MO calculation. (2) To develop materials of high optical nonlinearity, we search heavy metal oxide-based glasses and transition metal oxide thin films, and evaluate the nonlinear optical properties by THG and Z-scan methods. (3) Using sol-gel method, synthesis and microstructure control are carried out on ceramic/metal/organic dye composite thin films.

Professor
YOKO, Toshinobu
(D Eng)

Associate Professor
KOZUKA, Hiromitsu
(D Eng)

Instructor
UCHINO, Takashi
(D Eng)

Instructor
LIN, Hong
(D Eng)

Guest Research Associates
INNOCENZI, Plinio
ZHAO, Gaoling

Students
TERASHIMA, Kentaro (DC)
SAKIDA, Shin-ichi (DC)
NAKATA, Kunihiko (MC)
TAKAHASHI, Yasuhumi (MC)
HATTORI, Takeshi (MC)
TOKUDA, Youmei (MC)
KUMON, Souichi (UG)
NIIDA, Haruki (UG)

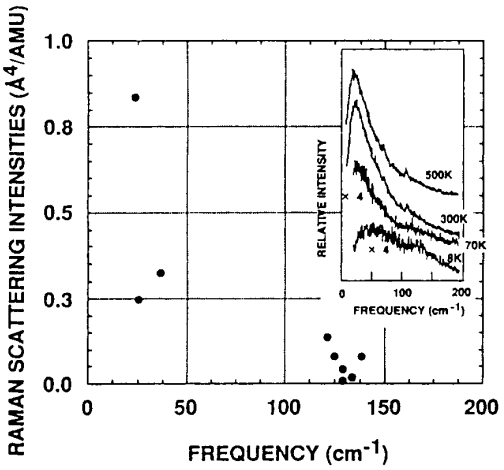

Figure 1. Calculated Raman scattering intensities at the HF/6-31G* level. Inset shows the observed Raman spectra of B_2O_3 glass (Ref.3).

orbital (MO) calculations were carried out to investigate the low-frequency vibrational properties of B_2O_3 glass [4]. It has previously been shown that ab initio MO calculations are useful to investigate the electronic and vibrational properties of glasses [5-7]. We employed the optimized $B_3O_3(OH)_2$-O-$B_3O_3(OH)_2$ cluster as a model of MRO in vitreous B_2O_3. The hydrogen atoms in the cluster are used to saturate the dangling bonds of "surface" oxygen atoms. The $B_3O_3(OH)_2$-O-$B_3O_3(OH)_2$ cluster is composed of two boroxol rings; the boroxol rings are considered to be the principal structural units in B_2O_3 glass. All ab initio MO calculations were carried out using the GAUSSIAN92 computer program [8] on CRAY Y-MP2E/264 super computer in this Institute.

We notice from Fig.1 that the low-frequency vibrational modes for the model cluster can be separated into two regions. One lies from 23 cm^{-1} to 37 cm^{-1} (group I) and the other from 121 cm^{-1} to 138 cm^{-1} (group II). Figure 1 also compares the calculated results with the observed Raman spectra [3]. It should be noted that the two vibrational regions satisfactorily correspond to the observed frequencies (24 and 137 cm^{-1}) of the two boson peaks of B_2O_3 glass at room temperature.

We next analyze the normal coordinates to investigate what kinds of motion yield the low-frequency vibrational modes. Figure 3 depicts the normal coordinates of the vibrational modes calculated at the 6-31G* level. All these vibrational modes exhibit a sort of out-of-plane bending motions of the whole skeleton of the cluster. We refer to these low-frequency vibrational motions as the "wavelike" motions because they can be regarded as swelling motions to form "waves" having specific "wavelengths." It appears from Fig. 2 that the "wavelength" becomes shorter with increasing frequency of the modes. For the modes in group I (see, for example, Fig.2 (a)) the "wavelengths" are the extent of the two boroxol rings (~ 10 Å), while for the modes in group II (see, for example, Fig.2 (b)) they are the extent of one boroxol ring or that of one O-B-O-B bond. Thus we suggest that the boson peak results from the harmonic vibrational motions localized in the extent of the medium-range order (MRO) in the respective glass-forming systems.

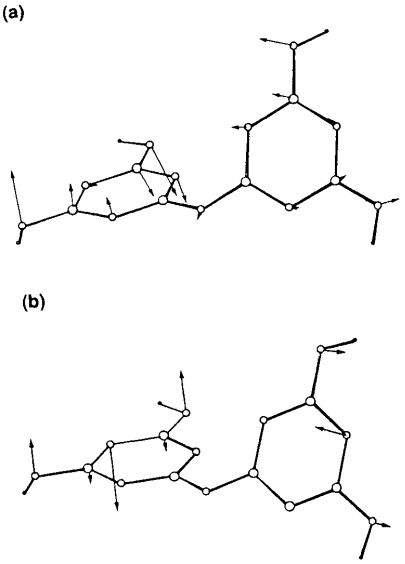

Figure 2. Calculated normal-mode coordinates for the modes at (a) 24 cm^{-1}, and (b) 129 cm^{-1}.

References

1. Götze W, in *Liquids, Freezing and the Glass Transition*, edited by Hansen J P, Levesque D, Zinn-Justin J, (North-Holland, Amsterdam, 1991), p.287.
2. Krüger M, Soltwisch M, Petscherizin I and Quitmann D, *J. Chem. Phys.* **96**, 7352 (1992).
3. Guha S and Walrafen G E, *J. Chem. Phys*. **80**, 3807 (1984).
4. Uchino T and Yoko T, *J. Chem. Phys*. **105**, 4140 (1996).
5. Uchino T and Yoko T, *Science* **273**, 480 (1996).
6. Uchino T and Yoko T, *J. Non-Cryst. Solids* **204**, 243 (1996).
7. Uchino T and Yoko T, *J. Ceram. Soc. Japan, in press.*
8. Frisch MJ et al., GAUSSIAN 92 (Gaussian, Inc., Pittsburgh, PA, 1992).

Molecular Rheology of Glassy Polymers

Tadashi Inoue, Hiroto Matsui, Hiroshi Watanabe, and Kunihiro Osaki

Molecular origin of the viscoelasticity around the glass transition zone is investigated by means of dynamic birefringence and dynamic viscoelasticity measurements. The present study show that the viscoelasticity around the glass transition zone has two molecular origins: One is the orientation relaxation of main chain axis and the other one is the rotational motion of structure units about the main chain axis.

Keywords: Viscoelasticity / Birefringence / Stress-optical rule / Orientation / Vinyl polymers

Viscoelasticity of amorphous polymers is brought about by molecular motions of polymer chain. The aim of our study is to find molecular origin which are responsible for viscoelasticity around the glass-to-rubber transition zone. We will discuss how a polymer chain is deformed in the glassy zone in this study.

For polymer melts or concentrated solutions, the strain-induced birefringence, Δn, is proportional to the stress. This rule is called the stress-optical rule (SOR). SOR indicates that molecular origin of the stress and birefringence of rubbery materials is the orientation of chain. However, SOR does not hold valid in the glass transition and glassy zones. We have found that the birefringence can be related to the stress through a modified stress-optical rule (MSOR) in these zones[1-3].

$$E^*(\omega) = E_G^*(\omega) + E_R^*(\omega) \quad (1)$$

$$O^*(\omega) = C_G E_G^*(\omega) + C_R E_R^*(\omega) \quad (2)$$

where $O^*(\omega) \equiv \Delta n^*(\omega)/\varepsilon$ is the complex strain-optical coefficient and $E^*(\omega)$ is the complex Young's modulus. $E_i^*(\omega)$ and C_i (i=R, G) are the component function and the stress-optical coefficient. MSOR is based on two experimental results; validity of the SOR, $O^*(\omega)=C_R E^*(\omega)$, in the rubbery zone and $O''(\omega)=C_G E''(\omega)$ in the glassy zone. $E_i^*(\omega)$ can be separated quantitatively by reducing eqs. 1 and 2. It has been found that MSOR holds valid for more than ten polymers with a few exceptions[3].

The birefringence and the stress can be related with two characteristic orientation functions of structure units by using a polymer model. In this model the polymer chain is supposed to be composed of identical *flat* units that do not change the shape over the studied time scale. The chain can change its shape by the rotation motion about the connecting bonds. The birefringence of this model can be written as follows[2].

$$\Delta n \propto \{\alpha_1 - (\alpha_2+\alpha_3)/2\}P_R + (1/4)(\alpha_2-\alpha_3)P_G \quad (3)$$

Here, aα_i and represents the principal values of the polarizability tensor of the structure unit. The subscript represents the coordinate of the molecular frame; "1" represents the direction of the chain axis and "2" is taken in the plane of the unit if the unit can be regarded as flat to any

FUNDAMENTAL MATERIAL PROPERTIES —Molecular Rheology—

Scope of research

The molecular origin of various rheological properties of materials is studied. Depending on time and temperature, homogeneous polymeric materials exhibit typical features of glass, rubber, and viscous fluids while heterogeneous polymeric systems exhibit plasticity in addition to these features. For a basic understanding of the features, the molecular motion and structures of various scales are studied for polymeric systems in deformed state. Measurements are performed of rheological properties with various rheometers, of isochronal molecular orientation with flow birefringence, and of autocorrelation of the orientation with dynamic dielectric spectroscopy.




Prof	Assoc Prof	Instr	Techn
OSAKI, Kunihiro	Watanabe, Hiroshi	INOUE, Tadashi	OKADA, Shinichi
(D Eng)	(D Sc)	(D Eng)	(B Eng)

Students

RYU, Deug-Soo (DC)
MATSUI, Hiroto (MC)
SATO, Tomohiro (MC)
ABE, Shuichi (MC)
ONOGI, Takayuki (MC)
KUWADA, Shozo (UG)
NAKAMURA,Shinya(UG)

extent. Here, the tensor was assumed to be diagonal with respect to the molecular frame for simplicity. The orientational functions P_G and P_R are given as follows.

$$P_R = (1/2)(3\langle\cos^2\theta\rangle - 1) \quad (4)$$

$$P_G = 3\langle\sin^2\theta\cos^2\phi\rangle \quad (5)$$

Here, θ and ϕ are the polar and azimuthal angles of the stretch direction in the local coordinates of each structure unit. P_R represents the orientation of the main chain axis and P_G reflects the tilting of the structure unit about main chain axis. Thus, the two components can be related to longitudinal and transverse anisotropies of the structure unit.

On the other hand, the local stress, σ_{ij}^m, acting on each structure unit, may vary from place to place and from time to time. However, it was shown that σ_{ij}^m is well constant in the stress relaxation process[2]. As a result the macroscopic stress, σ, can be written as follows.

$$\sigma = \{\langle\sigma_1^m\rangle - (\langle\sigma_2^m\rangle + \langle\sigma_3^m\rangle)/2\}P_R + (1/4)(\langle\sigma_2^m\rangle - \langle\sigma_3^m\rangle)P_G \quad (6)$$

Here, $\langle\sigma_i^m\rangle$ represent the principal values of the statistical average of the local stress tensor. Thus the stress can be related to the same orientation functions as the birefringence. The first terms in eqs. 3 and 6 correspond to the R component and the second to the G component.

Eq. 3 provides molecular origin of the birefringence and the relation between the birefringence and molecular structure. The validity of this molecular interpretation can be examined by a study on a series of vinyl polymers[2].

The characteristic birefringence of each component, $O_i'(\infty)=C_iE_i'(\infty)$ (I = R or G) reflects the orientation of the structure unit as well as the molecular anisotropy. We define a reduced strain-optical ratio at high frequencies.

$$O_i'(\infty) \equiv \{9nM_0/2\pi(n^2+2)^2\rho N_a\}O_i'(\infty) = \Delta\alpha_i P_i/\varepsilon \quad (7)$$

where ρ and M_0 are the density and molecular weight of the repeating unit and $\Delta\alpha_R=\alpha_1-(\alpha_2+\alpha_3)/2$ and $\Delta\alpha_G=(\alpha_2-\alpha_3)/4$. Assuming the additivity of bond polarizability and free rotation of the side group, it can be shown that $2\Delta\alpha_G=A-\Delta\alpha_R$ for vinyl polymers. Here, A is a constant independent of the side groups. With this relation, the relation between $O_R'(\infty)$ and $O_G'(\infty)$ can be reduced to the relation between P_R and P_G.

In Figure 1 $O_G'(\infty)$ is plotted against $O_R'(\infty)$. Two lines in the figure are due to two orientation models with the assumption of free rotation of the side chains[5]. In the first model, we assumed that the main chain axis(axis 1) and the side chain direction (axis 2) orient independently according to the quasi-affine deformation. This model gives $P_G=6P_R$.

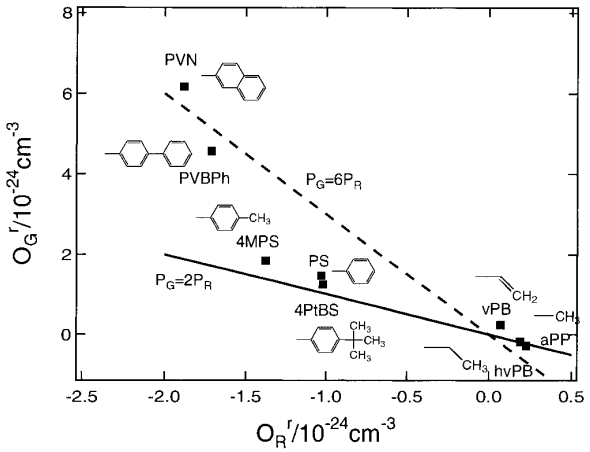

Fig. 1. Relation between the two reduced strain-optical coefficients for vinyl polymers; (-CH_2CHR-)n.

However, this model prediction is not correct because this model includes deformation of the structure units which is assumed to be rigid. In the second model, we assumed that the main chain axis orients quasi-affinely and the side chain axis rotates about main chain axis keeping orthogonality between the two axis by an angle which is obtained by quasi-affine orientation. This model gives $P_G=2P_R=(6/5)\varepsilon$. The data points for aPP, hvPB, vPB and PS are close to this line. On the other hand, the results for PVN and PVBPh suggest that P_G/ε values increases with increasing the size of side chain. Thus our molecular interpretation is in accord with experimental results

In conclusion, we have shown that the viscoelasticity and the birefringence of glassy polymers have the two molecular origin around the glass transition zone. One is the orientation relaxation of the structure units along the main chain axis and the other one is the rotational motion of the structure units about the main chain axis.

References

1. T. Inoue, H. Okamoto, and K. Osaki, *Macromolecules*, **24**, 5670(1991).
2. K. Osaki, H. Okamoto, T. Inoue, and E.-J. Hwang, *Macromolecules*, **28**, 3625(1995).
3. T. Inoue, and K. Osaki, *Macromolecules*, **29**, 1595 (1996).
4. T. Inoue, et al., *Macromolecules*, **29**, 6240(1996).
5. T. Inoue, et al., *Polymer*, in press.

How Does the Polymer Chain Expand by Intramolecular Electrostatic Repulsion

K. Nishida, K. Kaji and T. Kanaya

The electrostatic correlation lengths ξ in salt-free polyelectrolyte solutions have been measured as functions of charge density and polymer concentration using a small-angle X-ray scattering (SAXS) technique. Water soluble poly(vinyl alcohol) (PVA) was employed as a parent polymer to avoid increasing hydrophobic interactions with decreasing the charge density; partially sulfuric-acid esterificated PVA's were used as samples. The charge density was changed from 0.008 to 0.499 in degree of esterification α. It was found that the maximum position q_m of a characteristic SAXS peak, which is attributable to the electrostatic interchain correlation, is proportional to the square root of polymer concentration C at any charge density. This supports that the isotropic model of de Gennes et al. is valid. The α dependence of q_m agrees with the theoretical prediction from the blob chain model for weakly charged polyelectrolytes proposed by Pfeuty and Khokhlov. This is the first and important experimental data which tells how the polymer chain expands by intramolecular electrostatic repulsion.

Keywords: Polyelectrolytes / Correlation length / Blob chain model / Isotropic model / SAXS

It is well-known that in salt-free solutions the polymer chains having flexible backbones will behave as half-riged rods when they have high charge density. The driving force of the expansion is, of caurse, the intramolecular electrostatic repulsion between dissociation groups attached to the backbone. On the other hand, without charges they will behave as coils. So it is natural to consider that the low charge density polyions in salt-free solutions should have an intermediate conformation, something between a half-riged rod and a spherical coil. But, how ? The mechanism of chain expansion by charges is one of the most interesting problems in the field of polyelectrolyte solutions.

As the charge density α decreases, however, the flexibility of polyion chains does not continuously increase, but they collapse into blobs below a critical value of the charge density. This type of conformation has been modeled as a chain of blobs by de Gennes et al.[1], Pfeuty[2], and Khokhlov[3-4]. A single blob chain consists of a sequence of blobs inside which the chain conformation is approximated as Gaussian. The effective contour length of this blob chain is defined by the sum of blob diameters. As α decreases, the blob diameter increases proportionally to the square root of the molecular weight M_b of a blob while the number of blobs in a chain decreases proportionally to M_b. The contour length therefore decreases with decreasing α. Further, since the interchain correlation length in the semidilute region is related

FUNDAMENTAL MATERIAL PROPERTIES —Polymer Materials Science—

Scope of research

The structure and molecular motion of polymer substances are studied using mainly scattering methods such as neutron, X-ray and light with the intention of solving fundamentally important problems in polymer science. The main projects are: the mechanism of structural development in crystalline polymers from the glassy or molten state to spherulites; the dynamics in disordered polymer materials including low-energy excitation or excess heat capacity at low temperatures, glass transition and local segmental motions; formation process and structure of polymer gels; the structure and molecular motion of polyelectrolyte solutions; the structure of polymer liquid crystals.

Prof
KAJI, Keisuke
(D Eng)

Assoc Prof
KANAYA, Toshiji
(D Eng)

Instr
NISHIDA, Koji

Students

TAKESHITA, Hideki (DC)
KIRIYAMA Kohei (MC)
MIYAKAWA Masafumi (MC)
MATSUBA Go (MC)
NISHIKOJI Yuichi (MC)
MIYAMOTO, Keiko (UG)
OGAMI, Akinobu (UG)
TSUKUSHI, Itaru (RF)
HANSEN, Jan (RS)

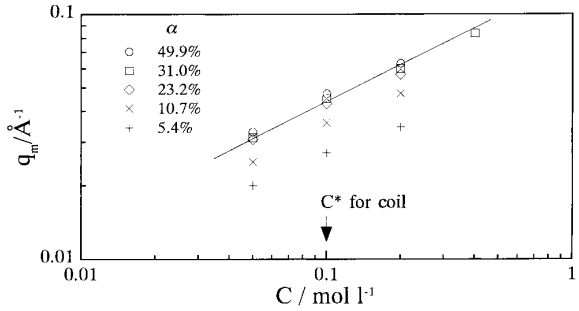

Figure 1. q_{max} vs. C plot in logarithmic scales for NaPVS solutions. α = 49.9 % (O), 31.0 % (❑), 23.2 % (◊), 10.7 % (×), and 5.4 % (+). The straight line represents a slop of 1/2.

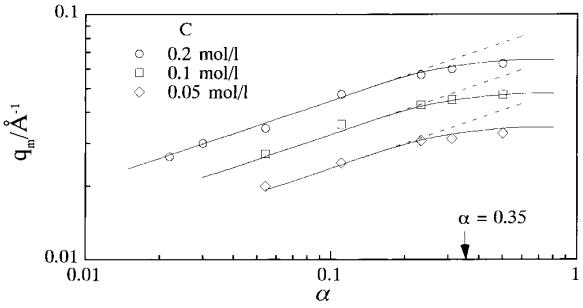

Figure 2. The q_{max} vs. α plot in logarithmic scales for NaPVS solutions. C = 0.2 mol/l (O), 0.1 mol/l (❑), and 0.05 mol/l (◊). Dashed lines represents a slop of 1/3. Solid lines are to guide the reader's eye.

to the density of the effective contour length, i.e., density of skeletal lines, the interchain correlation length ξ also increases with decreasing α under the constant C condition. Thus, based on this model the α dependence of the correlation length can be derived. When the correlation length $\xi \sim C^{-1/2}$ was derived in the isotropic model[1], the overlap concentration in rod limit was taken as N/L^3 where $L = a_0 N$ is contour length, a_0 and N being the length of a monomer and the degree of polymerization, respectively. For a chain consisting of blobs, replacing L by effective contour length L', the interchain correlation length becomes

$$\xi \sim (CL'/N)^{-1/2}. \quad (1)$$

According to the blob model[2-4]

$$L' \sim \alpha^{2/3} N, \quad (2)$$

and so

$$\xi \sim \alpha^{1/3} C^{-1/2} \quad (3)$$

or

$$q_m \sim \alpha^{1/3} C^{1/2}, \quad (4)$$

where q is the length of scattering vector $q = 4\pi \sin\theta/\lambda$, 2θ and λ being scattering angle and X-ray wavelength, respectively. Equations 3 and 4 are basic relations in the semidilute region for understanding the α dependence of the correlation length ξ and the peak position q_m, respectively. Here, it should be noted that these equations are valid only for $\alpha \le a_0/l_B$ because of the Oosawa-Manning counterion condensation theory[5-7] where l_B is the Bjerrum length defined by $e^2/4\pi\varepsilon kT$, e, ε, k and T being elementary charge unit, dielectric constant of solvent, Boltzmann constant and temperature, respectively. For $\alpha > a_0/l_B$, ξ and q_m become independent of α.

The SAXS measurements were carried out using a 6-m point focusing SAXS camera at the High-Intensity X-ray Laboratory of Kyoto University. In Figure 1, q_m is plotted against C for various α's. For $\alpha \ge 0.107$, the relationship in equation 4 is satisfied in respect to the C-dependence. This behavior of q_m for $\alpha \ge 0.107$ in Figure 1 is essentially the same as in the previous experiments[8-9] for the salt-free semidilute solution of NaPSS with α =1.0. It is therefore expected that the present systems with $\alpha \ge 0.107$ also assume the 'isotropic structure'. For $\alpha \le 0.054$, the exponent of C is rather small compared with 1/2. Considering this phenomenon and the crossover concentration C^* = 0.1 mol/l for the coil limit, these systems may no longer be regarded as semidilute in the whole range observed, especially at C < 0.1 mol/l, but they may be somewhere in the crossover region.

Figure 2 shows logarithmic plots of q_m against α for various concentrations. For α < 0.3, the relationship in equation 4 is satisfied in respect to the α-dependence. The decrease of the correlation length with increasing α means that polyion blob chains expand with increasing α.

The leveling-off of q_m for α > 0.3 is attributable to a phenomenon of counterion condensation. According to the condensation theory of Oosawa[5-6]-Manning[7], the counterion condensation occurs when the distance between the neighboring dissociation groups on the backbone chain is within the Bjerrum length l_B as above described. Since l_B is 7.16Å in water at 25°C and a_0 = 2.52 Å for a vinyl type of polymers, the critical charge density $\alpha = a_0/l_B$, at which the counterion condensation begins to occur, is 0.35. This almost corresponds to the observed value of 0.3. The structural change by electrostatic interaction is therefore no longer expected for α > 0.35.

These results indicate that the structure of semidilute solutions of weakly charged polyelectrolytes can also be understood within a frame work of the 'isotropic model'[1], and the mechanism of chain expansion by charge obeys the 'blob chain model'[1-4].

References

1. de Gennes P G, Pincus P, Velasco R M, Brochard F, *J. Phys. France*, **37**, 1461-1473, (1976).
2. Pfeuty P, *J. Phys. Colloq. France* **39**, C2-149-160, (1978).
3. Khokhlov A R, *J. Phys. A: Math. Gen.* **13**, 979-978, (1980).
4. Khokhlov A R, Khachaturian K A, *Polymer*, **23**,1742-1750, (1982).
5. Oosawa F, *J. Polym. Sci.* , **23**, 421-430, (1957).
6. Oosawa F, *Polyelectrolytes* : Marcel Dekker, NewYork, 1971.
7. Manning G S, *J. Chem. Phys.* , **51**, 924-933,(1969).
9. Kaji K, Urakawa H, Kanaya T, Kitamaru R, *Macromolecules*, **17**, 1835-1839, (1984).
10. Kaji K, Urakawa H, Kanaya T, Kitamaru R, *J. Phys. France*, **49**, 993-1000, (1988).

Solid-State ^{29}Si NMR Analyses of the Structure and Dynamics of Solid Poly(di-*n*-alkylsilane)s

Hironori Kaji and Fumitaka Horii

Solid-state ^{29}Si NMR analyses of the solid structure and dynamics have been performed for poly(di-*n*-butylsilane) with the order-disorder transition at 76 °C. ^{29}Si chemical shift anisotropy (CSA) spectra are measured with an ultraslow magic angle spinning at a rate less than 100 Hz. Almost rigid CSA spectra for the 7/3 helical structure are observed below the transition temperature. In contrast, axially symmetric CSA spectra with different principal values appear above the transition temperature, suggesting the onset of the rotational motion around the molecular chain axis with trans-rich conformation. The changes of the conformation and dynamics around the transition are also discussed for other poly(di-*n*-alkylsilane)s such as poly(dimethylsilane) and poly(di-*n*-hexylsilane).

Keywords: Poly(di-*n*-alkylsilane)s / CPMAS NMR / Chemical shift anisotropy / Ultraslow MAS / Solid structure / Dynamics

Polysilanes are a new class of polymers which contain only silicon atoms in the backbone. They have been attracting much interest because of their interesting electronic and chemical properties, such as photoconductivities, and nonlinear optical properties. These properties are dominated by σ-delocalization of electrons along the silicon backbone and thus considered to be strongly dependent on the chain conformation and molecular motion. For this reason, we have been particularly interested in the characterization of the conformational structure and dynamics of the silicon-based materials on the molecular level. Among them, poly(di-*n*-alkylsilane)s are known to have the order-disorder transition and the liquid crystalline state has recently been found above this transition temperature. In this report, we investigate the solid structure and dynamics of poly(di-*n*-butylsilane) (PDBS), poly(dimethylsilane) (PDMS) and poly(di-*n*-hexylsilane) (PDHS) by solid-state ^{29}Si NMR analyses, in particular around the order-disorder transition temperature.

PDBS and PDHS, which were kindly provided by Shin-Etsu Chemical Co., Ltd, were isothermally annealed at 100 °C for 10 hr in vacuum. DSC measurements were performed on TA Instruments DSC-2910. Solid-state ^{29}Si NMR measurements were conducted on JEOL JNM-GX400 and Chemagnetics CMX-400 spectrometers both operating under a static magnetic field of 9.4 T. ^{1}H and ^{29}Si field strengths $\gamma B_1/2\pi$ were 50 - 59.5 kHz. The contact time for the CP process was 3 and 10 ms for the ordered and disordered phases, respectively. The rate of sample spinning was set

FUNDAMENTAL MATERIAL PROPERTIES —Molecular Dynamic Characteristics—

Scope of research

The Research activities in this subdivision cover structural studies and molecular motion analyses of polymers and re-lated low molecular weight compounds in the crystalline, glassy, liquid crystalline, solution, and frozen solution states by high-resolution solid-state NMR, dynamic light scattering, electron microscopy, and so on, in order to obtain basic theories for the development of high-performance polymer materials. The processes of biosynthesis, crystallization, and higher-ordered structure formation are also studied for bacterial cellulose.

Prof
HORII Fumitaka
(D Eng)

Assoc Prof
TSUNASHIMA
Yoshisuke
(D Eng)

Instr
KAJI Hironori
(D Eng)

Assoc Instr
HIRAI Asako
(D Eng)

Techn
OHMINE
Kyoko

Guest Scholar
SHEN, Yimin (Assoc Prof, DSci)
Students
ISHIDA, Hiroyuki (DC)
KAWANISHI, Hiroyuki (MC)
KUWABARA, Kazuhiro (MC)
TAI, Toshihiro (MC)
MASUDA, Kenji (MC)
HATTORI Kimihiko (UG)
TAJIRI Kouji (UG)
ZHENG Jianming (RS)

to 4 kHz. ^{29}Si chemical shifts were expressed as values relative to tetramethylsilane (Me_4Si) by using the resonance line at -34 ppm for PDMS crystals as an external reference.

The order-disorder transition temperatures determined for PDMS, PDBS and PDHS by DSC were 157.8 °C, 75.9 °C and 44.4 °C , respectively. Figure 1 shows CP/MAS ^{29}Si NMR spectra of PDBS at different temperatures. The upfield and downfield resonance lines, which correspond to the ordered and disordered phases, are observed respectively below and above 70 °C , as is already reported by Schilling et al [1]. X-ray diffraction analyses revealed that PDBS has 7/3 helical structure in the ordered state [1]. Considering the γ-*gauche* effect, the higher chemical shift value in the disordered phase suggests that the chain conformation approaches to the planar *trans* conformation in this phase. In contrast, an upfield shift from -21.3 ppm at room temperature to -25.8 ppm at 80 °C is observed for PDHS, suggesting that the *trans* conformation in the ordered phase changes some helical structure in the disordered phase. No chemical shift change is observed for PDMS between room temperature and 200 °C within the experimental error.

Table 1 shows ^{29}Si spin-lattice relaxation times (T_1) for PDBS at different temperatures, measured by the CPT1 pulse sequence. T_1 values in the disordered phase are much shorter than those in the ordered phase. Such an evident difference in T_1 indicates the onset of the enhanced molecular motion in the disordered phase.

Table 1 Chemical shift and T_1 for PDBS.

Temperature/°C	rt	60	80	100
Chemical shift / ppm	-26.1	-25.0	-23.0	-22.3
T_1 / s	240	300	11	10

In order to characterize the detail of the molecular motion in the disordered phase, the spectra reflecting the ^{29}Si chemical shift anisotropy (CSA) are measured for PDBS at different temperatures. Figure 2 shows the ^{29}Si CSA spectra obtained under an ultraslow magic angle spinning at a rate less than 100 Hz, which is insensitive to CSA lineshapes. Typical CSA powder patterns, which reflect the principal values, σ_{11}, σ_{22}, and σ_{33}, of the chemical shift tensor in the rigid state are observed below the transition temperature. Such CSA spectra suggest that the molecular motion of the main chain is frozen in a time scale of 10^{-2} s. In contrast, axially symmetric CSA spectra are observed above the transition temperature. Assuming that σ_{11} corresponds to the molecular chain axis, these axially symmetric CSA spectra suggest that PDBS chains undergo the rotational motion around the chain axis with the frequency above 10^3 Hz. This result is consistent with the result of X-ray diffraction [1] which reveals the hexagonal packing in the disordered phase. Such rotational motion may be similar to the motion observed for *n*-alkane [2] in the hexagonal phases.

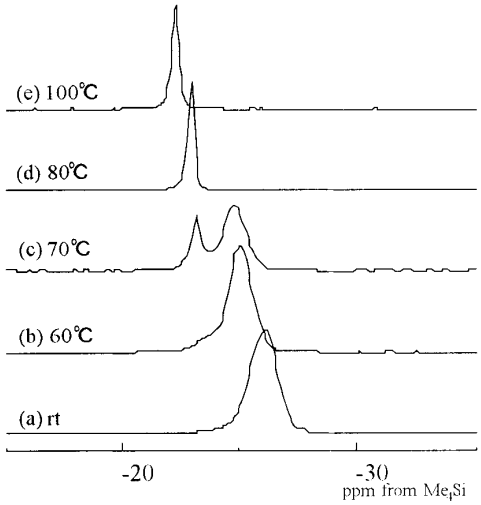

Figure 1. 79.6 MHz CP/MAS ^{29}Si NMR spectra of solid PDBS at various temperatures. The spinning rate is 4 kHz.

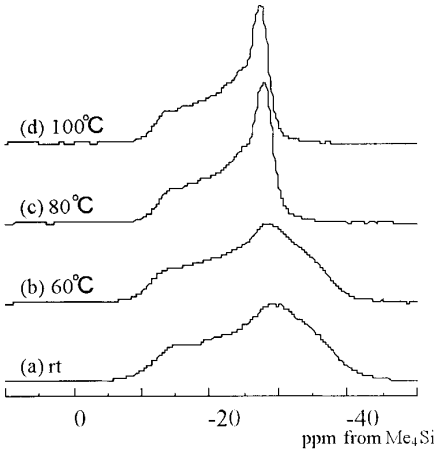

Figure 2. Ultraslow-MAS ^{29}Si CSA spectra of PDBS at various temperatures. The spinning rate is less than 100 Hz.

The analyses of T_1 and CSA powder patterns for PDMS and PDHS also suggest some enhanced molecular motion in the disordered phase. More detailed characterization of these polymers are in progress.

References

1. Schilling F C, Lovinger A J, Zeigler J M, Davis D D and Bovey F A, *Macromolecules*, **22**, 3055 (1989).
2. Kitamaru R, Horii F, Nakagawa M, Takamizawa K,Urabe Y and Ogawa Y, *J. Molec. Sturc.*, **355**, 95 (1995).

Mechanism and Kinetics of Nitroxide-Controlled Free Radical Polymerization

Takeshi Fukuda, Yoshinobu Tsujii and Takeaki Miyamoto

In the nitroxide-mediated free radical polymerization, the rate of polymerization is determined by the balance of the rates of thermal initiation and bialkyl termination, just like in the conventional system, while the polydispersity is determined by the dissociation-combination frequency of the polymer-nitroxyl adduct and the rate of decomposition of the adduct. These mechanisms were quantitatively confirmed by both experiments and computer simulations.

Keywords: Nitroxyl-polymer adduct / Reversible dissociation / Initiation / Termination / Decomposition / Narrow polydispersity

Introduction

Nitroxide-controlled free radical polymerization, first reported in 1985[1] and most extensively studied since 1993,[2] is a simple and robust method for preparing well-defined polymers. However, no unified views on the mechanism and kinetics have been established as yet. Here, we discuss the problems on the basis of our published and unpublished results.

Kinetic Schemes

A key role of the nitroxyl method is believed to be played by the reversible reaction among the polymer radical P*, the nitroxyl X*, and their adduct P-X[1,2,3]:

$$P^* + X^* \underset{k_d}{\overset{k_c}{\rightleftharpoons}} P\text{-}X \qquad (1)$$

while X* is active only to P*, P* should generally be active not only to X* and the monomer M (propagation) but also to other P* (termination). The concentrations of P* and X* should follow

$$d[P^*]/dt = R_i - k_t[P^*]^2 + k_d[P\text{-}X] - k_c[P^*][X^*] \qquad (2)$$

$$d[X^*]/dt = k_d[P\text{-}X] - k_c[P^*][X^*] \qquad (3)$$

where R_i is the rate of initiation, and k_t is the termination rate constant. If R_i is non-zero, a stationary state will be eventually reached, in which $d[P^*]/dt = d[X^*]/dt = 0$, and we have [3]

$$[P^*] = (R_i/k_t)^{1/2} \qquad (4)$$

$$[X^*] = K\,[P\text{-}X] / [P^*] \qquad (5)$$

Experimental Results and Discussion

For simplicity, here we confine ourselves to the polymerization of styrene in the presence of a purified adduct of polystyrene (PS) with TEMPO (2,2,6,6-tetramethylpiperidinyl-1-oxy) with no extra (free) nitroxyl added.

ORGANIC MATERIALS CHEMISTRY —Polymeric Materials—

Scope of research

Basic studies have been conducted for better understandings of the structure/property or structure/function relations of polymeric materials and for development of novel functional polymers. Among those have been the studies on (1) the synthesis and properties of cellulose- and oligosaccharide-based functional polymers, e.g., biodegradable polymers, liquid crystals and polymers of well-defined structure having pendant oligosaccharides, (2) the structure of polymer gels, ultrathin films and polymer alloys, and (3) the syntheses of new types of block and graft copolymers and fullerene(C_{60})-including polymers.

Prof MIYAMOTO, Takeaki (D Eng)

Assoc Prof FUKUDA, Takeshi (D Eng)

Instr TSUJII, Yoshinobu (D Eng)

Instr MINODA, Masahiko (D Eng)

Assoc Instr DONKAI, Nobuo (D Eng)

Students
IDE, Nobuhiro (DC)
TAKARAGI, Akira (DC)
OHNO, Kohji (DC)
OKAMURA, Haruyuki (DC)
YAMADA, Kenji (DC)
KUWAHARA, Shigenao (MC)
YAMAMOTO, Shinpei (MC)
GOTO, Atsushi (MC)
IMIYA, Chie (MC)
MIYAZONO, Koki (MC)
MUHAMMAD, Ejaz (MC)
IZU, Yasumasa (UG)
OGUCHI, Asahiro (UG)
BABA, Takeichiro (RF)
GAWRONSKI, Michael (RF)
KAMIYAMA, Fumio (RF)
LIU, Haiqing (RF)
NISHIMURA, Hiroshi (RF)

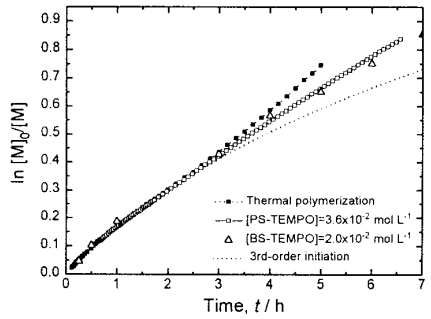

Figure 1 First-order plot for the polymerization of styrene at 125 °C in the presence (❑) and absence (■) of 10 wt% of PS-TEMPO adduct (M_n = 2300, M_w/M_n = 1.14). The dotted curve shows the $[M]^3$-dependent initiation (constant k_t): (Δ) batch polymerization with 2-benzoyloxy-1-phenylethyl adduct with TEMPO, a unimer model of PS-TEMPO ([BS-TEMPO] = 20 m mol L^{-1})

***Polymerization* Rate R_p.** According to eq 4, the polymerization rate $R_p = k_p [P^*][M]$ is independent of [P-X], being equal to that of the thermal (adduct-free) system. This has been verified experimentally, as Figure 1 shows.[4] The deviations observed at high conversions are ascribed to changes in k_t (changes in viscosity).

Equilibrium Constant K. The same styrene/PS-TEMPO system as was dilatometrically studied in Figure 1 was in situ followed by ESR to determine the concentration of free TEMPO as a function of time. The result was combined with the dilatometrically estimated [P*] with k_p = 2300 L mol^{-1} s^{-1} (125 °C), yielding K = 2.1 x 10^{-11} mol L^{-1}, independent of time.[4]

Dissociation Rate Constant k_d. Styrene was polymerized in the presence of a PS-TEMPO adduct and the initiator *t*-butylhydroperoxide (BHP). In this condition, a dissociated PS radical will undergo propagation until it is recombined with TEMPO, and hence it should be distinguishable from the never-dissociated species by use of GPC. BHP plays the role of capturing free TEMPO, thereby helping the chain propagate longer so that the GPC analysis becomes easier. This idea in fact worked, as shown in Figure 2. The concentration of the never-dissociated species, determined in an absolute manner independent of the grown components, was found to be first order in itself, giving $k_d = A \exp(-E/RT)$ with A = 3.0 x 10^{13} s^{-1}

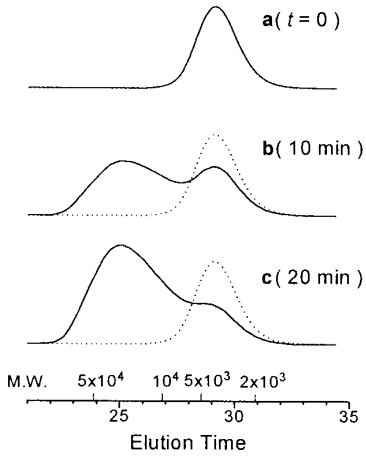

Figure 2 GPC charts for the styrene/BHP/PS-TEMPO(M_n = 2300, M_w/M_n = 1.14) mixture heated at 120 °C for varying times: [PS-TEMPO] = 18 m mol L^{-1}; [BHP] = 20 m mol L^{-1}.

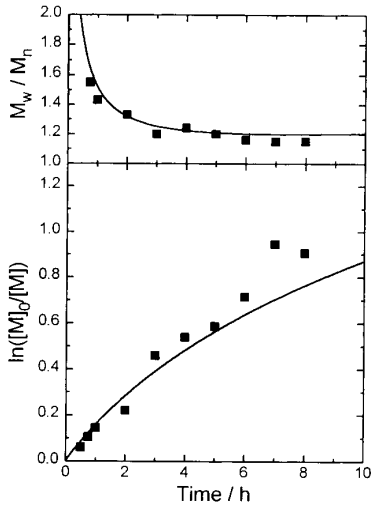

Figure 3 Plot of $\ln([M]_0/[M])$ and M_w/M_n vs. polymerization time for the styrene/BS-TEMPO/125°C system with [BS-TEMPO] = 50 m mol L^{-1} (cf. Caption to Figure 1): (❑) measured; (—) simulated.

and E = 124 kJ mol^{-1}.[5] The k_d value thus determined was independent of [BHP], which indicates that the degenerative transfer to the alkoxide is not a main mechanism of the controlled polymerization in this system.

Thermal Decomposition of the Alkoxide. The 1-phenylethyl adduct with TEMPO (S-TEMPO) thermally decomposes through the β-H abstraction to give styrene and the hydroxyamine.[6] We have made an NMR study to examine the decomposition of a PS-TEMPO (M_n = 1100, M_w/M_n = 1.03) according to a similar mechanism and evaluated the first-order rate constant of decomposition as $k_{dec} = A' \exp(-E'/RT)$ with A'= 5.7 x 10^{14} s^{-1} and E' = 153.3 kJ mol^{-1}. This result indicates that in the TEMPO-mediated polymerization of styrene, the decomposition of the active chain-end would occur less seriously than implied by the experiment with S-TEMPO.[6]

Computer Simulation. We have carried out a computer simulation on a styrene/BS-TEMPO/125°C system, for which all the main parameters are known including k_d, k_c (= k_d/K), k_{dec}, $k_p/k_t^{1/2}$, k_p, and k_i (the 3rd-order thermal initiation rate constant). The result predicts that the stationary state with both [P*] and [X*] will be reached in about 5 min for [BS-TEMPO] = 5.0 x 10^{-2} mol L^{-1}, for example. Figure 3 gives the time dependence of $\ln([M]_0/[M])$ and M_w/M_n of the same system. The experimental data are well reproduced by the simulation *without any adjustable parameters*. A main cause of the rather small deviations is the neglect of the conversion dependence of k_t in the simulation. The postulated mechanisms of the TEMPO-controlled polymerization of styrene are thus confirmed.

References

1 Solomon, D.H. et al., *U.S. Patent* 4,581,429.
2 Georges, M. K. et al., *Macromolecules* **1993**, *26*, 2987.
3 Fukuda, T. et al., *Chemistry Lett. (Tokyo)* **1996**, 293.
4 Fukuda, T. et al. *Macromolecules* **1996**, *29*, 6393.
5 Goto, T. et al., *Polym. Prepr., Jpn* **1996**, *45*, 1261.
6 Li, I. et al., *Macromolecules* **1995**, *28*, 6692.

Application of Solid-State and High-Pressure Reactions for Fullerene Derivatization and CO_2 Activation

Koichi Komatsu, Guan-Wu Wang, Yasujiro Murata,

Sadayuki Mori and Kiyoshi Kudo

Under the solid-state reaction conditions, a nucleophilic addition of organozinc reagent occurs on fullerene C_{60} to give a monoadduct together with a bisadduct and a cyclopropanofullerene. Surprisingly, the fullerene C_{60} also undergoes a clean [2+2] type dimerization by the action of KCN or Mg powder under the similar reaction conditions. The fullerene dimer thus obtained is the very first example of $(C_{60})_2$, and its structure has been determined by the X-ray crystallography. The use of high pressure (5000 atm) was also shown to be advantageous for a liquid-phase [4+2] cycloaddition of C_{60}. The high-pressure reaction of CO with supercritical CO_2 has been found to effect the C-C bond formation affording an oxalate salt in good yield in the presence of Cs_2CO_3.

Keywords: C_{60} / solid-state-reaction / cyclodimerization / organozinc reagent / supercritical CO_2 / CO

The use of extraordinary reaction conditions can sometimes bring about unique results which are hardly attainable by other methods. Here we report typical such examples recently obtained in our research group.

(1) A Solid-State Reformatsky-type Reaction of Fullerene C_{60} [1].

The chemical functionalization of fullerene C_{60} has been the subject of intensive research both from the academic standpoint and for exploring the applicability of this new carbon allotrope as functional materials. However, the researchers are often confronted with the extremely low solubility of C_{60} in common organic solvents. In order to circumvent such difficulty, we explored a novel method of reacting C_{60} with nucleophiles without any solvent.

As a typical example of Reformatsky-type reaction, a mixture of C_{60}, Zn powder, and ethyl bromoacetate (in a molar ratio of 1:20:5) was placed in a stainless-steel capsule of a vibrating mixer containing a stainless-steel mixing ball under nitrogen. The mixture was vigorously agitated for 20 min at room temperature, treated with toluene-CF_3CO_2H, and separated by chromatography to give adduct 1 in 63% yield

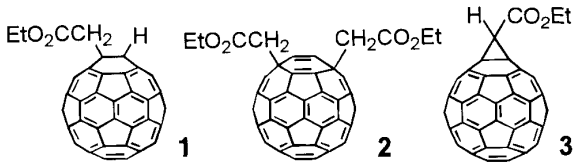

ORGANIC MATERIALS CHEMISTRY —High-Pressure Organic Chemistry—

Scope of Research

Fundamental studies are being made for creation of new functional materials with novel structures and properties and for utilization of high pressure in organic synthesis. The major subjects are: synthetic and structural studies on novel cyclic π-systems; chemical transformation of fullerene C_{60}; utilization of carbon monoxide and dioxide for organic synthesis under the transition-metal catalysis.

Prof KOMATSU Koichi (D Eng)

Instr MORI Sadayuki (D Eng)

Instr KUDO Kiyoshi (D Eng)

Instr NISHINAGA Tohru (D Eng)

Techn YASUMOTO Mitsuo

Assoc Instr TANAKA Toru

Guest Res Assoc
WANG, Guan-Wu
STAHR, Helmut

Students
MURATA, Yasujiro (DC)
KAWAMURA, Tetsu (MC)
TAKATA, Yuki (MC)
MATSUURA, Akira (MC)
NAKAYAMA, Hideaki (MC)
IZUKAWA, Yoshiteru (UG)
KOIZUMI, Satoshi (UG)
TAKAHASHI, Masayo (UG)
TERAUCHI, Hidenori (UG)
FUJIWARA, Koichi (RS)

based on consumed C_{60} together with minor products **2** and **3**. All the products were fully characterized by ^{1}H and ^{13}C NMR, IR, UV-vis, and MS spectra.

Preliminary experiments showed that a Grignard reagent can be prepared and can react with C_{60} under similar conditions.

(2) The First Synthesis of Fullerene Dimer $(C_{60})_2$ [2] .

The all-carbon fullerene polymers are quite promising as new carbon materials. However, there has so far been absolutely no experimental evidence for the all-carbon fullerene dimer, which should be an important structural unit of these polymers.

When we conducted the solid state reaction of C_{60} with KCN under the similar conditions as above, new C_{60} dimer **4** was isolated for the first time, in 60% yield based on consumed C_{60}, instead of a cyano derivative. The same dimer was similarly obtained by the reaction of C_{60} with magnesium powder albeit in a lower yield (6%).

Dimer **4** is a dark brown crystal, which is hardly soluble in most of the organic solvents except *o*-dichlorobenzene (ODCB). The structure of **4** was assigned first based on the ^{13}C NMR spectrum exhibiting 16 signals in the sp^2-carbon region and one signal (δ 76.22) in the sp^3-carbon region, and on the UV-vis spectrum (λ_{max} 328, 434, and 698 nm).

The structure was decisively determined by X-ray crystallography for a single crystal grown from ODCB. As shown in Figure 1, dimer **4** is composed of two C_{60} cages sharing a cyclobutane ring.

Reflecting the elongation of the linking bond between two C_{60} cores (1.575(7) Å), dimer **4** readily dissociates into two C_{60} molecules by heating at 175 °C for 15 min. This dissociation was also observed upon electrochemical reduction as examined by cyclic voltammetry and differential pulse voltammetry. This facile formation of **4** will open up the way to the fundamental study on the nature of fullerene polymers.

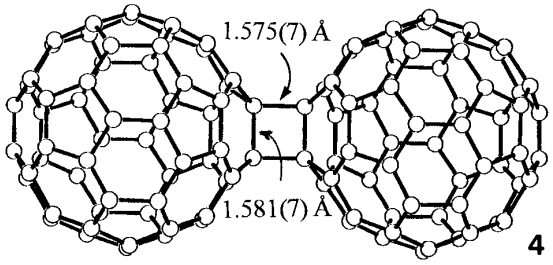

Figure 1. X-Ray crystal structure of the first fullerene dimer **4**. The crystallography was conducted by Dr. Motoo Shiro of Rigaku Corp.

Another reaction under extraordinary conditions, i.e. a liquid-phase high-pressure reaction (5000 atm), was also found to be advantageous for cycloaddition of C_{60} leading to the adduct such as **5** [3].

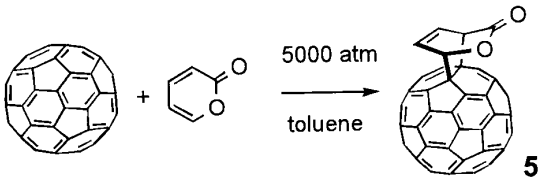

(3) Novel C-C Bond Formation between CO and Supercritical CO_2 in the Presence of Cs_2CO_3.

The efficient utilization of carbon dioxide is one of the most important issues of today, both from the chemical and environmental viewpoints. We found that a reaction of pressurized CO with CO_2 affords oxalate salt **6** in high yield in supercritical CO_2 in the presence of Cs_2CO_3.

As a typical example, **6** was obtained in 90% yield (based on charged Cs_2CO_3) after the reaction for 2 h at 380 °C under 50 atm of CO and 110 atm of CO_2 (0.28 mol) in the presence of Cs_2CO_3 (4.5 mmol) in a glass-lined autoclave (20 ml) with shaking.

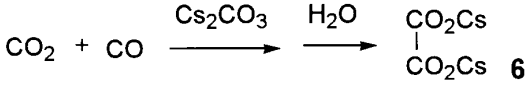

Based on results of various control experiments including ^{13}C labeling, it was unambiguously proven that the present C-C formation occurs by way of the reductive capture of CO_2 with CO in which Cs_2CO_3 is playing a crucial role [4].

On the other hand, the action of methanol in place of CO under the similar reaction conditions as above effected the formation of HCO_2Cs (135%), H_2 (715%), and CO (463%), thus demonstrating further applicability of supercritical carbon dioxide.

References

1. Wang G-W, Komatsu K, Murata Y and Wan T S M, *Chem. Commun*., 2059 (1996).
2. Komatsu K, Wang G-W, Murata Y and Shiro M, *Nature*, in press (1997).
3. Mori S, Karita T, Komatsu K, Sugita N and Wan T S M, *Synth. Commun*., in press (1997).
4. Kudo K, Ikoma F, Mori S, Komatsu K and Sugita N, *J. Chem. Soc., Chem. Commun*., 633 (1995).

Recent Developments in the Main Group Element Chemistry

Kohei Tamao, Akio Toshimitsu, and Shigehiro Yamaguchi

Some recent advances in the main group element chemistry, especially in the organosilicon chemistry and the organoselenium chemistry, are described herein as follows: (1) Asymmetric intramolecular hydrosilation yielding an optically pure spirosilane with axial chirality, (2) high electron-transporting abilities of new silole π-conjugated compounds, and (3) effective steric protection of the selenium atom of the episelenonium ion intermediate.

Keywords: Spirosilanes / Asymmetric intramolecular hydrosilation / Silole / Electron-transporting materials / Organic electroluminescent devices / Episelenonium ion / 2,4,6-Tri-*tert*-butylphenyl group

1. Axially Chiral Spirosilanes via Catalytic Asymmetric Intramolecular Hydrosilation [1].

Chiral spiranes having axially chirality are of special interest due to their rigid chiral environments of C_2 symmetry by perpendicularly arranging two planes. The spiranes would thus be promising chiral building units for material science, especially for chiral macromolecules such as molecular squares and polymers with main-chain chirality. However, there is only a limited number of optically pure spiranes available, because optical resolution has been the only methodology to attain them. To the best of our knowledge, asymmetric syntheses of the axially chiral spiranes have rarely been reported. We now report the first catalytic asymmetric synthesis of an axially chiral spirane of C_2 symmetry.

As the chiral spirane, we have designed a 5-silaspiro[4.4]nonane derivative **1** having a silicon atom on the

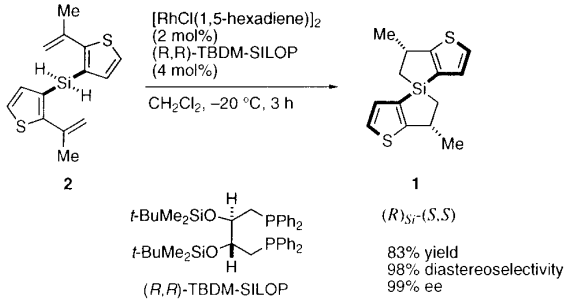

spiro center and two thiophene rings fused with the spiro[4.4]nonane skeleton. The spirosilane **1** has been successfully prepared via a Rh(I)-catalyzed intramolecular hydrosilation of bis(alkenyl)dihydrosilane **2**. The intramolecular hydrosilation of **2** would proceed sequentially in two steps: The first step involves a diastereotopic group selection and diastereotopic face selection, producing a chiral

SYNTHETIC ORGANIC CHEMISTRY —Synthetic Design—

Scope of research

(1) Synthesis, structural studies, and synthetic applications of organosilicon compounds, such as pentacoordinate silicon compounds, functionalized silyl anions, and functionalized oligosilanes. (2) Design and synthesis of novel π-conjugated polymers containing silacyclopentadiene (silole) rings, based on new cyclization reactions and carbon-carbon bond formations mediated by the main group and transition metals. (3) Chiral transformations and asymmetric synthesis via organosulfur and selenium compounds, especially via chiral episulfoniu and episelenonium ions.

Prof
TAMAO
Kohei
(D Eng)

Assoc Prof
TOSHIMITSU
Akio
(D Eng)

Instr
KAWACHI
Atsushi
(D Eng)

Instr
YAMAGUCHI
Shigehiro
(D Eng)

SUN, Guanri (Guest Scholar)
JIN, Ren-Zhi (Guest Scholar)
ASAHARA, Masahiro (DC)
TANAKA, Yoko (DC)
OHNO, Shigeki (MC)
DOI, Noriyuki (MC)
ISHII, Hiroyuki (MC)
TERADA, Masayoshi (MC)
ITAMI,Yujiro (UG)
MITSUDO, Koichi (UG)

center on the silicon atom as well as on a carbon atom. The second intramolecular hydrosilation is a simple diastereotopic face selection of the remaining olefin to carry the third chiral center on the carbon atom. In total, three pairs of enantiomers are possible. The asymmetric intramolecular hydrosilation in the presence of a Rh(I) complex with (*R*,*R*)-SILOPs, which have now been introduced by us as new C_2 symmetry chiral bidentate ligands, have afforded one of the six enantiomers as the major product with high diastereoselectivities up to 98 % and high enantiomeric excesses up to 99 %.

2. Silole Derivatives as Efficient Electron Transporting Materials [2].

Organic electroluminescent (EL) devices, generally composed of thin multilayers of hole transporting (HT), emissive, and electron transporting (ET) materials sandwiched between two electrodes, are enjoying a great deal of interest because of their possible application as large-area flat panel displays. One of the major current subjects in this field is the development of efficient ET materials. Here, several new 2,5-di(aryl)silole derivatives having 3-methylphenyl (PSP), 2-pyridyl (PYSPY), 5-*tert*-butyldiphenylsilyl-2-thienyl (SiTSTSi), and bithienyl (TTSTT) as aryl groups have been examined as electron transporting (ET) materials for thin multilayer organic electroluminescent devices. The silole

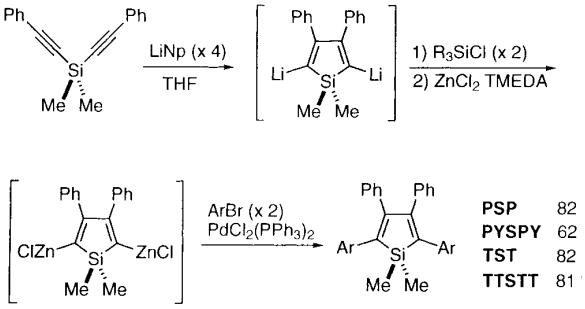

derivatives have been prepared in one pot starting from bis(phenylethynyl)silane based on an intramolecular reductive cylization promoted by lithium naphthalenide, followed by a palladium-catalyzed coupling reaction with appropriate aryl halides. Among these silole derivatives, PYSPY shows the highest ET ability, which also exceeds that of tris(8-hydroxyquinoline)aluminum (Alq), one of the best ET materials. Three other silole derivatives are found to act as emissive ET materials, emitting greenish-blue to reddish-orange lights with the colors being tuned with the aryl groups.

3. Steric Protection of the Selenium Atom of the Episelenonium Ion Intermediate To Prevent both the Racemization of the Chiral Carbon and the Selenophilic Attack of Carbon Nucleophiles [3].

Organic reactions *via* the three-membered cyclic episelenonium ion intermediate have been widely used in organic syntheses. Still, two basic drawbacks of the episelenonium ion intermediate have remained to be solved. Thus, in the episelenonium ion intermediate bearing a phenyl group on the selenium atom, (1) a chiral carbon present in the three-membered ring racemizes quite readily during reactions and (2) carbon nucleophiles such as ketene silyl acetals attack the selenium atom selectively rather than the carbon atom to give no carbon–carbon bond formation products. We have found that these drawbacks are both overcome by the steric protection of the selenium atom by 2,4,6-tri-*tert*-butylphenyl (TTBP) group.

Our strategy is based on our observation that the rate of racemization of the chiral carbon in the episelenonium ion intermediate is highly dependent on the concentration of the substrates, the arylseleno-substituted alcohol, indicating that the racemization is induced by the selenophilic attack on the selenium atom of the intermediate by the alcohol.

In fact, as shown in below, chiral alcohol bearing the TTBPSe group on the adjacent carbon atom was found to react with carbon nucleophiles such as alkenyl silyl ethers, trimethylsilyl cyanide, and allyltrimethylsilane in the presence of Lewis acid to afford the carbon–carbon bond formation products in satisfactory yields without loss of optical purity.

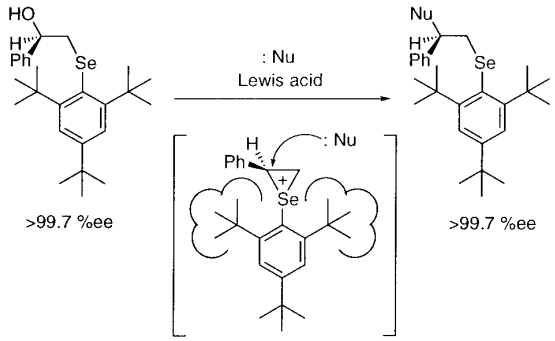

References

1. Tamao K, Nakamura K, Ishii H, Yamaguchi S and Shiro M, *J. Am. Chem. Soc.*, **118,** 12469 (1996).
2. Tamao K, Uchida M, Izumizawa T, Furukawa K and Yamaguchi S, *J. Am. Chem. Soc.*, **118**, 11974 (1996).
3. Toshimitsu A. Nakano K. Mukai T. and Tamao K. *J. Am. Chem. Soc*., **118**, 2756(1996).

Memory of Chirality: Direct Asymmetric α-Alkylation of Phenylalanine Derivatives

Takeo Kawabata, Thomas Wirth, Kiyoshi Yahiro, Hideo Suzuki, and Kaoru Fuji

The (*S*)-phenylalanine derivative 1 was treated with lithium 2,2,6,6-tetramethylpiperidide and then with methyl iodide at -78 °C to afford **3** in 82% ee without addition of any external chiral source. The asymmetric methylation reaction proceeded with retention of configuration.

Keywords: Asymmetric synthesis/ Amino acid/ Alkylation

Asymmetric synthesis of a-substituted α-amino acids has attracted considerable attention because of the biological and chemical importance of these compounds.[1] One of the most efficient methods for their synthesis has been *via* enolate chemistry utilizing chiral auxiliaries. However, it would be even more efficient if direct α-alkylation of the enolates generated from optically active α-amino acids could proceed enantioselectively without using any external chiral source. This has not been possible due to the loss of chirality at the α-carbon of α-amino acids in the corresponding enolates due to their achiral nature. However, enolates generated from optically active α-amino acids are not always achiral, according to the concept of *memory of chirality*, which we recently proposed.[2] In searching for conditions under which enolates are chiral, we discovered that optically active *N*-methyl-*N*-Boc-phenylalanine derivatives can undergo direct asymmetric α-alkylation with ee's as high as 82% without the addition of any external chiral source.

Treatment of **1** (>96% ee) with a variety of bases in THF followed by methyl iodide afforded **3**, whose ee was determined as its *N*-benzoyl derivative **4** (Table I). Among the bases screened, lithium 2,2,6,6-tetramethylpiperidide (LTMP) proved to be the most effective for the asymmetric induction (entries 1-4). Asymmetric methylation proceeded with retention of configuration when LTMP or lithium diisopropylamide (LDA) was employed, while inversion of configuration was observed with potassium hexamethyldisilazide (KHMDS). The absolute configuration of **3** was determined by chemical correlation with **5**. The degree of asymmetric induction depended on the amount of LTMP employed (entries 5-9). The best results (82% ee, 40% yield) were obtained when 1.0 eq of LTMP was employed. Increasing the amount of base decreased the efficiency of the asymmetric induction without affecting the yield of **3**. Deuteration of the enolate generated from **1** and 1.1 eq of LTMP was carried out by treatment with D_2O. Recovered **1** (76% yield) contained 51% deuterium and had 76% ee with *S* configuration. If all of the enolate was trapped with

SYNTHETIC ORGANIC CHEMISTRY —Fine Organic Synthesis—

Scope of Research

Fundamental studies are being made for creation of new functional materials with novel structures and properties and for utilization of high pressure in organic synthesis. The major subjects are: synthetic and structural studies on novel cyclic p-systems; chemical transformation of fullerene C60; utilization of carbon monoxide and dioxide for organic synthesis under the transition-metal catalysis

Prof
FUJI,
Kaoru
(D Pharm Sc)

Assoc Prof
TANAKA,
Kiyoshi
(D Pharm Sc)

Instr
KAWABATA,
Takeo
(D Pharm Sc)

Techn
TERADA,
Tomoko

Secretary
TAKEDA, Kyoko
Guest Scholar
POOLSAK, Sahakitpicnan
Guest Research Associate
AHN, Mija; LAKSHMAIAH, Gingipalli; CHEN, Jijun
Students
NAGATO, Minoru (DC); SUZUKI, Hideo (DC); TAKASU, Kiyosei (DC); FURUTA, Takumi (DC); SHANG, Muhong (DC); TSUBAKI, Kazunori (DC); WATANABE, Toshiyuki (DC); ASAKAWA, Naoyuki (MC); KONDOH, Masakatu (MC); WATANABE, Yukari (MC); OHNISHI, Hiroshi (MC); HAMADA, Masaki (MC); MORIYAMA, Shoko (MC); OHTSUBO, Tadamune (UG); TAKAOKA, Hiromi (UG); YAMAMOTO, Kensaku (UG); YOSHIDA, Masato (UG)
Research Fellow
HAMAJIMA, Yoshio; WATANABE, Joshu
Research Student
KOYAMA, Naohisa; NURUZZAMAN,Mohammad

deuterium, deuteration would proceed with retention of configuration in 55% ee. Enolate formation was estimated to be complete in entries 7-9 since the ee of recovered **1** was ~ 50%, whereas enolate formation in entries 5 and 6 was found to be incomplete. When the extent of enolate formation was low, a considerable amount of starting material was recovered (entry **5**). When it was high, on the other hand, formation of side products increased. As a result, a-methylation of **1** proceeded with ~40% yield, irrespective of the extent of enolate formation.

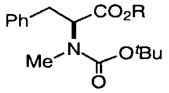

1 : R = Et
2 : R = ^{n}Bu

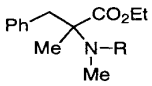

3 : R=$CO_2{}^t$Bu
4 : R=COPh

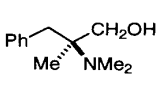

5

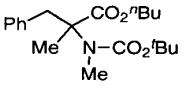

6

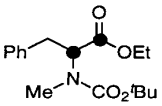

7

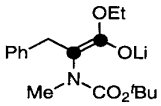

8

Mechanistic aspects of the present asymmetric induction were investigated. Shown in Chart I are plausible intermediates: (**A**) mixed aggregates of the *achiral* enolate with the undeprotonated optically active starting material, (**B**) a configurationally stable carbanion stabilized by the adjacent *N*-Boc group, (**C**) an enolate with chiral nitrogen strongly coordinated with lithium, (**D**) an enolate with a C-N chiral axis in which the steric bulk of the OLi group is increased by coordination with the amine originating from LTMP, and (**E**) an enolate with a chiral plane. To estimate the feasibility of **A**, cross-over experiments between **1** and the butyl ester **2** were done. A 1 : 1 mixture of **1** (96% ee) and racemic **2** was treated with LTMP (1.0 eq to the total amount of **1** and **2**) at -78 °C followed by addition of methyl iodide at the same temperature to afford optically active **3** (74% ee, 26% yield) and racemic **6** (30% yield). The same treatment of a 1 : 1 mixture of racemic **1** and optically active **2** (96% ee) afforded racemic **3** (17% yield) and optically active **6** (71% ee, 24% yield). These observations clearly indicate that **A** does *not* make a significant contribution to the asymmetric induction.

Table 1. Asymmetric α-Methylation of **1**.[a]

entry	base (eq)	yield of **3**	ee of **4**[b]	recovered **3**	
				yield	% ee[c]
1	LTMP (1.1)	38	79 (*S*)	23	87
2	LDA (1.2)	57	22 (*S*)	25	*d*
3	LHMDS (1.2)	0	-	*d*	*d*
4	KHMDS (1.2)	79	20 (*R*)	0	-
5	LTMP (1.0)	40	82 (*S*)	36	92
6	LTMP (1.5)	42	77 (*S*)	17	73
7	LTMP (2.0)	42	73 (*S*)	13	48
8	LTMP (4.0)	36	66 (*S*)	13	54
9	LTMP (6.0)	37	55 (*S*)	22	48

[a]**1** (98% ee) was treated with the base in THF at -78 °C for 15 min followed by methyl iodide at -78 °C for 4 h. [b]Determined by HPLC analysis using Daicel CHIRALPAK AS (3% EtOH/hexane). The letter in the parentheses indicates the absolute configuration. [c]The absolute configuration was S in each entry. Ee was determined by HPLC analysis using Daicel CHIRALPAK AS (3% EtOH/hexane). [d]Not determined.

Chart I

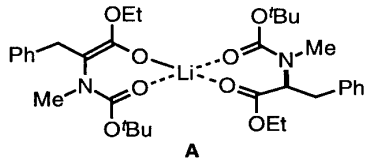

A

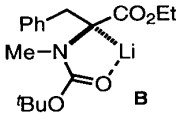

B

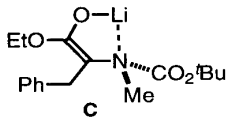

C

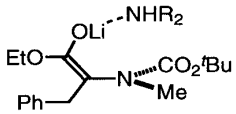

D

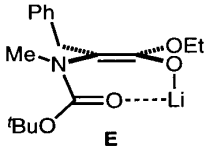

E

The anionic species generated from **1** and LTMP can be expected to contain some chiral information. To examine the structure of the anionic species, the ^{13}C-NMR spectrum was studied on the anionic species generated from [1,2-$^{13}C_2$]-phenylalanine derivative **7** (racemic) with ^{7}Li-LTMP (1.7 eq) in d_8-THF at -78 °C. Although the spectrum measured at this temperature gave complicated and uninterpretable signals, raising the temperature of the solution to 20 °C induced a complete change in the spectrum, in which two doublets now appeared at d 159.9 (J = 115 Hz) and 86.4 (J = 115 Hz). These signals could be assigned to a normal enolate structure **8**. Re-cooling the enolate solution to -78 °C did not lead to significant changes in the spectrum, the major signals of **8** remaining unchanged. Next, we investigated the effects of the observed structural changes caused by temperature variation on the asymmetric a-methylation of **1**. Racemic **3** was obtained in 26% yield when **1** (96% ee) was treated with LTMP (1.0 eq) at -78 °C for 15 min, then at 20 °C for 45 min followed by methyl iodide at -78 °C. Thus, it can be concluded that the initially formed anionic species at -78 °C could memorize the original chiral information, while the achiral enolate **8**, formed after raising the temperature, neither possessed chiral information nor could recall it even when re-cooled to -78 °C. Studies directed toward structure determination of the intermediary anionic species generated from **1** and LTMP at -78 °C are currently under way.

References and Notes

1. a) For examples, see: a) Seebach, D.; Boes, M.; Naef, R.; Schweizer, W. B. J. *Am. Chem. Soc*. **1983**, *105*, 5390. b) Schöllkopf U. *Tetrahedron* **1983**, *39*, 2085.
2. Kawabata, T.; Yahiro, K.; Fuji, K. *J. Am. Chem. Soc.* **1991**, 113, 9694.

Atropisomeric Flavoenzyme Models with a Modified Pyrimidine Ring

Atsuyoshi Ohno, Jun Kunitomo, and Yasushi Kawai

Abstract: Optically active 5-deazaflavin derivatives (3-aryl-10-(4-*tert*-butylphenyl)pyrimido[4,5-*b*]quinoline-2,4(3*H*,10*H*)-dione) with an axial chirality at the pyrimidine ring have been synthesized, and the physical properties of these compounds have been investigated. In addition, (net) hydride-transfer reactions with NAD(P)H analogs have been carried out to elucidate the stereochemistry at the transition state of the reactions.

Keywords: flavin/ axial chirality/ NAD(P)H analog/ (net) hydride transfer/ stereochemistry

Flavoenzymes are the enzymes that require flavin coenzymes such as flavin adenine dinucleotide (FAD) or flavin mononucleotide (FMN) and catalyze redox reactions in biological systems. At the active site of flavoenzymes, flavin coenzymes are covalently bound or tightly held to apoproteins to form chiral environments and polar functional groups of apoproteins in proximity to a flavin coenzyme have a significant influence on stereochemistry in the reactions between the flavin coenzyme and a substrate. Thus, we synthesized atropisomeric flavoenzyme models **1**—**8** and investigated the physical properties and stereochemical reactivities of these models.

We have studied the thermal enantiomerization of **1**—**6** kinetically in order to estimate the conformational stability (1). Although the free energy of activation for thermal enantiomerization decreases in the order R = $Bu^t \gg CF_3 > Pr^i > Et > Me \approx CH_2OH$ due to steric effect, the entropy term does not contribute meaningfully to the energy barrier. Furthermore, the difference in the energy barrier between **1**—**3** is small in spite of the difference in size of the substituent of the aryl group at the N(3) position. This is probably because the benzylic protons of the aryl group face toward the flavin skeleton in order to minimize the steric repulsion, which is supported by the results of X-ray crystallographic analyses of these compounds (1—2).

By comparing the geometry of a flavin molecule in the crystal of **3** with that in the crystal of **3**·urea·ethanol that includes hydrogen bonds to the pyrimidine ring of **3**, we have simulated geometrical change observed when an oxidized flavin coenzyme is activated through hydrogen bonding with apoproteins (3). The result has revealed that when hydrogen bonds to the pyrimidine ring of the flavin are formed, both bond lengths of N(1)—C(10a) and C(4a)—C(5) (which are represented formally by a double bond)

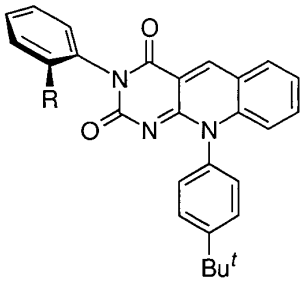

1 : R = CH_2OH
2 : R = CH_3
3 : R = CH_2CH_3
4 : R = $CH(CH_3)_2$
5 : R = $C(CH_3)_3$
6 : R = CF_3
7 : R = CO_2H
8 : R = CH_2OTBDM

BIOORGANIC CHEMISTRY —Bioorganic Reaction Theory—

Scope of research

Biochemical reactions are studied from the viewpoint of physical organic chemistry. Namely, the reaction mechanism and stereochemistry of NAD-dependent oxidoreductases are exploed. Stereospecific redox transformations mediated by certain biocatalists such as microbes, enzymes, cultured tissues are also studied. The results will be applied to develop new organic reactions.


Prof OHNO,Atsuyoshi (D Sc)


Assoc Prof NAKAMURA, Kaoru (D Sc)


Instr KAWAI, Yasushi (D Sc)


Assoc Inst YAMAZAKI, Norimasa


Techn HIRANO, Toshiko

Guest Research Associate:
HORNES, Sander
Students
TSUTSUMI, Akihiro (RF, D Sc)
KINOSHITA, Masamichi (RF, D Sc)
SHIOJI, Kosei (RF, D Sc)
KUNITOMO, Jun (DC)
HIDA, Kouichi (DC)
TAKENAKA, Keishi (DC)
SAITOU, Kentarou (MC)
NAKAGAWA, Toshiya (MC)
INABA, Yoshikazu (MC)
MATSUDA, Tomoko (MC)
ISHIKAWA, Yoshiteru (MC)
FUJII, Mikio (MC); MATSUO, Takashi (MC); DAO, Duc Hai (RS)

become longer by 0.023 Å, whereas that of C(10a)—C(4a) (which is represented formally by a single bond) becomes shorter by 0.021 Å than those in free **1**, respectively. This indicates that the hydrogen bonding at the pyrimidine ring affects the electronic structure of the flavin greatly: the π-electrons in the conjugated system are shifted to the N(1) position through hydrogen bonding with urea so that the geometry of the oxidized flavin can approach to that of its reduced form and that the electron density at the C(5) position is expected to become low.

It is necessary to determine the absolute configurations of these flavoenzyme models to elucidate the stereochemistry at the transition state in the reactions of these models. Thus, we synthesized **9** that was expected to maintain its conformation for a long time and confirmed that the (—)-enantiomer had the *S* configuration from the X-ray crystallographic analysis by means of anomalous dispersion effect of the bromine atoms (2). Next, (*S*)-(-)-**9** was debrominated by catalytic hydrogenation, and the resultant **2** was subjected to HPLC from which its conformation was determined to be (*R*)-(+). Finally, the (+)-**1** was converted into **2**, and the resultant **2** was subjected to HPLC, which confirmed that the compound was the (—)-enantiomer (1). Consequently, the absolute configuration of (+)-**1** has been assigned as *S*. Furthermore, all absolute configurations of **3**—**8** have been determined on the basis of circular dichroism spectra of **1** and **2**.

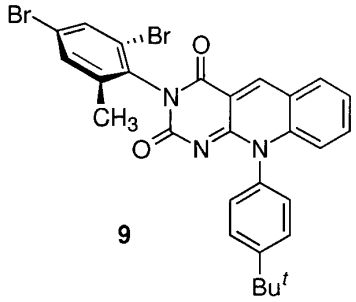

9

In order to investigate the selectivity of the faces in which a (net) hydride is transferred, reductions of several flavoenzyme models (**1**, **2**, **6**, and **8**) with 1-benzyl-1,4-dihydronicotinamide (BNAH) were studied (1,4). In the presence of Mg^{2+}, the (net) hydride transfer from BNAH to **2**, **6**, or **8** takes place predominantly in the *anti* face, whereas the selectivity observed in the reaction of **1** is the opposite of that of **2**, **6**, or **8**. Furthermore, in the absence of Mg^{2+}, the *syn/anti* selectivity is reversed from that observed under the Lewis acid (Mg^{2+})-catalyzed reaction. The association constant of **1** with Mg^{2+} is about twice as large as that of **2**, which predicts that the hydroxymethyl group of **1** in the presence of Mg^{2+} plays a significant role in coordinating onto Mg^{2+} to form a ternary complex with BNAH rigidly in the *syn* face. On the other hand, the hydroxymethyl group in the absence of Mg^{2+} is not different from other substituents such as methyl, trifluoromethyl, and [(*tert*-butyldimethylsilyl)oxy]methyl groups in terms of interaction with BNAH in the sense that it is nothing but a sterically interfering group. Consequently, these substituents result in the deactivative *anti* preference rather than a *syn* face reaction.

In addition, we studied asymmetric (net) hydride-transfer reactions between chiral **1** and chiral 1,4-dihydro-2,4-dimethyl-*N*-(α-methylbenzyl)-1-propylnicotinamide (Me_2PNPH) to elucidate the intermolecular arrangement between **1** and an NAD(P)H analog at the transition state of (net) hydride-transfer reactions (1). The results

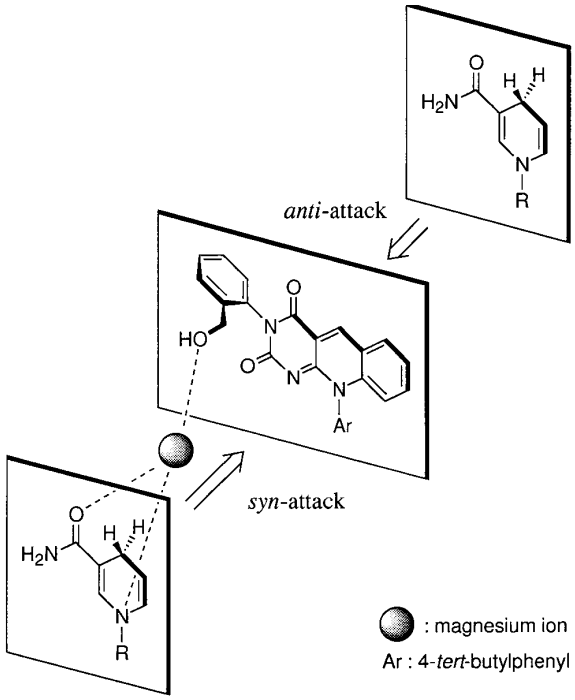

Figure 1. Most predominant intermolecular arrangements between (*S*)-(+)-**1** and an NAD(P)H analog at the transition states of (net) hydride-transfer reactions in the presence (*syn* face) and absence (*anti* face) of magnesium ion, respectively. The conformation of the side-chain carbamoyl group of NAD(P)H analog is drawn arbitrarily.

revealed that the most suitable intermolecular arrangement between **1** and NAD(P)H analog at the transition state of (net) hydride-transfer reactions is the one in which two molecules are arranged with maximum overlap of their molecular planes and the pyrimidine ring of **1** is set in front of the carbamoyl group of the analog, regardless of the presence or absence of Mg^{2+} (Figure 1). The intermolecular arrangement is similar to that reported for FAD and NADPH in the active site of glutathione reductase: the flavin moiety of FAD is stacked onto the nicotinamide ring of NADPH and the pyrimidine ring of the flavin and the carbamoyl group of the nicotinamide face each other. It is of great interest that the intermolecular arrangement can be seen in a model system even though no steric compulsion exists to arrange them in this order.

The present result strongly indicates not only a possibility that there might exist stabilizing effects due to the overlap of molecular planes of a flavin and an NAD(P)H coenzymes but also a possibility that functional groups in an apoprotein in proximity to a flavin coenzyme in the active site of a flavoenzyme have significant influence on the stereoselective interaction with a substrate.

References

1. Ohno A, Kunitomo J, Kawai Y, Kawamoto T, Tomishima M and Yoneda F, *J. Org. Chem.* **61**, 9344-9355 (1996).
2. Kawai Y, Kunitomo J and Ohno A, *Acta Crystallogr., Sect. C*, in press.
3. Kawai Y, Kunitomo J and Ohno A, *Tetrahedron Lett.* **37**, 8905-8908 (1996).
4. Ohno A, Kunitomo J, Kawamoto T, Tomishima M, Bessho K and Yoneda F, *Tetrahedron Lett.* **35**, 9729-9732 (1994).

Metal-Chelating Inhibitors of a Zinc Finger Protein HIV-EP1. Remarkable Potentiation of Inhibitory Activity by Introduction of SH Groups

Masami Otsuka, Mikako Fujita, and Yukio Sugiura

HIV-EP1 is a C_2H_2 type zinc finger protein which binds to DNA kB site present in the long terminal repeat of HIV provirus. Previously we have reported zinc chelators having histidine-pyridine-histidine skeleton and were successful to inhibit the DNA binding of HIV-EP1 by removing zinc from the zinc finger domain. Aiming at the potentiation of the inhibitory activity, we synthesized novel chelators comprising pyridine and aminoalkylthiol. These showed marked inhibitory activity on the DNA binding of HIV-EP1. In particular, one of them having bis(2-mercaptoethyl)amino side chain showed inhibitory activity (IC_{50}, ~4μM), 10 times stronger compared with the strongest inhibitor that we reported previously.

Key words: HIV-EP1 / Zinc finger / Transcription factor / DNA-binding

Zinc finger proteins constitute a major group of transcription factor and play important roles in the gene expression at the terminus of cellular signal transduction. Our interest has been focused on a C_2H_2 type zinc finger protein HIV-EP1 which binds to DNA kB site (5'-GGGACTTTCC-3') present in the long terminal repeat of HIV provirus to activate the HIV-1 gene expression. Inhibition of HIV-EP1 would lead to the interference of the replication of AIDS virus. In the previous ICR Annual Report, we described a new strategy for the inhibition of zinc finger proteins, i. e. removal of zinc from the finger domain by use of chelator. Thus, heterocyclic ligands comprising a dimethylaminopyridine and histidine units such as 1 exhibited remarkable zinc-binding capability and showed marked inhibitory effect on the DNA binding activity of HIV-EP1.

We now intended to replace the imidazole in the inhibitor **1** by mercapto group since mercapto group is contained in all known zinc finger proteins as a key ligating residue. It was considered that replacement of the imidazole moiety of our previous synthetic chelators by a mercapto group would alter the fundament of the metal binding characteristics and hence we prepared novel chelators **2** and **3** and some related sulfur-containing ligands.

Compounds **2** and **3** were found to be easily autoxidized under basic condition, resulting in the formation of disulfides whose main constituents were those assignable to **11** and **12**.

BIOORGANIC CHEMISTRY —Bioactive Chemistry—

Scope of research

The major goal of our laboratory is to elucidate the molecular basis of the activity of various bioactive substances by biochemical, physicochemical, and synthetic approaches. These include studies on the mechanism of sequence-specific DNA cleavage by antitumor or carcinogenic molecules, probing the DNA fine structure by various chemicals, studies on the DNA recognition of zinc-finger proteins, construction of artificial restriction enzyme, and model study on the cooperative mechanism of DNA binding by dimeric peptides. Also studied are the design and synthesis of functional molecules that effectively regulate the intracellular signal transduction or that applicable to fluorescence detection of DNA.

Prof
SUGIURA, Yukio
(D Pharm Sci)

Assoc Prof
OTSUKA, Masami
(D Pharm Sci)

Instr
MORII, Takashi
(D Eng)

Assoc Instr
OKUNO,Yasushi

StudentsNAGAOKA, Makoto (DC)
AIZAWA, Yasunori (DC)
INOUE, Teruhiko (DC)
KUBOTA, Naoki (MC)
SAWADA, Mamoru (MC)
YASOSHIMA, Kenichi (MC)
ARAKI, Michihiro (MC)
KAMIUCHI, Tatsuya (MC)
SASAKI, Daisuke (MC)
YOKONO, Masanori (MC)
SAEGUSA, Nana (UG)
SUZUKI, Kazuo (UG)
HARA, Yuji (UG)
MATSUSHITA, Keizo (RS)

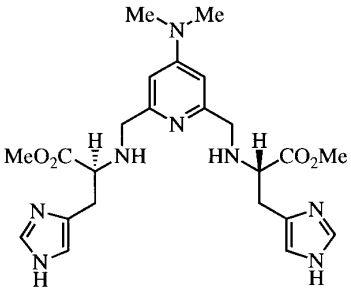

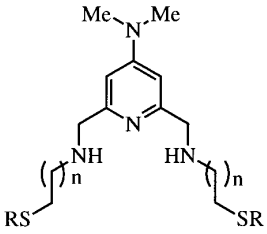

2 R = H, n = 1
3 R = H, n = 2
4 R = *t*-Bu, n = 1
5 R = *t*-Bu, n = 2
6 R = Trt, n = 1
7 R = Me, n = 1
8 R = Me, n = 2
9 R = S-Nps, n = 1
10 R = S-Nps, n = 2

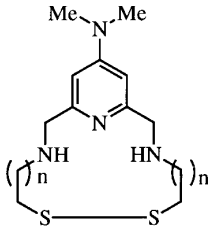

11 n = 1
12 n = 2

We found disulfides **9**—**12** to be stable in air, easy to handle, and quantitatively reducible by dithiothreitol to generate either **2** or **3** in *situ*. Therefore, we employed **9**—**12** as practical equivalents for **2** and **3** in the biochemical experiments described below.

The inhibitory effects of imidazole compound **1**, mercapto compounds **2**, **3**, and alkylthio compounds **4**—**8** on the DNA binding of HIV-EP1 were studied by electrophoretic mobility shift assay. Compound **2** or **3** generated from **9** or **10** was indistinguishable from that obtained from **11** or **12** in terms of the inhibitory activity. Mercapto compounds **2** and **3** exhibited remarkable inhibitory effect much stronger than that of imidazole compound **1**. The most potent was compound **2**, which inhibited DNA binding of HIV-EP1 almost completely at 30 μM concentration, whereas 300 μM of **1** was required for the effective inhibition. IC_{50} of **2** was ~4 μM. Thus, inhibitory activity of compound **2** was shown to be 10 times stronger than that of **1**. *tert*-Butylthio, trirylthio, and methylthio analogues **4**—**8**, and other thiols, e. g. 2-aminoethanethiol, glutathione, and dithiothreitol, showed markedly lowered inhibitory effect at 30 μM concentration. It should be noted that inhibitory effect of 2-aminoethanethiol was small but significant because this constitutes the side chain of the inhibitor **2**, demonstrating the effect of assembling the 2-aminoethanethiol units on a pyridine ring in potentiating the inhibitory activity.

As previously reported, compound **1** was shown to abstract zinc from the zinc finger site of HIV-EP1 because the DNA-HIV-EP1 binding was restored by the addition of zinc before or after the inhibition reaction. In contrast, when zinc was introduced after the DNA binding inhibition reaction with **2** or **3**, virtually no or limited recovery of HIV-EP1-DNA complex was observed. This mechanism of the inhibition, seemingly distinct from that of our previous inhibitors, could be a new clue to the specificity issue to distinguish zinc finger proteins, which is our next subgoal.

References

1. Otsuka M, Fujita M, Sugiura Y, Ishii S, Aoki T, Yamamoto T, Inoue J, *J. Med. Chem.*, **37**, 4267-4269 (1994).
2. Otsuka M, Fujita M, Aoki T, Ishii S, Sugiura Y, Yamamoto T, Inoue J, *J. Med. Chem.*, **38**, 3264-3270 (1995).
3. Fujita M, Otsuka M, Sugiura Y, *J. Med. Chem.*, **39**, 503-507 (1996).

Possible Involvement of Alzheimer Amyloid Precursor Protein and Its Associated Protein Kinase Activity in Signal Transduction Pathway

Kunihiro Ueda, Masayoshi Minakuchi, Terry D. Copeland and Yoshifumi Adachi

Amyloid precursor protein (APP) is one of the major causative agents of Alzheimer's disease and possesses a receptor-like structure with extracellular, single transmembrane, and cytoplasmic domains. To explore the physiological significance of APP in the cell, we focuses on the possible involvement of APP in signal transduction pathways. Using affinity precipitation followed by an *in vitro* kinase assay, we found an APP-associated protein kinase activity in the cytosol/membrane fraction of human cell lines derived from neuroblastoma, glioblastoma, embryo, epidermis, and cervix cancer. The kinase was capable of phosphorylating APP- and/or kinase-associated cellular proteins and of binding to a part of the extracellular domain of APP. The kinase activity was specific for serine residues. These results suggest that APP may function in a form of heteromer with a membrane-spanning receptor-like kinase via binding to the extracellular domain characteristic of other receptor systems.

Keywords: Alzheimer's disease /β/A4 Amyloid precursor protein / Protein interaction / Protein kinase / Phosphorylation / Signal Transduction

Alzheimer's disease is the most prevalent neurodegenerative disease, characterized clinically by progression of memory loss and pathologically by the presence of senile plaques, neurofibrillary tangles, and extensive neuronal loss (1). The major constituent protein (β/A4) of amyloid plaques, which are a hallmark of this disease, is proteolytically derived from the β/A4 amyloid precursor protein (APP). Encoded by a single gene on chromosome 21, APP belongs to a family of alternatively spliced Type I integral transmembrane glycoproteins (Figure 1), the cellular function of which is unknown. After the identification of APP695 (2), which consists of 695 residues, at least 10 isoforms of APP have been identified, resulting from alternative splicing of a single gene. Neurons express high amounts of APP695, while longer APPs (751 and 770), containing a Kunitz-type protease inhibitor (KPI) insert, and those lacking exon 15 (L-APPs) are more abundant in peripheral tissues (1). Genetic studies have revealed that point mutations cosegregate with the disease phenotypes (1). Therefore, structural alterations of APP are thought to be one etiology of the disease, although their molecular mechanisms remain unclear.

As shown in Figure 1, APP structurally resembles a type of cell-surface receptors consisting of a glycosylated extracellular domain with a cysteine-rich region, a single transmembrane

BIOORGANIC CHEMISTRY —Molecular Clinical Chemistry—

Scope of Research

This laboratory was founded in 1994 with the aim of linking biomedical research and clinical medicine. Thus, the scope of our research encompasses the structure/function/regulation of various biomolecules, the pathophysiological significance of divergent bioreactions, the specific abnormalities that cause diseases, and the application of molecular techniques to clinical diagnosis and therapy. Our current interest is focussed on poly(ADP-ribosyl)ation of cellular proteins in relation to carcinogenesis, phosphorylation and NuLS-dependent nuclear localization of proteins related to apoptosis and leukemogenesis, the pathophysiological role of Alzheimer β/A4 amyloid precursor protein (APP) and its associated kinase in signal transduction pathways, the aberrant splicing of the APP gene transcript, and the etiological linkage of Alzheimer's disease to the apolipoprotein ε4 allele.

Prof
UEDA, Kunihiro
(D Med Sc)

Assoc Prof
TANAKA, Seigo
(D Med Sc)

Instr
ADACHI,Yoshifumi
(D Med Sc)

Guest Scholar
STROSZNAJDER, Joanna (Prof, Ph D)
Students
MINAKUCHI, Masayoshi (DC)
ITOH, Taketo (DC)
MATOH, Naomi (DC)
SHO, Toh (DC)
YAMAGUCHI , Hiroshi (UG)
TAKESHITA, Ken (UG)
KITAGAWA, Koichiro (RF)
TAKANO, Emiko (RF)
WILLIAMS, Tyler (RS)

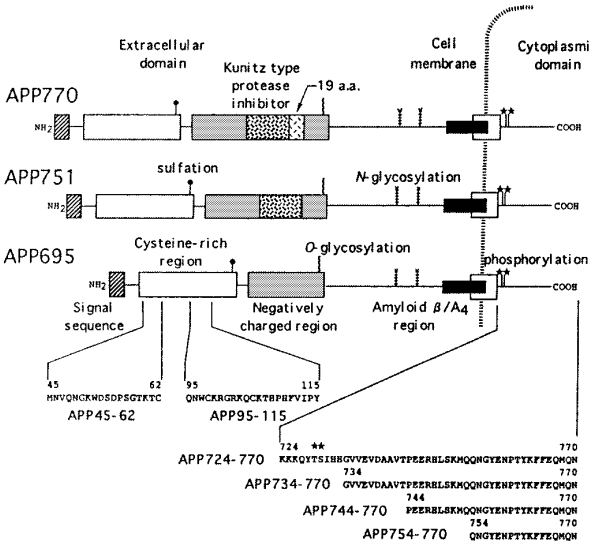

Figure 1. Molecular structure of Alzheimer β/A4 amyloid precursor proteins (APPs). Three major isoforms of APP, APP770, APP751 and APP695, have been identified as a result of alternative splicing of a single gene. The oligopeptides indicated were chemically synthesized using *t*-butoxycarbonyl amino acids and *p*-methylbenzhydrylamine resins, coupled to EAH-Sepharose 4B support by 1-ethyl-3-(3-dimethylaminopropyl)carbodiimido hydrochloride, and used for affinity precipitation followed by *in vitro* kinase assay (5,6).

domain, and a cytoplasmic domain (2). Actually, APP is localized in the cell membrane as an *N*- and *O*-glycosylated form (3). Immunohistochemical studies revealed a patchy and punctate appearance of APP on neurons in rat brain. It has been pointed out that the cytoplasmic domain of APP contains the tetrapeptide sequence, NPTY, which conforms to the consensus sequence, NPXY, required for the rapid endocytosis of the LDL receptor. Subsequently, it has been shown that APP expressed on the cell surface is internalized and delivered to the prelysosomal/lylsosomal branch of the endocytic pathway (3). Ser^{730} and Thr^{729} in the cytoplasmic domain are phosphorylatable

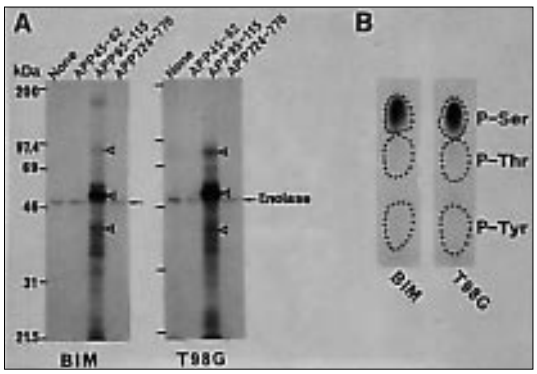

Figure 2. Detection of APP-associated protein kinase activity in human cell lines derived from neuroblastoma (BIM) and glioblastoma (T98G). A, APP peptide-Sepharose beads were incubated with cytosol/membrane fractions from BIM and T98G (6). Recovered affinity complexes on the beads were resuspended in the kinase reaction mixture containing [γ-^{32}P]ATP and exogeneous substrate, enolase, for 10 min at 25°C. After gel electrophoresis, the APP-associated kinase activities were detected by autoradiography. B, phosphoamino acids of proteins phosphorylated by APP-associated kinase were separated by high-voltage electrophoresis and identified by autoradiography (7).

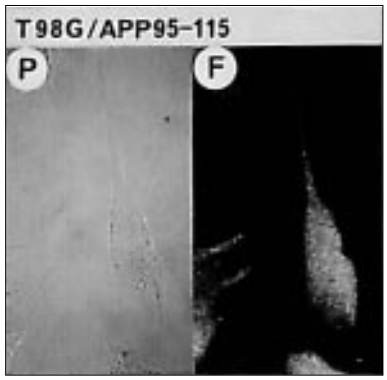

Figure 3. Subcellular localization of APP-associated kinase(s). T98G cells were incubated with fluorescein isothiocyanate-labeled APP95-115 peptide (5). Subcellular localization of the bound peptide (APP-associated kinase) was visualized by fluorescence microscopy (F). The cells were also viewed by phase-contrast microscopy (P).

by protein kinase C and Ca^{2+}/calmodulin-dependent kinase II (1). This phosphorylation might be involved in the regulation of unknown APP function(s) and/or the transduction of unknown signaling(s).

In order to explore the pathophysiological significance of APP, we focuses on the possible involvement of APP in signal transduction pathway. Based on computer analysis of the predicted secondary structures, surface probability, antigen index, flexibility, and hydrophobicity, we synthesized a series of APP peptides for affinity precipitation (Figure 1). By using the affinity precipitation method followed by *in vitro* kinase assay, we discovered an APP-associated kinase activity in the cytosol/membrane fraction from a variety of human cell lines. Figure 2 shows typical data with neuroblastoma cells, BIM, and glioblastoma cells, T98G (4). The APP95-115 sequence in the extracellular domain of APP is a binding site for the kinase or kinase-associated proteins. The APP-associated kinase is capable of phosphorylating APP- and/or kinase-associated protein(s) at serine residues but not tyrosine residues. The kinase requires Mn^{2+} and Mg^{2+} for activation. APP-associated kinase is distributed on the cell membrane (Figure 3). Taken together, we suggest that APP may function in a form of heteromer with a membrane-spanning receptor-like protein with a kinase activity via binding to the extracellular domain as known for other receptor signaling systems.

References

1. Katzman R and Saitoh T, *FASEB J.* **5**, 278-286 (1991)
2. Kang J, Lemaire HG, Unterbeck A, Salbaum JM, Masters CL, Grzeschik KH, Multhaup G, Beyreuther K and Müller-Hill B, *Nature* 325, 733-736 (1987)
3. Weidemann A, König G, Bunke D, Fischer P, Salbaum JM, Masters CM and Beyreuther K, *Cell* **57**,115-126 (1989)
4. Ishii K, Adachi Y, Hatanaka M, Sakamoto H and Furuyama J, *J. Cell. Physiol.* **143**, 569-576 (1990)
5. Adachi Y, Copeland TD, Hatanaka M and Oroszlan S, *J. Biol. Chem.* **268**, 13930-13934 (1993).
6. Kubota S, Adachi Y, Copeland TD and Oroszlan S, *Eur.J. Biochem.* **233**, 48-54 (1995).
7. Adachi Y, Pavlakis GN and Copeland TD, *J. Biol. Chem.* **269**, 2258-2262 (1994).

Mechanism-Based Inactivation of *E.coli* γ-Glutamylcysteine Synthetase by Phosphinic Acid- and Sulfoximine-Based Transition-State Analogues

Makoto Katoh, Jun Hiratake, Hiroaki Kato, and Jun'ichi Oda

On the basis of the proposed reaction mechanisms of γ-glutamylcysteine synthetase, tetrahedral phosphinic acid- and sulfoximine-based compounds **1** and **2** were synthesized and evaluated as inhibitors of *E. coli* γ-glutamylcysteine synthetase. Both compounds inactivated the enzyme in a time-dependent manner with an overall inhibition constant K_i of 4.95 and 0.39 μM, respectively. The enzyme inactivation was observed only when ATP was present, suggesting that the inhibitors are phosphorylated in the enzyme active site, serving as a mechanism-based inactivator. The inhibition potency was 10 and 100 times, respectively, higher than L-buthionine-*SR*-sulfoximine, a well known inhibitor of this enzyme. In particular, the sulfoximine **2** served as an almost irreversible enzyme inactivator with a very slow regain of enzyme activity ($t_{1/2}$ = 3.9 day). This compound may find a potential use as chemotherapeutic agent.

keywords: γ-glutamylcysteine synthetase/ transition-state analogue/ phosphinic acid/ sulfoximine/ time-dependent inactivation/ mechanism-based phosphorylation

Glutathione biosynthesis is mediated consecutively by two mechanistically related ligases, γ-glutamylcysteine synthetase (γ-GCase, EC 6.3.2.2) and glutathione synthetase (EC 6.3.2.3). The design and synthesis of specific inhibitors of these physiologically important enzymes are of critical importance for the development of therapeutic agents as well as for use as mechanistic and physiological probes in glutathione metabolism (1). Following the success in determining the three dimensional structure of glutathione synthetase (2) and in developing and characterizing a specific inhibitor of this enzyme (3), we started the program for the design and synthesis of transition-state analogue inhibitors of γ-GCase, which is a physiologically more relevant enzyme regulating the glutathione biosynthesis. The reaction catalyzed by γ-GCS is thought to proceed *via* the initial formation of an acyl phosphate intermediate followed by nucleophilic attack of cysteine to yield γ-Glu-Cys, ADP and

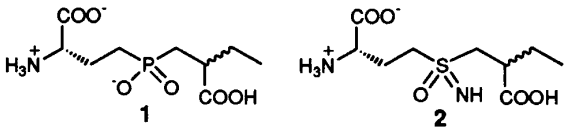

MOLECULAR BIOFUNCTION —Functional Molecular Conversion—

Scope of research

Our research aims are to elucidate structure-function relationships of biocatalysts in combination with organic chemistry, molecular biology and X-ray crystallographic technique, and to design and generate a novel biocatalysts for use as a tailor-made catalyst for organic reactions. Major subjects are (1) X-Ray diffraction analysis of asparagine synthetase, (2) Design and synthesis of transition-state analogue inhibitors of ATP-dependent synthetases, (3) Time-resolved X-ray crystallographic study of glutathione synthetase, (4) Characterization of an activation protein of Pseudomonas lipase, and (5) Design and preparation of catalytic antibodies for chemiluminescence.

Prof
ODA, Jun'ichi
(D Agr)

Assoc Prof
HIRATAKE, Jun
(D Agr)

Instr
KATO, Hiroaki
(D Agr)

Instr
TANAKA, Takuji
(D Agr)

NAKATSU, Toru (DC)
SHIBATA, Hiroyuki (DC)
AOYAGI, Amane (DC)
KATOH, Makoto (DC)
SAWA, Masaaki (DC)
YAMASHITA, Atsuko (DC)
TANOUE, Shintaro (MC)
HISADA, Hiromoto (MC)
IRIE, Takayuki (MC)
OOKI, Yasushi (MC)
KOIZUMI,Mitsuteru (MC)
TOKUTAKE, Nobuya (RF)

inorganic phosphate. According to this proposed reaction mechanism, we designed the phosphinic acid- and sulfoximine-based transition-state analogues **1** and **2**, in which the γ-carboxyl group of L-Glu was replaced by tetrahedral phosphorus and sulfur atom, respectively, and the attacking cysteine moiety was mimicked by α-ethylpropionic acid. Diastereomeric mixture of **1** and **2** were synthesized from a vinylglycine derivative and homocystine, respectively (4).

Both phosphinate **1** and sulfoximine **2** were found to serve as potent inactivators of *E. coli* γ-GCS. Treatment of γ-GCS with varying concentration of **1** or **2** in the presence of ATP caused a time-dependent inactivation of the enzyme (Figure 1).

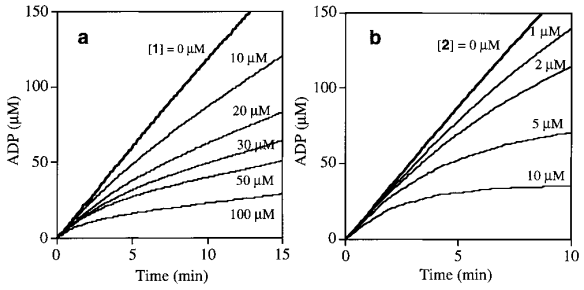

Figure 1. Progress curves for the inactivation of γ-GCS by (a) phosphinate **1**, and (b) sulfoximine **2**. The reaction was initiated by adding the enzyme to an assay mixture containing L-Glu (0.75 mM), L-2-aminobutyric acid (150 mM), ATP (1 mM), $MgSO_4$ (10 mM) and **1** (10-100 μM) or **2** (1-10 μM) in 0.1 M Tris-HCl (pH 7.5) at 37°C.

The shape of the progress curves represents a typical slow binding inhibition as observed with the inhibition of glutathione synthetase by a phosphinic acid transition-state analogue (3). Table 1 depicts the extent of inhibition, the second order rate constants for time-dependent inhibition (k_{inact}/K_i), and the overall dissociation constants (K_i*) obtained from the steady-state reaction rates after the binding equilibrium was reached. For comparison, the inhibition by sulfone **3** and L-buthionine-*SR*-sulfoximine (L-BSO), a well known inhibitor of this enzyme (5), was also examined.

Table 1. Inhibition of *E. coli* γ-glutamylcysteine synthetase

Compound	Conc. [μM]	% Inhibition[a]	k_{inact} / K_i [$M^{-1}sec^{-1}$]	K_i* [μM]
Phosphinate **1**	5.7	35	436 ± 33	4.95 ± 0.27
Sulfoximine **2**	5.1	98	1206 ± 117	0.39 ± 0.11
L-BSO[b]	25.0	9.7	ND[c]	49.3 ± 7.40
Sulfone **3**	16.3	32	—[d]	9.23 ± 1.76[e]

[a] As measured by steady state inhibited velocities (v_s);
[b] L-Buthionine-*SR*-sulfoximine (Sigma); [c] Not determined;
[d] No time-dependent inhibition was observed; [e] Initial inhibition constant (K_i).

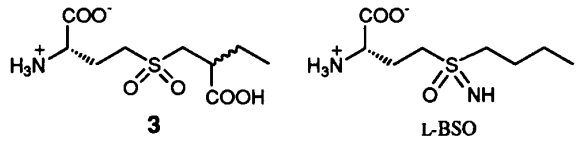

The overall binding of phosphinate **1** and sulfoximine **2** is one and two orders of magnitude greater than that of L-BSO, respectively. In particular, sulfoximine **2** acted as an extremely powerful inactivator: although the sulfoximine **2** is a mixture of eight diastereomers, it inhibited γ-GCS about 126 times more effectively than did L-BSO. Assuming that the sulfoximine **2** contains equal amounts of diastereomers and only one stereoisomer inhibits the enzyme, it could be more than 500 times as effective as an active diastereomer of L-BSO. Both phosphinate **1** and sulfoximine **2** required ATP for enzyme inactivation: Non-hydrolyzable ATP analogue such as 5'-adenylylimidodiphosphate (AMPPNP) failed to cause the inactivation of the enzyme, suggesting a mechanistic scheme involving phosphorylation of the inhibitors by ATP within the enzyme active site (3, 5). This is also supported by the fact that sulfone **3** served as a simple reversible inhibitor. Although sulfone **3** did not cause ATP-dependent inactivation of the enzyme, its inhibition potency was more than five times higher than that of L-BSO as measured by the inhibition constant. The difference is still underestimated because the initial inhibition constant of sulfone **3** (K_i = 9.2μM) is compared with the overall inhibition constant of L-BSO (K_i* = 49μM) where the ATP-dependent tight binding equilibrium was established.

Another criterion relevant to inhibitor potency is the duration of enzyme inactivation. We therefore measured the extent of recovery of enzyme activity upon 1000-fold dilution after the enzyme was completely inactivated with sufficient concentrations of **1** or **2** and ATP. Under a standard assay condition, no regain of enzyme activity was observed with sulfoximine **2**, whereas a significant enzyme reactivation ($t_{1/2}$ < 1 min) was noted with phosphinate **1**. Although the inhibition by sulfoximine **2** was virtually irreversible within the time scale of assay, a very slow regain of enzyme activity was observed ($t_{1/2}$ = 3.9 day) when the inactivated enzyme was gel filtered and incubated in the absence of ATP. Under the same conditions, the enzyme inactivated by L-BSO regained almost 40% of activity immediately after gel filtration. Thus, the inhibition potency of sulfoximine **2** is much higher than L-BSO in terms of both binding affinity and duration of enzyme inactivation. The sulfoximine **2** is a promising candidate for use as a physiological probe and chemotherapeutic agent to cause a long-lasting glutathione depletion in the living organisms.

References

1. Meister, A., Anderson, M. E. *Ann. Rev. Biochem.* **52**, 711 (1983).
2. Kato, H., Tanaka, T., Yamaguchi, H, Hara, T., Nishioka, T., Katsube, Y., Oda, J. *Biochemistry* **33**, 4995-4999 (1994).
3. Hiratake, J., Kato, H. *J. Am. Chem. Soc.* **116**, 12059-12060 (1994).
4. Katoh, M., Hiratake, J., Kato, H., Oda, J. *Bioorg. & Med. Chem. Lett.* **6**, 1437-1442 (1996).
5. Griffith, O. W. *J. Biol. Chem.* **257**, 13704-13712 (1982).

Stereospecificity of Thermostable Ornithine 5-Aminotransferase for the Hydrogen Transfer in the L- and D-Ornithine Transamination

Nobuyoshi Esaki, Tohru Yoshimura, Kenji Soda and Kwang-Hwan Jhee

The thermostable ornithine 5-aminotransferase of a thermophile, *Bacillus* sp. YM-2 is unique in acting on both enantiomers of ornithine, although less effectively on the D-enantiomer. We studied the stereospecificity of the enzyme for the hydrogen abstraction from C-5 of the substrate moiety and the addition and removal of the hydrogen at C-4' of the cofactor (pyridoxal phosphate and pyridoxamine phosphate) moiety of the external Schiff base intermediate in the transamination of L- and D-ornithine. [5-^{3}H]L- and D-ornithines were prepared by incubation of L- and D-ornithines with the *B.* sp. YM-2 ornithine 5-aminotransferase in $^{3}H_2O$, respectively. The C-5 of the tritiated L-and D-ornithine was proved to have the *S*-configuration with L-ornithine 5-aminotransferase of a mesophile, *Bacillus sphaericus*, catalyzing the stereospecific abstraction of pro-*S* hydrogen from C-5 of L-ornithine and amino acid racemase with low-substrate specificity of *Pseudomonas putida* . When apo-form of the enzyme was incubated with pyridoxamine 5'-phosphates that was stereospecifically tritiated at C-4' and 2-oxoglutarate in the presence of L-ornithine or D-ornithine, tritium was released exclusively from (4'*S*)-[4'-^{3}H] pyridoxamine. These results suggest that the *B.* sp. YM-2 ornithine 5-aminotransferase stereospecifically abstracts the pro-*S* hydrogen from C-5 of L- and D-ornithine. The hydrogen abstracted is then transferred to C-4' of the cofactor moiety stereospecifically on the *si* face of the external Schiff base intermediate irrespective of the C-2 configuration of amino donor.

Keywords: Stereochemistry/ Ornithine transaminase/ Pyridoxal phosphate

The pyridoxal phosphate (PLP)-dependent aminotransferase reactions proceed through the abstraction of a hydrogen from the carbon bearing the amino group to be transferred, and the anionic intermediate is formed from the external Shiff base complex of a substrate and a cofactor. The hydrogen abstracted is transferred to C-4' of the cofactor, and consequently the pyridoxamine 5'-phosphate (PMP) form of enzyme and keto acid are produced through the ketimine

MOLECULAR BIOFUNCTION —Molecular Microbial Science—

Scope of research

Structure and function of biocatalysis, in particular, pyridoxal enzymes, NAD enzymes, and enzymes acting on xenobiotic compounds are studied to elucidate the dynamic aspects of the fine mechanism for their catalysis in the light of recent advances in gene technology, protein engineering and crystallography. In addition, the metabolism and biofunction of selenium and some other trace elements are investigated. Development and application of new biomolecular functions of microorganisms are also studied to open the door to new fields of biotechnology. For example, molecular structures and functions of thermostable enzymes and their application are under investigation.

Prof
ESAKI,
Nobuyoshi
(D Agr)

Assoc Prof
YOSHIMURA,
Tohru
(D Agr)

Instr
KURIHARA,
Tatsuo
(D Eng)

Technician: SEKI, Mio; NISHIKAWA, Kumiko;
Guest Scholar:GORLATOV,Sergey;GORLATOVA,Natalia;
Guest Research Associate: GALKIN, Andrey;
Students: KUROKAWA, Youichi (DC); JHEE, Kwang-Hwan (DC); KISHIMOTO, Kazuhisa (DC); GUTTIERREZ, Aldo Francisco (DC); CHOO, Dong-Won (DC); PARK, Chung (DC); LIU, Lidong (DC); MIHARA, Hisaaki (DC); FUCHIKAMI, Yoshihiro(DC); LI, Yongfu (DC); KITTIWORAKARN, Jongrak (DC); WATANABE, Akira (DC); KURONO, Takeshi (MC); MIYAKE, Hitoki (MC); ICHIYAMA, Susumu (MC); UO, Takuma (MC); ENDO, Keiji (MC); NISHIHARA, Mitsuhiro (MC); KULAKOVA, Ludmila (MC); SHIOMI, Kazuo (MC); HIRANO, Yuriko (MC); MAEDA, Masaki (MC); YOSHIMUNE, Kazuaki (MC); SUZUKI, Takeshi (RF); TAKADA, Shin-ichi (RS); BAHK, Song-Chul (RS); DOI, Yousuke

intermediate. Three stereochemical possibilities exist for the hydrogen transfer: the stereospecific transfer on the *si*- or *re*-face, alternatively the non-stereospecific transfer on both faces of the plane of the π-electron system of the intermediate. The stereospecificities of various α-aminotransferases for the hydrogen transfer have been examined. However, no information is available about the stereospecificity of ω-aminotransferases such as ornithine 5-aminotransferase (OAT, EC 2.6.1.13). The stereospecificity reflects the active-site structure of the enzyme, especially the geometrical relationship between the catalytic base of enzyme for the hydrogen transfer and the bound cofactor. Thus, we determined the stereospecificity for the hydrogen transfer catalyzed by the thermostable OAT from *Bacillus* sp. YM-2 (1). The enzyme is unique in acting on both enantiomers of ornithine, although D-ornithine is poorer as an amino donor than the L-enantiomer (2).

In ω-aminotransferase reactions, one of two prochiral hydrogens of the distal carbon is abstracted and transferred to the C-4' of the bound cofactor. At first, we determined the stereospecificity for the hydrogen abstraction from C-5 of L- and D-ornithine catalyzed by the thermostable OAT from *B.* sp. YM-2. When L- and D-ornithines were incubated with the *B.* sp. YM-2 OAT in $^{3}H_2O$, they were tritiated. The specific radioactivities of L- and D-ornithines were 3.9 x 10^{2} and 3.7 x 10^{4} (dpm/mmol), respectively. The rate of the tritium incorporation to D-ornithine was about 1 % of that to L-ornithine. The tritium was probably incorporated into C-5 of L- and D-ornithine. Because, ^{1}H-NMR spectral change of L-ornithine during the incubation with the *B.* sp. YM-2 OAT in $^{2}H_2O$ demonstrated that the enzyme catalyzes the exchange of one of the two hydrogen atoms at C-5 with a solvent deuteron in the half reaction of transamination.

When the L-[5-^{3}H] ornithine prepared was incubated with the *B. sphaericus* OAT which specifically abstracts the pro-*S* hydrogen from C-5 of L-ornithine (3), 78.5 % of the initial radioactivity was released into the solvent. Thus, the C-5 of the tritiated L-ornithine has the *S*-configuration. The tritiated D-ornithine also reacted with the *B. sphaericus* OAT in the presence or absence of the amino acid racemase with low substrate specificity of *Ps. putida* which catalyzes the racemization of ornithine. In the presence of amino acid racemase, 85.6 % of the initial radioactivity was released from the tritiated D-ornithine into the solvent. In contrast, tritium was only little released into the solvent in the absence of the amino acid racemase. The amino acid racemase does not act on C-5 of ornithine. Thus, tritium was abstracted from C-5 of the tritiated D-ornithine, after D-ornithine was converted to the L-enantiomer. These results suggest that the *B.* sp. YM-2 OAT stereospecifically abstracts a pro-*S* hydrogen from C-5 of both D- and L-ornithines.

Then, we studied the stereospecificity of the *B.* sp. YM-2 OAT for the abstraction and addition of hydrogen at C-4' of the cofactor in the half and overall reactions according to the method of Yoshimura et al (4). When (4'*S*)-[4'-^{3}H] PMP or (4'*R*)-[4'-^{3}H] PMP was incubated with the apo-form of the *B.* sp. YM-2 OAT in the presence of 2-oxoglutarate, tritium was exclusively released from (4'*S*)-[4'-^{3}H] PMP into the solvent. Accordingly, the pro-*S* hydrogen at C-4' of PMP is abstracted in the half reaction. Stereospecificities for the abstraction and addition of hydrogen at C-4' of the cofactor in the overall transaminations were also determined with L- and D-ornithines as a substrate. When each enantiomer of the stereospecifically tritiated PMP was incubated with the apo-enzyme and 2-oxoglutarate in the presence of L- or D-ornithine, tritium was released from (4'*S*)-[4'-^{3}H] PMP into the solvent specifically. This suggests that the abstraction and addition of hydrogen at C-4' of the cofactor occur on the *si* -face of the plane of the conjugated π-system of the intermediate in the overall transamination of the *B.* sp. YM-2 OAT irrespective of the C-2 configuration of amino donor.

In the α-transaminase reactions, the intramolecular hydrogen transfer between C-2 of the substrate and C-4' of the cofactor was observed (5). The pro-*S* hydrogen abstracted from C-5 of D- or L-ornithine is probably transferred to the C-4' of PLP on the *si* -face of the planar π-system of the substrate-cofactor complex in the transamination catalyzed by the *B.* sp. YM-2 OAT. The stereospecificity for the hydrogen transfer is not dependent on the configuration of ornithine. The geometrical relationships between the C-5 of L- and D-ornithines and the plane of the π-electron system of the external Schiff base intermediates are the same. The C-2 moiety of D-ornithine is probably bound to the same binding-site as that for L-ornithine.

References

1. Jhee K, Yoshimura T, Esaki N and Soda K, *Biochemistry*, **30**, 9792-9796 (1996)
2. Jhee K, Yoshimura T, Esaki N, Yonaha K and Soda K, *J. Biochem.*, **118**, 101-108 (1995)
3. Tanizawa K, Yoshimura T, AsadaY, Sawada S,Misono H and Soda K, *Biochemistry*, **21**, 1104-1108 (1982)
4. Yoshimura T, Nishimura K, Ito J, Esaki N, Kagamiyama H, Manning J. M. and Soda K, *J. Am. Chem. Soc.*,**115**, 3987-3900 (1993)
5. Gehring H, *Biochemistry* , **23**, 6335-6340 (1984)

Solution X-ray Scattering Study of Reconstitution Process of Tobacco Mosaic Virus Particle Using Low-Temperature Quenching

Yuzuru Hiragi and Yoh Sano

The reconstitution process of tobacco mosaic virus (TMV) was investigated by the solution X-ray scattering measurements with the synchrotron radiation source using low-temperature quenching. TMV assembly in an aqueous solution is completely stopped below 5℃. The TMV assembly was traced by the small-angle X-ray scattering (SAXS) measurements at 5℃ on a series of solutions prepared by low-temperature quenching after incubation either at 15, 20 or 25℃ appropriate interval between 0 and 60 min. The SAXS results were analyzed by the Guinier plot, the Kratky plot and the distant distribution function. In order to account the time course of SAXS profiles in terms of the elongation of TMV assembly, a model calculation was performed by applying Glatter's multibody method. The simulated model functions support the conclusion that the incubation of the RNA and protein of TMV began to reconstitute TMV instantly after mixing, proceeded steeply to a long rod.

Key words: Solution X-ray scattering/ Tobacco mosaic virus/ Reconstitution/ Quenching

Tobacco mosaic virus (TMV) is one of the well-characterized plant viruses, and consists of single stranded RNA long surrounded by a single type of coat protein of subunits. It forms a hollow cylinder of a length 3000Å, inner diameter of 40Å, and an outer diameter of 180Å. The TMV particles can be reconstituted *in vitro* from its constituents under physiological conditions in two steps of nucleation and elongation. Real-time observation of the elongation process of the assembly may be attainable by using time-resolved (TR) small-angle X-ray (SAXS) scattering measurements. Fortunately, TMV assembly in aqueous solution can be stopped below 5℃ (1). If a reaction mixture of TMV-RNA and TMV-protein kept at 25℃ is quenched into ice water, this quenched mixture maintains the assembly as long as it is kept at 5℃. We can trace the TMV reconstitution process by carrying out SAXS measurements on a series of reaction solutions quenched at 5℃ with appropriate time intervals. We refer this method as a low-temperature Quenching. SAXS method is available at the Photon Factory in KEK, Japan.

Tobacco mosaic virus, Japanese common strain OM was

MOLECULAR BIOLOGY AND INFORMATION —Biopolymerstructure—

Scope of research

Our research aims are to elucidate structure-function relationships of biological macromolecules, mainly proteins, by using phisicochemical methods such as spectroscopic and X-ray diffraction methods. The following attempts have been mainly made in our laboratory for that purpose. (1) Peptide secondary or supersecondary structures in aqueous or hydrophobic environments are studied to get a principle of protein architecture, employing various spectroscopic methods. (2) X-ray diffraction studies on protein structures in crystal and in solution are carried out by crystallographic and/or small-angle X-ray scattering techniques to elucidate structure-function relationships of proteins.


Prof
TAKAHASHI
Sho
(D Sc)


Assoc Prof
HATA
Yasuo
(D Sc)


Instr
HIRAGI
Yuzuru
(D Sc)


Instr
FUJII
Tomomi


Assoc Instr
AKUTAGAWA
Tohru

Students
HISANO, Tamao (DC)
MATSUMOTO, Tomoharu (DC)

propagated in inoculated leaves of *Nicotiana tabacum* L. cv Xanthi. Leaves harvested were homogenized with 100 mM phosphate buffer (pH 7.0) containing 0.1% (v/v) thioglycolic acid. The virus was collected by two cycles of differential centrifugation. RNA was isolated by phenol/bentonite extraction; coat protein was isolated by the acetic acid method.

After mixing each 5 ml of RNA and protein solution in a tube at 5℃, the tube was immersed into a thermostat at either temperature of 15, 20, or 25℃. At an appropriate time interval between 0 and 60 min, each 0.5 ml of the reaction solution was subtracted from the tube and was quenched in ice water below 5℃ as quick as possible. The elongation reaction was completely stopped by quenching at 5℃.

SAXS experiments were carried out at 5℃ with the optics and detector system of SAXES installed on the 2.5 GeV storage ring in the Photon Factory, KEK, Tsukuba, Japan. Scattering intensities were registered with wave length of 1.49Å in the range $0.013Å^{-1} < Q < 0.355Å^{-1}$, where Q denotes the amplitude of the scattering vector equal to $4\pi\sin\theta/\lambda$ and 2θ is the scattering angle. Specimen chamber was kept at 5℃ throughout the experiments in order to prevent the elongation reaction. Net scattering intensities were calculated by subtracting the scattering intensities of a blank buffer solution from those of the assembly solution.

The TMV assembly solutions observed contain different degrees of elongation, and thus each radius of gyration Rg evaluated from SAXS measurements corresponds to the z-average radius of gyration Rg,z.

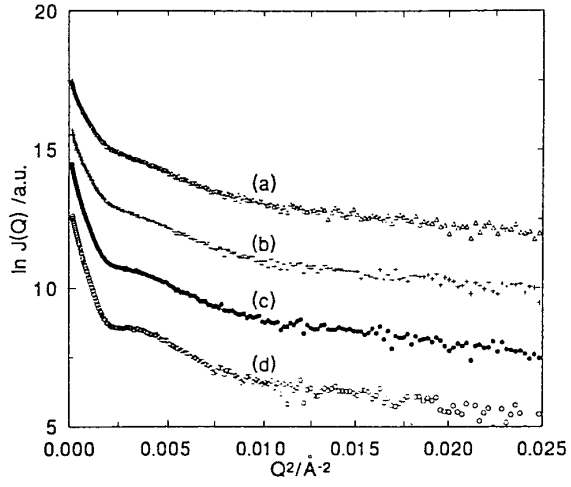

Figure 1. Guinier plots derived from the TMV assembly process. The TMVP solution was quenched at (a) 0 min, (b) 2 min, (c) 8 min, and (d) 25 min after mixing RNA at 20℃.

Fig.1 shows the Guinier plots of a series of TMV assembly samples as an example, quenched at 0, 2, 8 and 25 min after mixing at 20℃. In a low Q range a straight line was depicted in each Guinier plot, and its slope yields Rg,z. An initial slope increases with incubation time at 20℃, and a peak at around $Q^2=0.003Å^{-2}$ becomes steeper. The value of Rg,z(TMVP+RNA) increases more rapidly at 20℃ with the incubation time, compared to that at either 15℃ or 25℃, while the value of Rg,z(TMVP) hardly changes with time.

The Kratky plot is more sensitive than the Guinier plot to the changes in polymer chain configuration. Fig.2 shows the time variation of Kratky plots during TMV assembly at 20℃, where the SAXS data are obtained from the solutions quenched at 1 min, 5 min, 11 min and 25 min. A pronounced increase is observed in the first peak at around $0.002Å^{-1}$, whereas the second peak is almost invariant at about $0.07Å^{-1}$. A similar time variation in the Kratky plots was obtained for the TMV assembly at 15℃ and at 25℃ (data not shown).

Another index is, distant distribution ($p(r)$) function represents a statistical distribution of a pair of points being

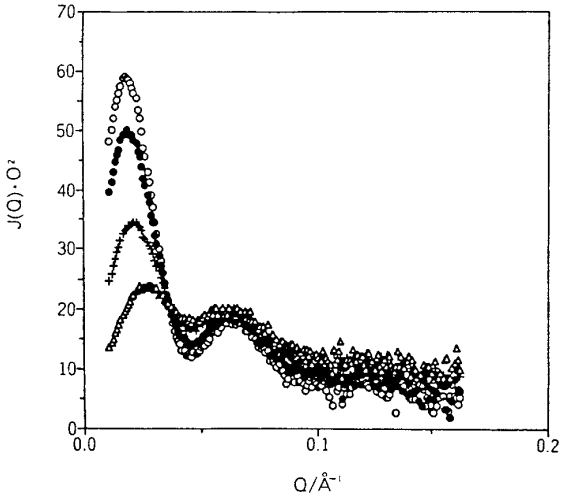

Figure 2. Time variation of the Kratky plots during TMV assembly at 20℃. (Δ) 1 min, (+) 5 min, (●) 11 min and (○) 25 min incubation time.

separated by a distance of rÅ within a molecule. The $p(r)$ function changes with the time during TMV assembly at 20℃ for 1, 5, 11 and 25 min after mixing of TMV-RNA with the protein. A relative ratio of $p(r)$ at around 100Å to that at around 60Å was found to increase gradually with the incubation time. A similar incubation-time dependence in the function was observed during TMV assembly at 15℃ and 25℃ and 25℃ (data not shown).

The results calculated from the SAXS measurements on TMV assembling solutions indicate that at the incubation of TMV-RNA and TMV-protein at 20℃ the reconstitution of TMV starts immediately after mixing, and proceeds fast enough to form a long rod within 10 to 20 min. The full length of TMV particle seems to be formed in 40 to 60 min in this condition. Simulated curves of the Guinier plot, the Kratky plot and the $p(r)$ function from four types of models qualitatively reproduce the experimental curves.

Time course of the Rg,z increases for the TMV assembly system at 20℃ is considerably similar to that obtained from the electron microscopic studies.

The present study proves that low-temperature quenching is useful technique to trace biological phenomena in order of minutes by SAXS or SANS.

References

1. Durham A C H and Klug A, *Nature New Biol.*, **229**, 42-46 (1971).

Analysis of the *Arabidopsis CDC2a* Promoter

Yoshiro Imajuku, Takashi Aoyama, Koji Goto, and Atsuhiro Oka

The eukaryotic cell division cycle is tightly controlled by a class of protein kinases. *Arabidopsis CDC2a* has been considered to encode one of those protein kinases because it is expressed in proliferating tissues and can complement defects in the *cdc2* gene of *Schizosaccharomyces pombe*. The promoter of *CDC2a* was investigated as a first step in exploring the regulation of plant cell proliferation. We found that its transcription is started at the position 677-base-pairs upstream from the *CDC2a* initiation codon. To localize the *cis*-element for proliferating-cell-specific expression, histochemical analysis was done with *β*-glucuronidase fusion genes containing various upstream regions of *CDC2a*. Results from the experiment indicated that a region downstream from the transcription start site is required for the proliferating-cell-specific expression of *CDC2a* and that an upstream region contains a *cis*-element directing transcription during trichome development.

Keywords: Cell cycle/ Transcription start site/ Transgenic plant/ GUS fusion/ Trichome

Proliferation of eukaryotic cells is tightly controlled according to a common cell cycle program. At various points of the cell cycle, specific protein kinase activities are required. Genetic studies of cell division in fission yeast *Schizosaccharomyces pombe* have identified the product of the *cdc2* gene ($p34^{cdc2}$) as a key component of those kinase activities (for reviews, see 1 and 2). $p34^{cdc2}$ is a catalytic subunit of such kinases and its activity is regulated by association with cyclin and post-translational modifications throughout the cell cycle (for reviews see 2-4).

Many genes encoding protein kinases similar to $p34^{cdc2}$ have been cloned from higher plants so far. In *Arabidopsis*, two *cdc2*-related genes, *CDC2a* and *CDC2b*, have been identified (5, 6). Yeast complementation analysis have demonstrated that *CDC2a*, but not *CDC2b*, encodes a functional homolog of $p34^{cdc2}$ (5,6). During plant development, accumulation of *CDC2a* mRNA is correlated with cell proliferation and with increased competence for cell division in certain tissues (7,8). From these facts, transcriptional regulation of *CDC2a* is thought to be closely linked to the regulation under which plant cells are destined to proliferate. In this work, the promoter of *CDC2a* was investigated as a first step in exploring the regulation of plant cell proliferation.

We first determined the transcription start site of *CDC2a*. Total RNA was prepared from seedlings of wild type *Arabidopsis thaliana* (Columbia ecotype) and subjected to primer extension and S1-nuclease mapping. An intense signal band at the position 677-base-pairs (bp) upstream from the

MOLECULAR BIOLOGY AND INFORMATION —Molecular Biology—

Scope of research

Attempts have been made to elucidate structure-function relationships of genetic materials and various gene products. The major subjects are mechanisms involved in signal transduction and regulation of gene expression responsive to environmental stimuli, development of plant leaves and flowers, and plant-microbe interaction. As of December 1996, study is being concentrated on (1) roles of homeodomain proteins and MADS box proteins in developmental processes and transcriptional control in higher plants and (2) contribution of protein phosphorylation and dephosphorylation toward cell cycle control and signal transduction in plants and plant pathogens.

Prof
OKA, Atsuhiro
(D Sc)

Assoc Prof
AOYAMA, Takashi
(D Sc)

Instr
GOTO, Koji
(D Sc)

Assoc Instr
IMAJUKU, Yoshiro

Students
ITAHANA, Koji (DC)
ISHIDA, Norihiro (DC)
TSUKUDA, Mayumi (DC)
HOMMA, Takashi (MC)
OHGISHI, Maki (MC)
SAKAI, Hiroe (MC)
LIANG Ya Jie (MC)
UEDA, Yumi (MC)
YANO, Hiroyuki (MC)

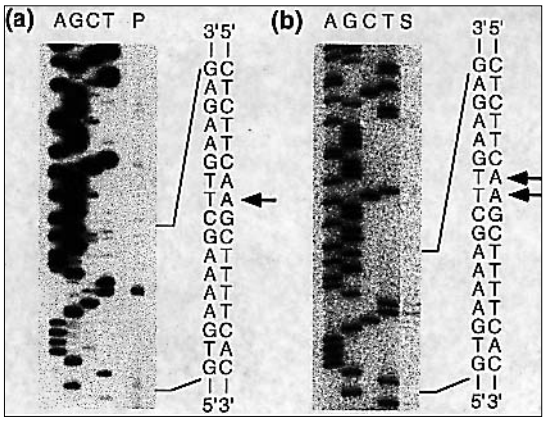

Figure 1. Primer-extension and S1-mapping analyses of the CDC2a promoter. The products of the reverse transcriptase reaction (lane P) (a) and the S1-nuclease reaction (lane S) (b) were electrophoresed together with reference sequence ladders (lanes A, G, C, and T). All the labeled products have the same 5' end so that the position of the signals can be referred easily. The sequence of the both strands in the relevant region are shown on each right side and the signal positions are indicated by arrows.

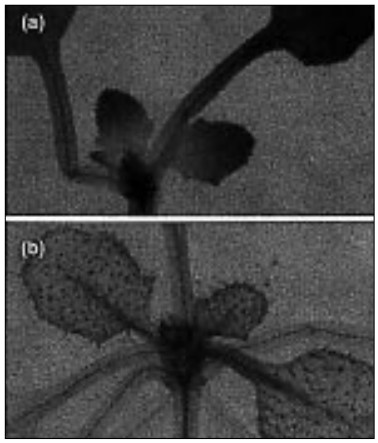

Figure 2. Histochemical analysis of the *CDC2a* promoter. Transgenic *Arabidopsis* plants 2-weeks-old after germination were examined histochemically: (a) transgenic plant carrying 35S-GUS; (b) transgenic plant carrying -591/+4-GUS, respectively.

CDC2a initiation codon and signal bands around the same position were observed in the primer-extension and the S1-mapping analysis, respectively (Figure 1). We concluded that the transcription of the *CDC2a* gene is started at the position 677-bp upstream from the initiation codon.

Activity of the *CDC2a* promoter in proliferating cells has been demonstrated in both histochemical analysis with a translational β-glucuronidase (GUS) fusion gene (8) and *in situ* hybridization analysis (7). In order to localize the *cis*-element required for the proliferating-cell-specific activity, we constructed three GUS fusion genes and introduced them into transgenic *Arabidopsis*. The GUS-coding sequence is preceded by the fragment between the positions 1301-bp upstream and 4-bp downstream from the transcription start site in the fusion gene designated as -1301/+4-GUS, and by the fragment between the positions 591-bp upstream and 4-bp downstream in that designated as -591/+4-GUS. The other designated as -986/+680-GUS is a translational fusion gene in which the fragment between the position 986-bp upstream from the transcription start site and the *CDC2a* initiation codon is fused to the GUS-coding sequence in an in-frame manner.

Several independent lines of transgenic plants for each GUS fusion gene were examined histochemically at the stage of juvenile plants 2-weeks-old after germination. Transgenic plants carrying the GUS-coding sequence preceded by the cauliflower mosaic virus 35S promoter (9) was used as a positive control of GUS staining (Figure 2a). Expression of -986/+680-GUS was detected in apical shoot and root meristems (data not shown) as reported before (7 and 8). On the other hand, -591/+4-GUS conferred no GUS activity to meristematic cells (Figure 2b). Instead, developing trichome cells showed strong GUS activity in plants carrying the fusion gene (Figure 2b). As trichomes maturated, the GUS activity gradually decreased and finally disappeared (data not shown). The same pattern of GUS expression was observed with -1301/+4-GUS (data not shown).

We concluded from these results that a region downstream from the transcription start site is required for the proliferating-cell-specific activity of the *CDC2a* promoter. Our results indicate another interesting fact that the 595-bp region located just upstream from the transcription start site contains a *cis*-element acting during trichome development. In *Arabidopsis*, a trichome is a unicellular organ existing on the leaf surface and its development consists of unique processes including endoreplication, extraordinary cell enlargement, and complicated cell morphogenesis (for review, see 10). The 595-bp region directs transcription during one of these unique processes. From a view point of protein function, endoreplication is a highly probable process because CDC2a function might be needed for DNA replication repeated without mitosis. CDC2a might act in outgrowth of trichome cells as CDK5 plays a critical role in nurite outgrowth during neuronal differentiation (11). In order to examine these possibility, it will be required to identify the responsible *cis*-element and the developmental process in which the *cis*-element is involved.

References

1. Forsburg S and Nurse P, *Annu. Rev. Cell Biol.* **7**, 227-256. (1991).
2. Reed S I, *Annu. Rev. Cell Biol.* **8**, 529-561.(1992).
3. Heichman K A and Roberts J M, *Cell*, **79**, 557-562.(1994).
4. Pines J, *Semin. Cell Biol.* **5**, 399-408. (1994).
5. Hirayama T, Imajuku Y, Anai T, Matsui M and OkaA, *Gene*, **105**, 159-165. (1991).
6. Imajuku Y, Hirayama T, Endoh H and Oka A.(1992). *FEBS Lett.* **304**, 73-77.
7. Martinez M C, Jorgensen J-E, Lawton M A, Lamb C J and Peter W D, *Proc. Natl. Acad. Sci. USA*, **89**, 7360-7364. (1992).
8. Hemerly A S, Ferreira P, de Almeida Engler J, Van Montagu M, Engler G and Inze D, *Plant Cell*, **5**, 1711-1723. (1993).
9. Odell J T, Nagy F and Chua N-H, *Nature*, **313**, 810-812. (1985).
10. Hulskamp M, Misera S and Jugens G, *Cell*, **76**, 555-566. (1994).
11. Nikolic M, Dudek H, Kwon Y T, Ramos Y F M and Tsai L-H, *Genes Devel.* **10**, 816-825. (1996).

A Survey on *E. coli* Enzymes: Correlation between Metabolic Pathway and Gene Location

Hiroyuki Ogata and Minoru Kanehisa

Deciphering the meaning of the gene location on the chromosome is one of the basic demands of molecular biology. Here we report a correlation between the position of enzymes on the metabolic pathways and the locality of the genes on the chromosome. We performed a window base search to identify functionally related enzymes coding segments (FRECS) for the *Escherichia coli* chromosome. Among 52 FRECS identified, 32 (~60%) were related to the known operons. It is also suggested that gene duplication has no connection to the observed correlation.

Keywords: Function and structure / Metabolism / Genome / Chromosome / Operon / Gene duplication

What function is coded in the gene location along the chromosome? Many examples in which the gene location has critical roles for the expression of gene functions have emphasized the importance of this basic question on genome structure and evolution. However, the recent completion of sequencing the bacterial gemomes and the extensive comparisons of gene order revealed that gene location is highly shuffled in the course of bacterial evolution and that the gene order is not a conservative entity except for the short-range colinearity (1). Although this striking feature of the gene disposition could be interpreted as the absence of functional role of the long-range gene order, direct comparisons of the gene locations with their functions must be necessary before deriving the answer to the question.

When this kind of questions are addressed, a major difficulty is in the definition of gene function. A recently developed database by Kanehisa *et al*. dealing with biological pathways provides excellent opportunities for the investigation of gene functions (2,3). The database named KEGG (Kyoto Encyclopedia of Genes and Genomes) stores wide coverage of the known metabolic pathways in a computable form called "binary relations", which enabled us to introduce a new measure to capture the degree of functional link between two enzymes (4).

In this study, we performed a statistical analysis on the relation between the distance of *Escherichia coli* enzyme genes along the chromosome and the functional link measured by the shortest path length between these enzymes on the metabolic pathways.

The information of *E. coli* metabolic pathways, operons

MOLECULAR BIOLOGY AND INFORMATION —Biological Information Science—

Scope of research

This laboratory aims at developing theoretical frameworks for understanding the information flow in biological systems in terms of genes, gene products, other biomolecules, and their interactions. Toward that end a new deductive database is being organized for known molecular and genetic pathways in living organisms, and computational technologies are being developed for retrieval, inference, and analysis. Other studies include: functional and structural prediction of proteins from sequence information and development of sequence analysis tools.

Prof
KANEHISA,Minoru
(D Sc)

Instr
GOTO, Susumu
(D Eng)

Instr
FUJIBUCHI,
Wataru

Instr
OGATA, Hiroyuki

Research Fellows
SATO, Kazushige
SUGIYAMA, Yukiteru (D Agr)

Students
TOMII, Kentarou (DC);
SUZUKI, Kenji (DC);
KIHARA, Daisuke (DC);
BONO, Hidemasa (MC);
HATTORI, Masahiro (MC);
KAWASHIMA, Shuichi (MC);
PARK, Keun-joon (MC);
IGARASHI, Yoshinobu (MC);
KATAYAMA Toshiaki (MC)

and the protein sequences of the enzymes were taken from KEGG. The genomic map positions of the enzymes were from EcoCyc (5). When an enzyme represented by an EC number is related to multiple genes as in the case of a multi-component enzyme, we omitted it from the results for the simplicity of the assignment on the genomic map.

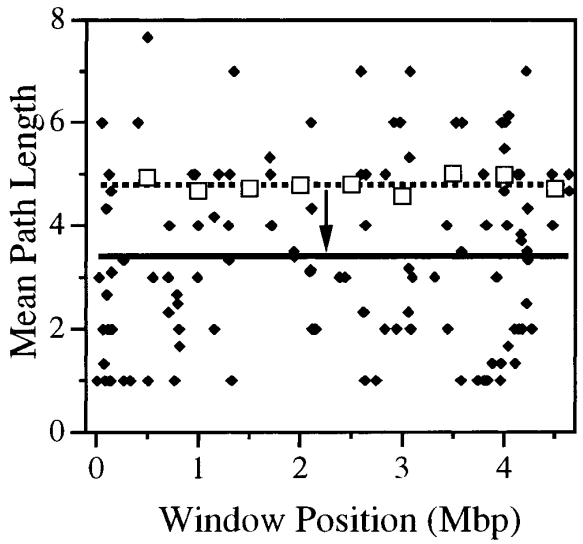

Figure 1. The mean path length of enzyme pairs is plotted for different sizes of the search window. White boxes and black boxes are those for 1 Mbp and 10 Kbp size window, respectively. Dotted and solid lines show the avarage levels of the path length.

Investigation here focused on whether the functional link of the enzymes has any relation to the physical distance of the genes on the *E. coli* chromosome. To this purpose, we performed a window search for the identification of the sets of enzymes coded on close positions along the chromosome, and calculated the mean path length of enzyme pairs appearing in the window. In Figure 1, the mean path length was plotted for two different window sizes. Interestingly, when we changed the window size from 1 Mbp to 10 Kbp, the path length was decreased, on the average, from 4.8 (10 samples) to 3.4 (139 samples) as indicated by the arrow in the Figure 1. If the enzymes appearing in close positions on the metabolic pathways are coded randomly on the chromosome, the average values of path length are expected to be the same for different window sizes. We considered that this correlation would be due to the existence of relatively short (~10 Kbp) DNA segments that encode enzymes playing their rolls at close position on the metabolic pathways. Here we call these segments functionally related enzymes coding segments (FRECS). After merging overlapped 10 Kbp segments, we obtained 52 FRECS with the mean path length less than 4. We examined these segments in terms of two possibilities that might explain this observation.

First, operon enzymes were examined. If we omitted operon enzymes from the above analysis, the average value of the path length raised from 3.4 to 4.2, and the number of the FRECS mentioned above decreased from 52 to 20. The enzymes coded in these twenty FRECS were 45 in all.

Second, we examined the chromosomal distance between 64 paralogous enzyme pairs identified by the BLASTP search (6). In the previous study, we revealed that the paralogous enzymes often play their rolls at close positions in the metabolic pathways (4). Thus we expected that this heterogeneity of the *E. coli* metabolic pathways might be reflected on the disposition of these duplicated enzymes. However, there were no paralog pairs in any of the 52 FRECS.

In conclusion, we identified 52 DNA segments that code enzymes appearing in close position on the metabolic pathways. Most of these segments (60%) were related to the operon enzymes. These segments contributed to the apparent correlation between the metabolic pathway and the gene location (Fig. 1). Further investigation on the remaining 20 DNA segments will elucidate the meaning of the feature that connects the *E. coli* chromosome and metabolic pathways .

Acknowledgment
This work was supported in part by a Grant-in-Aid for Scientific Research on Priority Areas, 'Genome Science', from the Ministry of Education, Science, Sports and Culture of Japan. The computation time was provided by the Supercomputer Laboratory, Institute for Chemical Research, Kyoto University.

References

1. Mushegian AR and Koonin EV, *Trends Genet.*, **12**, 289-290 (1996).
2. Kanehisa M, *Science & Technology Japan*, No. 59, pp. 34-38 (1996).
3. Goto S, Bono H, Ogata H, Fujibuchi W, Nishioka T, Sato K and Kanehisa M, *Proc. Pacific Symposium on Biocomputing '97*, pp. 175-186 (1996).
4. Ogata H, Bono H, Fujibuchi W, Goto S and Kanehisa M, *Proc. 7th Workshop on Genome Informatics*, pp. 128-136 (1996).
5. Karp PD, Riley M, Paley SM and Pelligrini-Toole A, *Nucleic Acids Res.*, **24**, 32-39 (1996).
6. Altschul SF, Gich W, Miller W, Myers EW and Lipman DJ, *J. Mol. Biol.*, **215**, 403-410 (1990).

Electron Storage and Stretcher Ring, KSR

Akira Noda, Hirokazu Fujita, Makoto Inoue, Yoshihisa Iwashita, Hiromi Okamoto, Toshiyuki Shirai, Takashi Sugimura and Hiromu Tonguu

An electron storage ring with the maximum energy of 300 MeV and critical wavelength from the dipole section of the 17 nm is under construction. It will also improve the duty factor of the electron beam with the energy of ~100 MeV attaining the average number of 10^{12} electrons per second with the fairly lower peak current of 0.3 μA, which is suitable for counter experiments.

Keywords: Storage Ring/ Synchrotron Radiation/ Insertion Device/ Pulse Stretcher/ Duty Factor

In order to provide a synchrotron light source in the wavelength of vacuum ultraviolet and soft X-ray region, an electron storage ring KSR with the maximum energy and the curvature radius of 300 MeV and 0.835 m, respectively has been under construction. The critical wave length of the synchrotron radiation from the dipole magnets is 17 nm, while the insertion device can provide radiation with an additional wavelength region. For example, superconducting wigler might generate the light with the wave length of several nm[1,2]. The detailed specification of the insertion device should be fixed after enough discussion on the research capabilities utilizing the light source. Further KSR has also such a role as enables the preparatory researches for experiments at the large research facility like Photon Factory at KEK or SPring-8 in Harima Science City.

The researches utilizing the 100 MeV electron beam of the linac[3] such as Parametric X-radiation from crystals [4] and transition radiation from multi-layers of thin foils are being carried out. Its small duty factor as 2×10^{-5}, however, causes a severe limitation on these experiments. The peak current of the linac must be reduced to 1mA to avoid the pile up of the signal pulses which results in the average number of electrons of the order of 10^9 per second. So the possibility to improve the duty factor of the electron beam to ~90 % with use of KSR is also studied. With this method, the average number of electrons per second is expected to increase to ~10^{12} keeping the peak current as low as 0.3 μA if the output beam from the linac with the peak current of 100 mA is injected and stretched at repetition rate of 10 Hz[5]. For this purpose, the electron beam is injected into the KSR by three-turn injection during 0.3μs. Then immediately after the injection, the beam emittance is increased with use of the transverse RF electric field which resonates with the horizontal betatron oscillation. The electrons which come to

NUCLEAR SCIENCE RESEARCH FACILITY —Particle and Photon Beams—

Scope of research

Particle and photon beams generated with accelerators and their instrumentations both for fundamental research and practical applications are studied. The following subjects are being studied: beam dynamics related to the space charge force in the accelerators: beam handling during the injection and extraction processes of the accelerator ring: radiation mechanism of photon by electrons in the magnetic field: interactions in the few-nucleon systems: R&D to realize a compact proton synchrotron dedicated for cancer therapy: and irradiation of materials with particle and photon beams.

Prof
NODA, Akira
D Sc

Assoc Prof
KAKIGI, Shigeru
D Sc

Instr
SHIRAI, Toshiyoki

Techn
TONGUU, Hiromu

Lecturer (part-time)
KITAMURA, Hideo
(Prof of National Laboratory for High Energy Physics, KEK / The Institute of Physical and Chemical Research, RIKEN)

Students
IKEGAMI,Masanori (DC)
KANDO, Masaki (DC)
SUGIMURA, Takashi (DC)
KIHARA, Takahiro (MC)
URAKABE, Eriko (M C)
NISHI Masatsugu (RF)

the boundary of the separatrix will become unstable and jump into the electrostatic septum to be extracted out from the ring[6],[7]. The KSR ring has two long straight sections 6.2 m in length. One of them will be dedicated for an insertion device and the other should include both injection and extraction channels. Such configuration has a merit of utilizing common beam dump between the linac and the stretcher ring, KSR.

The magnets had been precisely aligned with the precision of better than ±0.1 mm in 1995 and this year the vacuum vessels have been installed into the magnets in two arcs. Evacuation of the arc part has already been started. These sections are considered to require longer aging time to realize good enough vacuum pressure because of the heating due to synchrotron radiation compared with the straight sections. The control and power feeding system of the magnets and vacuum has also been completed to prepare the beam circulation test. Detailed design of the insertion device and injection and extraction apparates is now under way.

References

1. Noda A., Dewa H., Fujita H., Ikegami M., Iwashita Y., Kakigi S., Kando M., Mashiko K., Shirai T. and Inoue M., *Bull. Inst. Chem. Res., Kyoto Univ.*, 73, 27-32 (1995).
2. Noda A., Dewa H., Fujita H., Lkegami M., Iwashita Y., Kakigi S., Kando M., Mashiko K., Okamoto H., Shirai T., Inoue M., *Proc. of the 1995 Particle Accelerator Conf.* 278-280 (Dallas, USA, 1995).
3. Shirai T., Sugimura T., Iwashita Y., Kakigi S., Fujita H., Tonguu H., Noda A. and Inoue M., Proc. of LINAC96, 240- 242 (Geneva, Switzerland, 1996).
4. Hayakawa Y., Seto M., Maeda Y., Shirai T. and Noda A., Beam Science and Technology, 2 in print.
5. Noda A., Dewa H., Fujita H., Ikegami M., Inoue M., Iwashita Y., Kakigi S., Kando M.,Mashiko K.Okamoto H., Shirai T., Sugimura T., and Tonguu H., *Proc. of the 5th European Particle Accelerator* Conf. in print (Barcelona, Spain, 1996).
6. Tomizawa M., Yoshizawa M., Chida K., Yoshizawa J., Arakaki Y, Nagai R., Mizobuchi A., Noda A.,Noda K., Kanazawa M., Ando A., Muto H. and Hattori T., Nucl. Instr. and Meth. A326 399-406 (1993).
7. Noda K., Kanazawa M., Itano A., Takada E., Torikoshi M., Araki N., Yoshizawa J., Sato K., Yamada S.,Ogawa H., Itoh H., Noda A., Tomizawa M. and Yoshizawa M., Nucl. Instr and Meth. A374 269-277 (1996).

Table 1. Parameters of KSR

Beam Energy	
Storage Ring Mode	100~300 MeV
Stretcher Mode	~100 MeV
Circumference	25.689 m
Lattice Structure	Triple Bend Doubly Achromatic
Radius of Curvature	0.835 m
Bending Angle	60°
n-value	0
Edge Angle	0°
Length of the Long Straight Section	6.19 m
RF Frequency	116.7MHz
Harmonic Number	10
Number of Betatron Oscillations	
Horizontal Direction	2.75
Vertical Direction	1.25
Superperiodicity	
Storage Ring Mode	2
Stretcher Mode	1
Critical Wavelength (Dipole Section)	17 nm

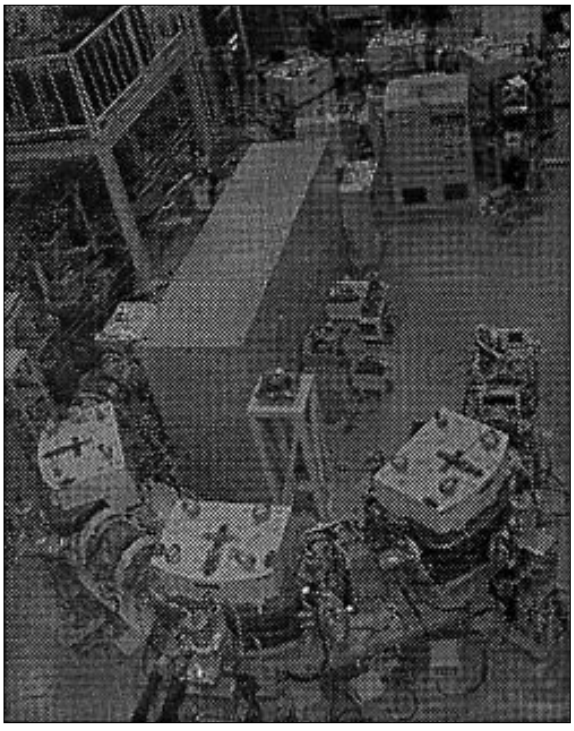

Figure 1. Overall View of the KSR.

Biperiodic L-Support Disk and Washer Structure

Yoshihisa Iwashita, Hiroyuki Ao, Akira Noda, Hiromi Okamoto,

Toshiyuki Shirai and Makoto Inoue

A high power model of the biperiodic L-support Disk and Washer structure for electron acceleration is fabricated and under test. Two 1.2m long accelerating tubes are coupled by a bridge coupler, which has an RF coupler, a vacuum port, and three frequency tuners. Each end of the bridge-coupled tube set is terminated by a full-cell endplate for the accelerating mode.

Keywords: linear accelerator/ DAW/ coaxial bridge coupler/ power model

An electron linac[1] has been installed at the Accelerator Laboratory, Institute for Chemical Research, Kyoto University. Its use is mainly intended as the injector for the electron storage ring KSR [2], which is being assembled. Three of 3-m disc-loaded wave-guides are installed as the accelerator tubes, which are operated at 2857MHz. By replacing one of the wave-guides with a new accelerating tube with a higher shunt impedance and the higher accelerating gradient, the output energy can be increased with the same input RF power.

The Disk and Washer (DAW) structure has outstanding features in high stability, good vacuum properties, high shunt impedance, and ease of fabrication.[3,4] Because the stability is related to the square of the coupling constant between cells, DAW, which has about ten times larger coupling constant than that of conventional coupled cell linac structures, should be almost hundred times stable than those. The large coupling constant is achieved by the confluence of the two modes in a cell. (See Fig. 1). They are called as the accelerating mode and the coupling mode. The former has the strong electric field on the axis, which is suitable for the acceleration. The latter has weak electric field on the axis, but has stored energy on the outer

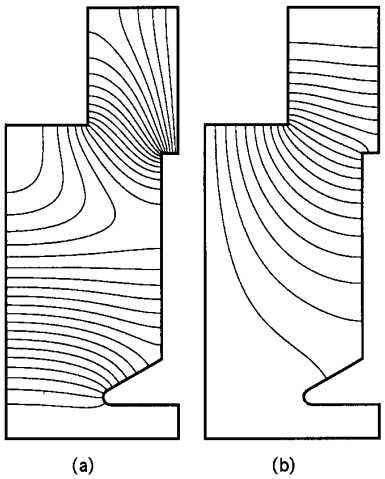

Figure. 1 Flux plots by SUPERFISH
(a) Accelerating mode (b) Coupling mode

NUCLEAR SCIENCE RESEARCH FACILITY —Beams and Fundamental Reaction—

Scope of research

Particle beams, accelerators and their applications are studied. Structure and reactions of fundamental substances are investigated through the interactions between beams and materials such as nuclear scattering. Tunable lasers are also applied to investigate the structure of unstable nuclei far from stability and to search for as yet unknown cosmological dark-matter particles in the Universe.

Prof
INOUE, Makoto
D Sc

Assoc Prof
MATSUKI, Seishi
D Sc

Instr
IWASHITA, Yoshihisa
D Sc

Instr
OKAMOTO, Hiromi
D Sc

Students
NAKAMURA, Shin (DC)
KAPIN, Valeri (DC)
YOSHIMURA, Tadahiko (DC)
TADA, Masaru (DC)
KISHIMOTO, Yasuhiro (DC)
AO, Hiroyuki (MC)
IKEDA, Kazumi (RF)
OGAWA, Izumi (RF)
DEWA, Hideki (RF)

region, which acts as the coupling cell.

Because of the extra volume, some of the higher order modes come down and overlap the operating frequency. It was found that the mode overlapping problem can be overcome by the biperiodic support configuration with the careful choice of the tank diameter. There are variety of options for DAW linac structure with such biperiodic washer support. For example, in a large tank-diameter configuration, the operating frequency drops between the two split TM11(-like) mode passbands, and the shunt impedance is higher. When the tank diameter is small, both TM11 mode passbands are above the operating frequency, and the mode density becomes smaller. The basic configuration used here is the extension of the PIGMI[5] geometries, except for the thicker washers and the reduced tank diameter by 20%. This geometry has the smaller density of the unwanted modes and the shorter filling time compared with the large diameter 4-T support DAW. The washer thickness is increased to provide the space for the cooling water channels machined in the washers. Because the L-support configuration has only two supports on the washer, there are only one inlet and one outlet for the water (see Fig. 2). It may simplify the fabrication problem compared with the 4-T support geometry, which has two inlets and two outlets on the washer.

Firstly, the three dimensional electro-magnetic field distributions including the supports are calculated by MAFIA, for the parameter optimization. Then a cold model made of Aluminum is fabricated (see Photo 1). The RF characteristics such as the resonant frequencies and the electric field distribution on the axis are measured on the cold model[6] (see Fig.3). The coaxial bridge coupler is also studied for stable operation[7] (see Fig.4). The high power accalerating tube is being fabricated and under test.

The present work is supported by Grant-in Aid for Scientific Research from Ministry of Education, Science, Sports and Culture Government of Japan. The version of the MAFIA used here is release 2.04. The version of SUPERFISH is Release 4.12. Computation time was provided by the Supercomputer Laboratory, Institute for Chemical Research, Kyoto University.

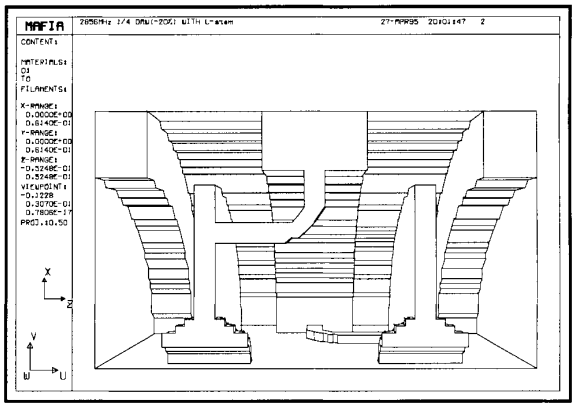

Figure.2 DAW with Biperiodic support

Photo 1 Close view of the disk-support-washer assembly

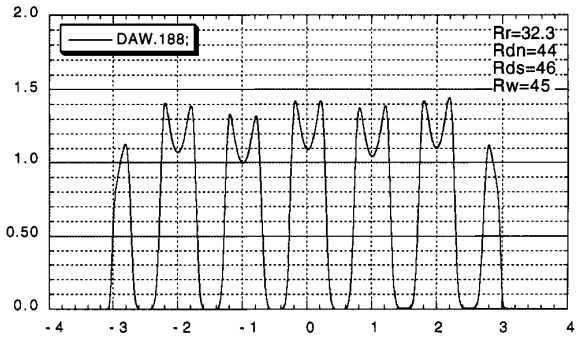

Figure. 3 The typical result of field distribution measurements

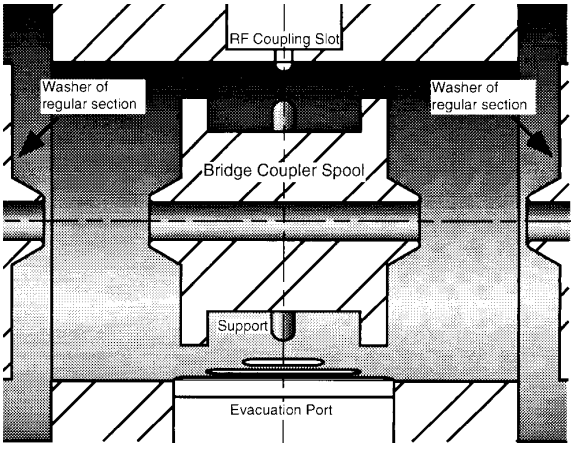

Figure. 4 Coaxial bridge coupler

References

1. T.Shirai, et al., "A 100 MeV Injector for the Electron Storage Ring at Kyoto University", Proc. of the 1995 Particle Accelerator Conference, Dallas, p.1079 (1995)
2. A.Noda et al., "Electron Storage and Stretcher Ring, KSR", Proc of the 1996 European Accelerator conference, Barcelona, in print.
3. R.K.Cooper, Y.Iwashita, J.M.Potter, S.O.Schriber, D.A.Swenson, J.M.Watson, L.C.Wilkerson and L.M.Young, "Radio-Frequency Structure Development for the Los Alamos/NBS Racetrack Microtron", LosAlamos National Laboratory document LAUR-83-95 (Jan. 1983)
4. Y.Iwashita, "Disk-and-Washer structure with biperiodic support", Nucl. Instrum. and Meth. in Phys. Res. A 348(1994)15-33
5. L. D. Hansbrough, Compiler, "PIGMI: A Design Report for a Pion Generator for Medical Irradiation", LANL report LA-8880(1980).
6. Y.Iwashita, et al., "Cold Model Test of Biperiodic L-Support Disk-and-Washer Linac Structure", Proc. of the 1995 Particle Accelerator Conference, Dallas, p.1093 (1995)
7. Y.Iwashita, et al., "Power Model of Biperiodic DAW Cavity", Proc. of the 1996 Linear Accelerator Conference, CERN Geneva, p. 857 (1996)

Kinetoplast Minicircles Carrying Guide RNA Genes of *Leishmania tarentolae*

Hiroyuki Sugisaki

The nucleotide sequences of the minicircles from the kinetoplast DNA network of Leishmania tarentolae have been determined. Each minicircle encoded a single unique guide RNA (gRNA) gene located approximately 150 base pairs from the conserved region which contains the replication origins for both strands. Out of seven minicircle-encoded gRNA genes identified, three were involved in RNA editing of the blocks I, II and V of the mitochondrial unidentified reading frame 4 gene (MURF4), four in RNA editing of the blocks II, V, VII and VIII of ribosomal protein S12 gene. Sequence comparison of the surrounding of the genes showed some similarity in the 5' flanking region which may contain signal sequences for transcriptional initiation of gRNAs

Keywords: kinetopalstid protozoa/RNA editing/mitochondria

Several mitochondrial mRNA in kinetoplastid protozoa such as *Crithidia*, *Leishmania* and *Trypanosoma* are extensively edited after transcription. The location of editing blocks, number of editing sites within a single editing domain, and number of U residues to be added or deleted at each editing site are very specific to individual mRNAs. The information for insertion and deletion of the uridine residues in the primary sequence of other mitochondrial RNA transcripts , so called guide RNAs (gRNA). The molecules have a length of 50-70 nucleotides, contain posttranscriptionally added 3' oligo(U) extensions and function as templates in the editing reaction by base complementarity to editing domains of the mRNAs (1,2).

The guide RNAs are transcribed from the maxicircle and the minicircle DNA molecules present in the kinetoplast DNA network (kDNA). The minicircle component of *L. tarentolae* consists of approximately 10^4 molecules 850-880 base pairs (bp) in size. Each minicircle is organized into a conserved region of 170-180 bp, which contains the replication origins for both strands, GGGCGT and GGGGTTGTGTGTAAA and a bent DNA region (see Figure 1), and a variable region of approximately 700 bp which defines the sequence class.

Unit-length linearized minicircles were released from networks by treatment with each of restriction enzymes *Bam*HI, *Bgl*I, *Eco*RI, *Kpn*I *Sma*I and *Xba*I. A recognition site of *Sma*I is located within the conserved region of all minicircles sequenced so far. In practice, however, some network DNA remained uncut by this enzyme. The unit-length linearized minicircle molecules were isolated from agarose gels and ligated into pUC118 or pUC119. The total sequence of each minicircle clone was obtained with the universal and reverse primers for

RESEARCH FACILITY OF NUCLEIC ACIDSS

Scope of Research

With emphasis on regulatory mechanisms of gene expression in higher organisms, the research activity has been focused on analysis of signal structures at the regulatory regions of transcriptional initiation and of molecular mechanisms involved in post-transcriptional modification by the use of eukaryotic systems appropriate for analysis. As of December 1994, studies are concentrated on the molecular mechanism of RNA editing in mitochondria of kinetoplastids.5

Assoc Prof
SUGISAKI,Hiroyuki
(D Sc)

Techn
YASUDA, Keiko

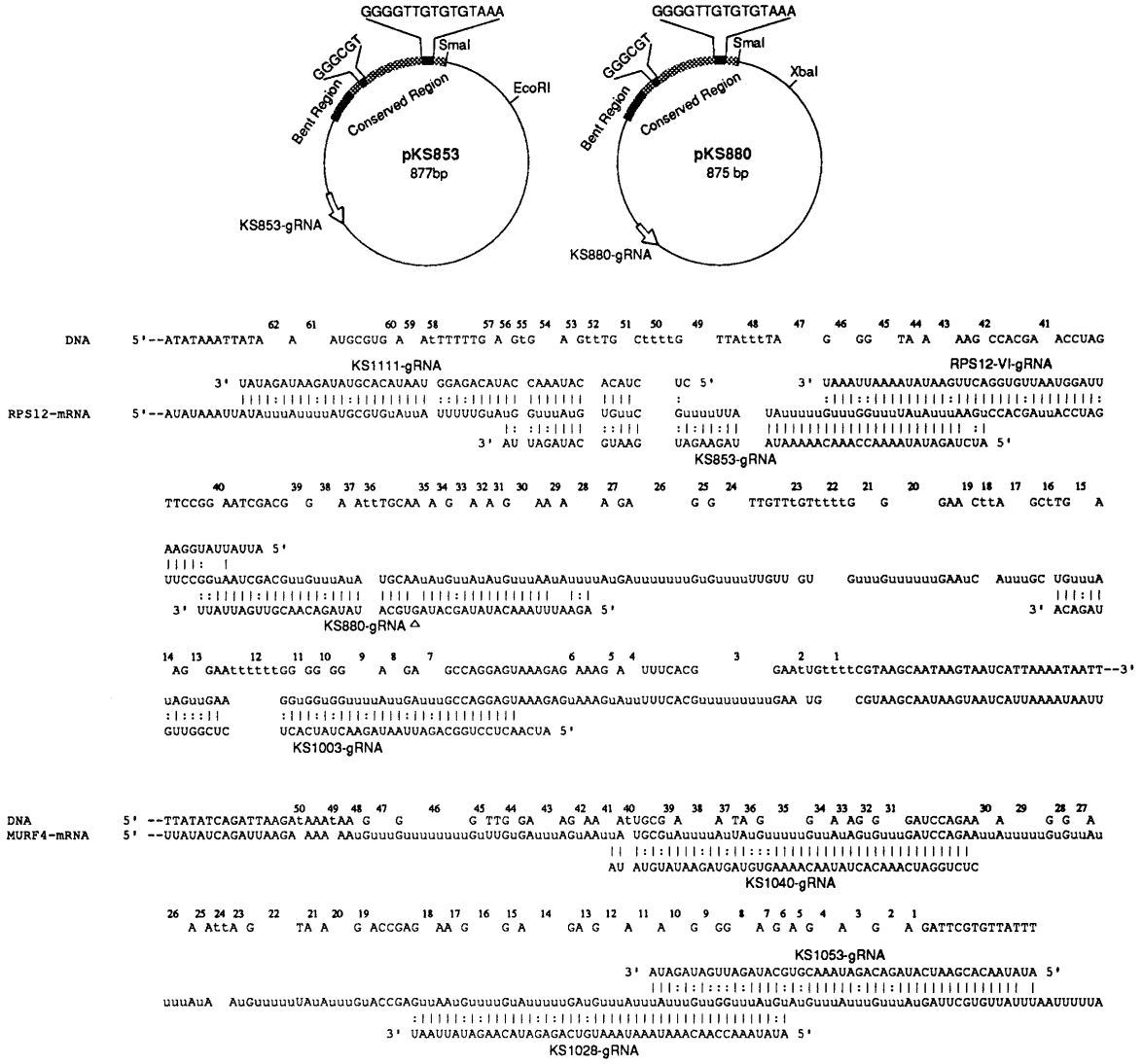

Figure 1. gRNAs mediating the RNA editing reactions of the MURF4 and RPS12 genes
The 5' portion of the mature edited MURF4 mRNA and the entire mature edited RPS12 mRNA are shown with the editing sites numbered. Edited nucleotides are indicated as lowercase u's in mRNA sequence for insertion and lowercase t's in DNA sequences for deletion. The complementary sequences are shown with G-C and A-U base pairs indicated by parallel lines and G-U base pairs by colons. Maxicircle-encoded RPS12 VI-gRNA is also shown.

the pUC sequencing system using the Applied Biosystems DNA sequencing system. Ninety nine sequences were determined from the *Sma*I library, two from the *Xba*I library and each one from the *Bam*HI, *Bgl*I, *Eco*RI, and *Kpn*I libraries.

The minicircle sequences were analyzed for potential gRNA sequences involved in the known editing of the cytochrome oxidase subunit III, mitochondrial unidentified reading frame 4 (MURF4) or ribosomal protein S12 gene (RPS12) mRNA, using the local alignment program. Each minicircle encoded a single unique gRNA located approximately 150 bp from the conserved region. Out of nine kinetoplast minicircle-encoded genes identified, minicircle-encoded gRNAs from pKS1053, pKS1028, and pKS1040 was involved in the RNA editing reaction for the blocks I, II and V, respectively, of the MURF4 gene, those from pKS1003, pKS880, pKS853, and pKS1111 for the blocks II, V, VII and VIII, respectively, of the RPS12 gene(Fig. 1), the remaining two for the blocks of unassigned genes.

The molecular mechanisms of transcriptional initiation and posttranscriptional addition of oligo(U) extension for gRNAs are interesting problems. When the sequences of the 5' flanking region the gRNA genes were compared with each other, two conserved blocks, AT(A/T)(G/T)T and AA(A/T)(G/T)T were located approximately -43 and -20 downstream from the 5' terminals of the gRNA genes. The sequences would be promoters which recognized by mitochondrial RNA polymerase of kinetoplastids. Sequence comparison of the surrounding regions of the 3' terminals of the gRNA genes which would contain the signal sequences responsible for posttranscriptional addition of oligo(U) extension showed little similarity. Specific secondary structures surrounding the 3' terminals of the transcription products from the gRNA genes may requited for the processing.

References

(1) Simpson L & Thiemann O H, Cell, **81**, 837-840 (1995)
(2) Sollner-Webb B, Science, **273**, 1182-1183 (1996)

LABORATORIES OF VISITING PROFESSORS

SOLID STATE CHEMISTRY —Structure Analysis—

Vis Prof
TERAUCHI, Hikaru
(D Sc)

Professor
TERAUCHI, Hikaru
Department of Physics, Faculty of Science, Kwansei Gakuin University
(1-155 Uegahara-Ichiban-cho, Nishinomiya 662)

Lectures at *ICR*
Crystal Symmetry and Physical Properties
X-ray Diffraction
Some Thermal Effects in Solids
Structural Phase Transitions
Artificial Structures

Vis Assoc Prof
TAKAGI Hidenori
(D Eng)

Associate Professor
TAKAGI, Hidenori
Institute for Solid State Physics, University of Tokyo (Roppongi 7-22-1, Minato-ku, Tokyo 106)

Lectures at *ICR*
Introduction to Solid State Physics: I, II and III
Transport Properties I,II and III
Disorder Induced Metal-Insulator Transitition I, II and III

FUNDAMENTAL MATERIAL PROPERTIES —Composite Material—

Vis Prof
KAKUGO
(D Eng)

Professor
KAKUGO, Masahiro (Dr. Eng.)
Director and Research Director of Petrochemicals Research Lab. and Plastic Technical Center of Sumitomo Chemical Co.

Lectures at *ICR*
History, Trend and Future of Polymer Industry
Recent Progress of Co-ordination Polymerization Catalysts
Metallocene Catalysts
Recent Progress of Polyolefin Production Process
Recent Progress of Plastic Processing Technology
Recent Progress of Precision Polymerization
Recent Progress of Polymer Alloy

Vis Assoc Prof
KAWASHIMA, Takayuki
(D Sc)

Associate Professor
KAWASHIMA, Takayuki (D Sc)
Department of Chemistry, Graduate School of Science, The University of Tokyo (7-3-1 Hongo, Bunkyo-ku, Tokyo 113)

Lectures at *ICR*
The Wittig Reaction, Peterson Reaction, and the Chemistry of the Corresponding Reactive Intermediates

SYNTHETIC ORGANIC CHEMISTRY —Synthetic Theory—

Vis Prof
MURAI, Akio
(D Sc)

Professor
MURAI, Akio
Faculty of Sciences, Hokkaido University (8 West, Kitajujo, Kita-ku, Sapporo 060)

Lecture at *ICR*
Synthesis of Marine Cyclic Polyethers
Synthetic Studies on Marine Toxins

Vis Assoc Prof
INENAGA, Junji
(D Eng)

Associate Professor
INENAGA, Junji
Institute for Fundamental Research of Organic Chemistry, Kyushu University (6-10-1 Hakozaki, Higashi-ku, Fukuoka, 812-18)

Lecture at *ICR*
Organic Reactions Using Rare Earth Metal: Recent Development

PUBLICATIONS

STATES AND STRUCTURES

I. Atomic and Molecular Physics

Nakamatsu H, Mukoyama T: Ionic and Covalent Bonds in CeO_2 Crystal, *ICR Annual Report 1995 (Institute for Chemical Research, Kyoto University, Uji, 1996)*, pp. 4-5.

Mukoyama T: Estimation of Atomic Parameters for Electron Capture Decay of ^{163}Ho, in *Study of the Mass of the Electron Neutrino in Japan, ed.by S. Yasumi and H. Maezawa, KEK REPORT 95-17 (National Laboratory for High Energy Physics, Tsukuba, 1996)*, pp. 71-82.

Yasui J, Mukoyama T, Shibuya T: Analytical Expressions of Atomic Wave Functions and Molecular Integrals for the X-Ray Transition Probabilities of Molecules, *Adv. in X-Ray Chem. Anal*., Japan **27**, 329-338 (1996).

Sarkadi L, Mukoyama T, Smit Z: Investigation of the Vacancy Sharing Process in L-Shell Ionization of Gold and Bismuth by Bare Ions, *J Phys. B: At. Mol. Opt. Phys*., **29**, 2253-2264 (1996).

Tökési K, Némethy A, Kövér L, Varga D, Mukoyama T: Modeling of electron scattering in thin manganese films on silicon by Monte Carlo methods, *J. Appl. Phys*., **79**, 3763-3769 (1996).

Onoe J, Nakamatsu H, Mukoyama T, Sekine R, Adachi H, Takeuchi K: Relativistic Change in Bond Overlap Population for the Study of Relativistic Effects on Bond Length of Diatomic Molecules, *J. Phys. Soc. Japan*, **65**, 2459-2462 (1996).

Ishizuka T, Vlaicu A M, Tochio T, Ohsawa D, Yamaguchi K, Ito Y, Mukoyama T, Nisawa A, Omote K, Shoji T, Yoshikado S: K and L X-Ray Spectra of Copper Metal Radiated by the Electron Bombardment, in *Abst. X96, 17th Internat. Conf. X-ray and Inner-Shell Processes, Hamburg, Germany, Sept. 9-13, 1996 (HASYLAB at DESY, Hamburg, 1996)*, p. 85.

Song B, Taniguchi K, Nakamatsu H, Mukoyama T: Titanium $L_{\alpha,\beta}$ X-Ray Emission Spectra in Several Titanium Compounds, in *Abst. X96, 17th Internat. Conf. X-ray and Inner-Shell Processes, Hamburg, Germany, Sept. 9-13, 1996 (HASYLAB at DESY, Hamburg, 1996)*, p. 87.

Tochio T, Vlaicu A M, Ishizuka T, Ohsawa D, Ito Y, Mukoyama T, Kawai S, Motoyama M, Yoshikado S: Investigation on Chromium Kb X-Ray Emission Spectrum in Several Chromium Compounds, *in Abst. X96, 17th Internat. Conf. X-ray and Inner-Shell Processes, Hamburg, Germany, Sept. 9-13, 1996 (HASYLAB at DESY, Hamburg, 1996)*, p. 93.

Ito Y, Tochio T, Mukoyama T, Takahashi M, Emura S, Azuma Y: Double Electron Transitions in the X-Ray Absorption near Xe L Edges, in *Abst. X96, 17th Internat. Conf. X-ray and Inner-Shell Processes, Hamburg, Germany, Sept. 9-13, 1996 (HASYLAB at DESY, Hamburg, 1996)*, p. 145.

Mukoyama T, Kaji H: K-Shell Ionization of Atoms by Mesons, in *Abst. X96, 17th Internat. Conf. X-ray and Inner-Shell Processes, Hamburg, Germany, Sept. 9-13, 1996 (HASYLAB at DESY, Hamburg, 1996)*, p. 313.

Mukoyama T, Tökési K, Ito Y: Monte Carlo Code for the study of the Response Function of Si(Li) Detectors for X Rays, in *Abst. X96, 17th Internat. Conf. X-ray and Inner-Shell Processes, Hamburg, Germany, Sept. 9-13, 1996 (HASYLAB at DESY, Hamburg, 1996)*, p. 374.

Yamaguchi K, Mukoyama T: Wavelet representation for the solution of radial Schrödinger equation, *J. Phys. B: At. Mol. Opt. Phys.*, **29**, 4059-4071 (1996).

Shigemi A, Nakamatsu H, Mukoyama T, Ikeda S: Shake-up Transition Probability for Molecule (in Japanese), *Bull. Soc. Discrete Variational Xa* **9**, 23 (1996).

Mukoyama T: X-ray emission rates of molecules in the relaxed-orbital approximation (in Japanese), *Bull. Soc. Discrete Variational Xa* **9**, 41 (1996).

Hirata M, Sekine R, Onoe J, Nakamatsu H, Mukoyama T, Adachi H: The electronic structures of actinyl nitrate-extractant complexes using the relativistic DV-DS method (in Japanese), *Bull. Soc. Discrete Variational Xa* **9**, 50 (1996).

Kurakado M, Ohsawa D, Katano R, Ito S, Isozumi Y, Shimizu H, Ebisu T, Watanabe T: Radiation spectroscopy of new generation (in Japanese), Nihon Genshiryoku Gakkai-shi, **38**, (9), 18-23 (1996).

Tochio T, Ito Y, Mukoyama T, Takahashi M, Emura S, Azuma Y: Multielectron transitions above the Xenon L edges, in *Abstracts of 9th Intern Conf. on X-ray Absorption Fine Structure, Grenoble, France, 26-31 Aug.*, PS3-112, 269 (1996).

Ito Y, Mukoyama T, Takahashi M, Emura S, Kanamaru F, Yoshikado S, Koto K: A possibility of phase transition at a low temperature in β-Pb F_2, in *Abstracts of 9th Intern Conf. on X-ray Absorption Fine Structure, Grenoble, France, 26-31 Aug.*, PS3-113, 269 (1996).

Emura S, Takahashi M, Osawa D, Yamaguchi K, Ito Y, Mukoyama T, Yoshikado S: Multielectron excitation in X-ray absorption spectra of RbCl and $RbNO_3$, in *Abstracts of 9th Intern Conf. on X-ray Absorption Fine Structure, Grenoble, France, 26-31 Aug*., PS3-114, 269 (1996).

Takahashi M, Emura S, Ishida A, Osawa D, Yamaguchi K, Ito Y, Mukoyama T, Yoshikado S: Multielectron excitation in X-ray absorption spectra of KOH, in *Abstracts of 9th Intern Conf. on X-ray Absorption Fine Structure, Grenoble, France, 26-31 Aug*., PS3-115, 270 (1996).

Ichihara J, Takahashi M, Emura S, Tochio T, Ito Y, Mukoyama T: XAFS study on the heterogeneous reaction between lead fluoride and benzyl bromide in acetonitrile, in *Abstracts of 9th Intern Conf. on X-ray Absorption Fine Structure, Grenoble, France, 26-31*

Aug., PS3-136, 277 (1996).

Emura S, Ito Y, Takahashi M: x-ray absorption hyper fine structure, in Abstracts *of 9th Intern Conf. on X-ray Absorption Fine Structure, Grenoble, France, 26-31 Aug*., PS3-161, 285 (1996).

Ito Y, Vlaicu A M, Mukoyama T, Sato S, Yoshikado S, Chong I, Takano M, Julian C: The strutural investigation of Pb rich Bi-2201 and its related super- conductors, in *abstracts of NATO-ASI Materials Aspects of H Tc-Superconductivity: 10 years After the Discovery, Delphi, Greek, 19-31 Aug*., 76 (1996).

Mukoyama T, Tochio T, Ito Y, Takahashi M, Emura S, Azuma Y: Multi-Electron transitions above the Xenon L edges, in *abstracts for the DAMOP Meeting of the American Physical Society, Ann Arbor, May 15-18*, 1 (1996).

II. Crystal Information Analysis

Kurata H., Moriguchi S., Isoda S. and Kobayashi T.: Attainable Resolution of Energy-Selecting Image Using High-voltage Electron Microscope. *J. Electron Microsc*., 45, 79-84 (1996).

Kuwamoto K., Irie S., Ogawa T., Miles M.J., Isoda S. and Kobayashi T.: Crystal Formation of 2,4,6-tris(1,3-dithiol-2-ylidene)-1,3,5-cyclohexanetrione by a Process in Dry System. *Technical Report of IEICE*, 96/31, 31-36 (1996) (in Japanese).

Kurata H., Isoda S. and Kobayashi T.: Chemical Mapping by Energy-Filtering Transmission Electron Microscopy. *J. Electron Microsc*., 45, 317-320 (1996).

Kobayashi T., Isoda S. and Kubono K.: Cyclophosphazene; Structure and Molecular Selectivity. p.399-420, in "Comprehensive Supramolecular Chemistry, vol.3", Pergamon, (1996).

Hoshino A., Isoda S. and Kobayashi T.: STM Analysis of the Interfacial Structure in Organic Epitaxy. *Denshi-Kenbikyo*, 31, 10-14 (1996) (in Japanese).

Komatsu K., Kim D., Kobayashi T., Watanabe K., Aguekian V.F., Karasawa T., Akai I. and Iida T.: Size Effects on Excitons of BiI_3 in Layered Matrices. Surface Review and Letters, 3, 1127-1131 (1996).

III. Polymer Condensed States Analysis

Yoon J R, Hashim A S, Kawabata N and Kohjiya S: Blends of Brominated EPDM and NR, *Rubber World*, **213**, 20-24 (1996).

Kohjiya S and Ikeda Y: Progress of Rubbery Materials I. From Natural Rubber to Functional Elastomer, *Shinsozai*, **7**, 41-45 (1996) (in Japanese).

Ikeda Y and Kohjiya S: Molecular Design of Thermoplastic Elastomers, *Kobunshi*, **45**, 136-140 (1996) (in Japanese).

Kohjiya S and Ikeda Y: Progress of Rubbery Materials II. From Natural Rubber to Functional Elastomer, *Shinsozai*, **7**, 28-31 (1996) (in Japanese).

Kohjiya S, Tanaka A, Wada Y and Ikeda Y: Study on the Reaction Condition for in situ Silica Reinforcement of Butadiene Rubber by Sol-Gel Method, *J. Soc. Rubber Ind., Jpn*., **69**, 442-446 (1996) (in Japanese).

Kohjiya S and Sato H: Enzyme Immobilization, in "Polymeric Materials Encyclopedia", Salamone J C Ed., CRC Press, NY, pp. 2135-2139 (1996).

Sando K, Kohjiya S, Ikeda Y, Yamashita S and Kawabata N: Liquid Rubber as a Reactive Softener for 1-Chlorobutadiene-Butadiene Rubber, *J. Appl. Polym. Sci*., **62**, 1093-1098 (1996).

Urayama K and Kohjiya S: Crossover of the Concentration Dependence of Swelling and Elastic Properties for Polysiloxane Networks Crosslinked in Solution, *J. Chem. Phys*., **104**, 3352-3359 (1996).

Kohjiya S, Takada Y, Urayama K, Tezuka Y and Kidera A: GPC Analysis of Polymer Network Formation : 1. Bifunctional Siloxane Monomer/Crosslinker System, *Bull. Chem. Soc. Jpn*., **69**, 565-574 (1996).

Takigawa T, Oodate M, Urayama K and Masuda T: Structure and Viscoelastic Properties of Segmented Polyurethane Blends, *J. Appl. Polym. Sci*., **59**, 1563-1568 (1996).

Takigawa T, Morino Y, Urayama K and Masuda T: Poisson's Ratio of Polyacrylamide (PAAm) Gels, *Polymer Gels & Networks*, **4**, 1-5 (1996).

Takigawa T, Yamasaki S, Urayama K, Takahashi M and Masuda T: Stress-Strain Behavior of Segmented Polyurethaneureas under Pure Shear Deformation, *Rheologica Acta*, **35**, 288-295 (1996).

Urayama K, Kawamura T and Kohjiya S: Elastic Modulus and Equilibrium Swelling of Networks Crosslinked by End-linking Oligodimethylsiloxane at Solution State, *J. Chem. Phys*., **105**, 4833-4840 (1996).

Takigawa, T, Urayama K, Yamasaki S and Masuda T: Elastic Properties of Real Elastomers at Small Deformations, *Angew. Makromol. Chem*., **240**, 197-203 (1996).

Takigawa, T, Morino Y, Urayama K and Masuda T: Osmotic Poisson's Ratio and Equilibrium Stress of Poly(acrylamide) Gels, *Polym. J*., **28**, 1012-1013 (1996).

Murakami S, Yamakawa M, Tsuji M and Kohjiya S: Structure Development in the Uniaxial-Drawing Process of Poly(ethylene naphthalate), *Polymer*, **37**, 3945-3951 (1996).

Uehara H, Kanamoto T, Kawaguchi A and Murakami S: Real-time X-ray Diffraction Study on Two-Stage Drawing of Ultra-High Molecular Weight Polyethylene Reactor Powder above the Static Melting Temperature, *Macromolecules*, **29**, 1540-1547 (1996).

Nishikawa Y, Murakami S, Kohjiya S and Kawaguchi A: Dynamical Observation of Structural Transition of Polymers Using an X-ray Diffraction System with Imaging Plates. 1. Reversible Helix/Helix Transformation of Poly(vinylcyclohexane), *Macromolecules*, **29**, 5558-5566 (1996).

Torii H, Tsuji M and Kawaguchi A: Oriented Over-

growth of Metals onto Poly-1,4-phenylene, *J. Mater. Res*., **11**, 970-980 (1996).

Magoshi A, Yamakawa M, Tsuji M and Kohjiya S: Structural Study on the Blend of Poly(aryl-ether-ether-ketone) and Poly(*p*-phenylene sulfide) by Electron Diffraction, *Kobunshi Ronbunshu*, **53**, 375-380 (1996) (in Japanese).

Ihn KJ and Tsuji M: Electron Microscopy for *Polymers, Polym. Sci. Technol.(Korea)*, **7**, 437-444 (1996) (in Korean).

Tsuji M: Structural Studies on Polymer Crystals by Electron and X-ray Diffraction, in *Proc. 41th Symp. Japn. Soc. E.M., (Kyoto)*, pp.11-14 (1996) (in Japanese).

Tsuji M: Structural Studies on Fibers and Polymer Solids by Crystal Lattice Imaging, *SEN'I GAKKAISHI*, **52**, P486-P493 (1996) (in Japanese).

Yamaguchi S, Tatemoto M and Tsuji M: Fine Structures in As-polymerized and Sintered Poly (tetrafluoroethylene), *SEN'I GAKKAISHI*, **52**, 657-659 (1996).

Tosaka M: Epitaxial growth of polymers on the friction-transfered oriented thin film, *Kaigai Kobunshi Kenkyu*, **42**, 10-11 (1996) (in Japanese).

INTERFACE SCIENCE

I. Solutions and Interfaces

Wakai C and Nakahara M : Attractive Potential Effect on the Rotational Correlation Times for Benzene-d_6 in Organic Solvents, *Bul. Chem. Soc. Jpn.*, **69**, 853-860 (1996).

Nakahara M, Wakai C, Yoshimoto Y and Matubayasi N : Dynamics of Hydrophobic Hydration of Benzene, *J. Phys. Chem*., **100**, 1345-1349 (1996).

Nakahara M : Attractive Force and Repulsive Force, *Kagaku (Chemistry)*, **51**, 432-434 (1996) (in Japanese).

Nakahara M : Structure of Supercritical Water, *Kagaku (Chemistry)*, **51**, 691-694 (1996) (in Japanese).

Yonezawa Y, Sato T, Miyama T, Takami A, Umemura J and Takenaka T : Photoinduced Formation of Aggregated Silver Particles from Silver Salt of Polysaccharide, *Surf. Rev. Lett*., **3**, 1109-1112 (1996)

Takenaka T and Umemura J : Application of Vibrational Spectroscopy to the Study of Structure-Function Relationship in Langmuir-Blodgett Films, in *"New Developments in Construction and Functions of Organic Thin Films"* (T. Kajiyama and M. Aizawa, eds), Elsevier, 145-180 (1996).

Nakagawa T, Umemura J, Hayashi S, Oobatake M, Miwa Y and Machida K : Molecular Dynamics Study of the Spectroscopic Properties of Liquid Benzene, *Mol. Phys*., **88**, 1635-1643 (1996).

Sakai H and Umemura J : Structure Disordering during Surface Pressure Relaxation of Langmuir Films of Stearic Acid as Studied by Infrared External Reflection Spectroscopy, *Chem. Lett*., 465-466 (1996).

Tano T and Umemura J : Gel to Liquid Crystal Phase Transition of Black Lipid Films in Air as Studied by FT-IR Spectroscopy, *Chem. Lett*., 801-802 (1996).

Kimura N, Umemura J and Hayashi S : Polarized FT-IR Spectra of Water in the Middle Phase of Triton X100-Water System, *J. Colloid and Interface Sci*., **182**, 356-364 (1996).

Ishiguro R, Matsumoto M and Takahashi S : Interaction of Fusogenic Synthetic Peptide with Phospholipid Bilayers: Orientation of the Peptide a-Helix and Binding Isotherm, *Biochemistry*, **35**, 4976-4983 (1996).

Matsumoto M, Tsuji Y, Nakamura K and Yoshimoto T : A Trough with Radial Compression for Studies of Monolayers and Fabrication of Langmuir-Blodgett Films, *Thin Solid Films*, **280**, 238-243 (1996).

Morita M, Kubo M and Matsumoto M : Interfacial Properties and Emulsification in Systems of Perfluoropolyether/Non-fluorinated Oil/Partially Fluorinated Oligomeric and Polymeric Compounds, *Colloids and Surfaces*, **A109**, 183-194 (1996).

Matubayasi M and Levy R M : Thermodynamics of the Hydration Shell. 2. Excess Volume and Compressibility of a Hydrophobic Solute, *J. Phys. Chem*., **100**, 2681-2688 (1996).

Matubayasi N : Mean-field Theory of Solutions: Chemical Potential and Solution Structure in the Superposition Approximation, *J. Chem. Phys*., **104**, 5265-5278 (1996).

II. Molecular Aggregates

Asami K: Dielectric Imaging of Biological Cells, *Colloid and Polym. Sci*., **273**, 1095-1097 (1995).

Asami K and Yonezawa T: Dielectric Behavior of Non-spherical Cells in Culture, *Biochim. Biophys. Acta*, **1245**, 317-324 (1995).

Nagaoka Y, Iida A, Kambara T, Asami K, Tachikawa E and Fujita T: Ion-channel-forming and Catecholamine-releasing Activities of Elongated and Truncated Analogues of Trichosporin-B, *J. Chem. Soc., Chem. Commun*., 2203-2204 (1995).

Asami K: Evaluation of Colloids by Dielectric Spectroscopy, *Hewlett-Packard Application Note*, **380** (3), 1-19 (1995).

Sato N, Oda M, Okuno T, Izuoka A and Sugawara T: Change of Electronic Absorption Spectra Observed through Heating Evaporated Thin Films of a Diacetylene Compound, *Mol. Cryst. Liq. Cryst*., **277**, 195-203 (1996).

Sato N and Yoshikawa M: Valence Electronic Structure at the Interface of Organic Thin Films, *J. Elect. Spectrosc. Relat. Phenom*., **78**, 387-390 (1996).

Shirotani I, Takeda K, Onuma F and Sato N: Electrical Properties of Thin Films of Bis(1,2-benzoquinone dioximato)platinum(II), $Pt(bqd)_2$, *Mol. Cryst. Liq. Cryst*., **285**, 119-124 (1996).

Nagaoka Y, Iida A, Kambara T, Asami K and Fujita T: Role of Gln7 in the Ion-channel-forming Properties of

the Peptaibol Trichosporin-B-VIa, *J. Chem. Soc., Chem. Commun*., 1079-1080 (1996).

Asami K, Yonezawa T, Wakamatsu H and Koyanagi N: Dielectric Spectroscopy of Biological Cells, *Bioelectrochem. Bioenerg*., **40,** 141-145 (1996).

Matsubara A, Asami K, Akagi A and Nishino N: Ion-channels of Cyclic Template-assembled Alamethicins that Emulate the Pore Structure Predicted by Barrel-Stave Model, *J. Chem. Soc., Chem. Commun*., 2069-2070 (1996).

Asami K and Yonezawa T: Dielectric Behavior of Wild-type Yeast and Vacuole-deficient Mutant over a Frequency Range of 10kHz to 10GHz, *Biophys. J*., **71**, 2192-2200 (1996).

Nagaoka Y, Iida A, Kambara T, Asami K, Tachikawa E and Fujita T: Role of Proline Residue in the Channel-froming and Catecholamine-releasing Activities of the Peptaibol, Trichosporin-B-Via, *Biochim. Biophys. Acta*, **1283**, 31-36 (1996).

Wada S, Iida A, Asami K and Fujita T: Ion Channel-forming Property of Trichorovin-XII, an 11-residue Peptaibol from the Fungus Trichoderma viride, in Planar Lipid Bilayer Membranes, *Bioorga. Medicin. Chem. Lett*., **6**, 2275-2278 (1996).

Yoshida H, Terasaki A and Kondow T: Photoelectron Spectroscopy of Co_n^- and Product Anions of Co_n^- with O_2 and N_2, *Surf. Rev. Lett*., **3**, 667-670 (1996).

Iseda M, Nishio T, Yoshida H, Terasaki A and Kondow T: Electronic Structure of Vanadium Cluster Anions - Measurement and DV-$X\alpha$ Calculation of Photoelectron Spectra, *The Science Reports of the Research Institutes, Tohoku University, Ser. A, Tohoku University* **A41,** 215-218 (1996).

III. Separation Chemistry

Umetani S, Le T H Q, Tomita T, and Matsui M: Design of Novel ß-Diketones of High Selectivity: Role of the Distance of the Two Donating Oxygens in *"Value Adding through Solvent Extraction"* (Shallcross D C, Paimin R, and Prvcic L M, Eds), The University of Melbourne, Melbourne, **1**, 347-352 (1996).

Tsurubou S, Sasaki T, Umetani S, and Matsui M: Highly Selective Extraction-Separation System Utilizing Macrocyclic Ionophores as Masking Reagents in *"Value Adding through Solvent Extraction"* (Shallcross D C, Paimin R, and Prvcic L M, Eds), The University of Melbourne, Melbourne, **1**, 623-628 (1996).

Matsui M: Ligand Design for Ion Size Recognition, *Bunseki Kagaku*, 45, 209-223 (1996) (in Japanese).

Kokusen H, Sohrin S, Matsui M, Hata Y, and Hasegawa H: Selectivity Design Using Interligand Contact: Solvent Extraction and Structures of First-series-transition Metal-bis(pyrazol-1-yl)borate Complexes, *J. Chem Soc., Dalton Trans*., 195-201 (1996).

Fujino O, Umetani S, Matsui M, Nishida S, Sanada K, and Orimi K: Determination of Rare Earth Elements, Uranium and Thorium in Apatite Minerals by Inductively Coupled Plasma-Mass Spectrometry, *Nippon Kagaku Kaishi*, 650-655 (1996) (in Japanese).

Li Q, Zhou D, Yao G, Huang C, Umetani S, and Matsui M: Synthesis, Fluorescence Characteristics and Langmuir-Blodgett Film of a Green Strongly Fluorescent Terbium-Isobutyryl Pyrazolone Complex, *Chem. J. Chinese Univ*., **17**, 1016-1018 (1996) (in Chinese).

Sasaki T, Umetani S, Le T H Q, Matsui M, and Tsurubou S: Improved Extraction-Separation of Alkaline Earths and Lanthanides with the Aid of an Ion Size Selective Masking Reagent, *Analyst*, **121**, 1051-1054 (1996).

Ying L, Yu A, X Zhao X, Li Q, Zhou D, Huang C, Umetani S, and Matsui M: Excited State Properties and Intramolecular Energy Transfer of Rare-Earth Acylpyrazolone Complexes, *J. Phys. Chem*., **100**, 18387 - 18391 (1966).

Zhou D, Huang C, Luo C, Yao G, Xu J, Li T, Umetani S, and Matsui M: Synthesis, Luminescent Properties and Langmuir Films of Four New Amphiphilic N-Hexadecyl Pyridinium Tetrakis(3-phenyl-4-benzoyl-5-isoxazolone) Lanthanide Complexes, *Chem. J. Chinese Univ*., **17**, 1828-1832 (1996) (in Chinese).

SOLID STATE CHEMISTRY

I. Artificial Lattice Allolys

Kikuchi H, Nagasawa H, Mibu K, Ono T, Hosoito N and Shinjo T: Susceptibility Measurements of the Haldane System $NiC_2O_4 \cdot$ (2DMIz Doped with Nonmagnetic Zn Ions, *J.Phys.Soc.Jpn*., **64**, 3429-3433(1995).

Levy P M, Zhang S, Ono T and Shinjo T: Electrical Transport in Corrugated Multilayered Structures, *Phys.Rev.B*, **52**, 16049-16054 (1995).

Passamani E C, Baggio-Saitovitch E, Mibu K and Shinjo T: ^{151}Eu Mössbauer Study of Transition-Metal/ Eu Multilayers, *Phys.Rev.B*, **53**, 6566-6571(1995).

Sugimoto T, Ueda K, Kanehisa N, Kai Y, Shiro M, Hosoito N, Takeda N and Ishikawa M: Weak-Ferromagnetism and Ferromagnetism in Tetrafluorotetracyanoquinodimethanide Salts, *ACS Symposium Series 644, Molecule-Based Magnetic Materials, Theory, Techniques, and Applications*, Chap.19, 276-295 (1996).

Sugimoto T, Ueda K, Tsujii M, Fujita H, Hosoito N, Kanehisa N, Shibamoto Y and Kai Y: Ferromagnetic Behavior of a Tetrafluorotetracyanoquinodimethanide Salt at Roo.m Temperature, *Chem.Phys.Lett*., **249**, 304-308(1996).

Ueda K, Tsujii M., Suga T, Sugimoto T, Kanehisa N, Kai Y and Hosoito N: Remarkably Strong Antiferromagnetic Interaction through an Intervening Hydrogen Atom in N-(*n*-propyl)pyridinium-substituted Imidazolin-1-oxyl Iodide, *Chem.Phys.Lett*., **253**, 355-360 (1996).

Ueda K, Sugimoto T, Endo S, Toyota N, Hohama M, Yamamoto K, Suenaga Y, Morimoto H, Yamaguchi T, Munakata M, Hosoito N, Kanehisa N, Shibamoto Y and Kai Y: 1:2 TCNQ/$TCNQ^-$ (Mixed Salts Exhibiting Ferromagnetic Behavior at Room Temperature, *Chem.Phys.Lett*., **261**, 295-300(1996).

Kobayashi Y, Nasu S, Emoto T and Shinjo T: ^{197}Au and ^{57}Fe Mössbauer Study of Au/Fe Multilayers, *Conf.Proc. Vol. 50, "ICAME-95"*, SIF, Bologna, 619-622(1996).

Tappert J, Keune W, Brand R A , Vulliet P, Sanchez J -P and Shinjo T: Magnetism and Structure of Dy/Fe Multilayers Studied by ^{57}Fe and ^{161}Dy Mössbauer Spectroscopy, *J.Appl.Phys*., **80**, 4503-4511(1996).

Shinjo T and Ono T: Magnetoresistance of Multilayers on Microstructured Substrates, *J.Magn.Magn.Mater*., **156**, 11-14(1996).

Kobayashi Y, Nasu S, Emoto T and Shinjo T: ^{197}Au Mössbauer Study of Au/M (M=Fe, Co, Ni) Multilayers, *J.Magn.Magn.Mater*., **156**, 45-46(1996).

Emoto T, Hosoito N and Shinjo T: Spin Penetration in Au Layers: ^{119}Sn Mössbauer Study of Co/Au Multilayers, *J.Magn.Magn.Mater*., **156**, 47-48(1996).

Mibu K, Nagahama T and Shinjo T: Magnetoresistance Studies of Multilayers Including Hard Magnetic CoSm Layers, *J.Magn.Magn.Mater*., **156**, 299-300(1996).

Hosoito N, Mibu K, Ono T, Emoto T and Shinjo T: Relationship between Magnetoresistance Change and Antiparallel Magnetization Estimated by Neutron Diffraction in Giant Magnetoresistance Systems, *J. Magn. Magn.Mater*., **156**, 325-326(1996).

Trhlík M, Mibu K, De Moor P, Pari P P, Rotter M, Severijns N, Shinjo T, Van Geert A and Vanneste L: Evidence for Perpendicular Magnetic Anisotropy of Tb in Tb/Fe Multilayers, *J.Phys.: Condens. Matter*, **8**, 8907-8913(1996).

Kobayashi Y, Aoki Y, Sato H, Ono T and Shinjo T: Hall Effect and Thermoelectric Power in Multilayers Prepared on Microstructured Substrate, *J.Phys.Soc.Jpn*., **65**, 1910-1913(1996).

Ono T, Shugita Y and Shinjo T: Magnetization Relaxation in Multilayer Wire Arrays Observed by GMR Effect, *J.Phys.Soc.Jpn*., **65**, 3021-3024(1996).

Shinjo T: Recent Progress in Preparation of Metallic Multilayers, *Materia*, **35**, 190-195(1996) (in Japanese).

Nagahama N, Mibu K and Shinjo T: Spring Magnetization Process of Hard-Magnetic/Soft-Magnetic Bilayers, *Nippon Oyo Jiki Gakkaishi*, **20**, 389-392(1996) (in Japanese).

Ono T, Sugita Y and Shinjo T: GMR Effect of Multilayers Prepared on Microstructured Substrates, *Nippon Oyo Jiki Gakkaishi*, **20**, 397-400(1996) (in Japanese).

Shinjo T: Magnetic Structure and Magnetoresistance of Metallic Multilayers, *Thin Solid Films*, **281-282**, 469-473(1996).

II. Artificial Lattice Compounds

Kusano Y, Kikuchi T, Takada J, Ikeda Y, Takano M and Bando Y: Phases and their Relations in the $BaO(BaCO_3)$-CaO-CuO System. *Funtai oyobi Funmatsu Yakin* **43**, 157-161 (1996) (in Japanese).

Kikuchi T, Kusano Y, Takada J, Ikeda Y, Takano M and Bando Y: Phases and their Relations in the $YO_{1.5}$-$BaO(BaCO_3)$-SrO-CuO System. *Funtai oyobi Funmatsu Yakin* **43**, 162-167 (1996) (in Japanese).

Kiyama T, Yoshimura K, Kosuge K, Ikeda Y and Bando Y: Invar Effect of $SrRuO_3$: Itinerant Electron Magnetism of Ru 4d electrons. *Phys. Rev. B* **54**, R756-R759 (1996).

Kiyama T, Yoshimura K, Kosuge K, Ikeda Y and Bando Y: Itinerant Electron Magnetism of (Sr-Ca)RuO_3 System -Invar Effect-. *Funtai oyobi Funmatsu Yakin* **43**, 1090-1094 (1996) (in Japanese).

Takada J, Ikeda Y and Takano M: Phases and their Relationships in the Bi-Pb-Sr-Ca-Cu-O System. Bismuth-Based *High-Temperature Superconductors, Applied Physics (ed. Maeda H and Togano K), Marcel Dekker, Inc., New York* **6**, 93-128 (1996).

Terashima T, Komai E, Nakazawa K, Bando Y, Kawahara T and Suzuki T: Electric Field Effects in $YBa_2Cu_3O_{7-\delta}$ Ultrathin Films. *Proceedings of the Seventh US-Japan Workshop on High-T_c Superconductors, Oct. 24-25, 1995, Tsukuba, Japan (ed. Tachikawa K, Kitazawa K, Togano K and Muromachi E)*, 184-187 (1996).

Kawahara T, Suzuki T, Komai E, Nakazawa K, Terashima T and Bando Y: Electric-Field Effect on Transport and Superconducting Properties of $YBa_2Cu_3O_{7-x}$. *Physica C* **266**, 149-156 (1996).

Tsuchiya Y, Kosuge K, Ikeda Y, Shigematsu T, Yama guchi S and Nakayama N: Non-Stoichiometry and Antiferromagnetic Phase Transition of NaCl-Type CrN Thin Films Prepared by Reactive Sputtering. *Materials Transactions, JIM* **37**, 121-129 (1996).

III. Multicomponent Materials

Kawasaki S, Takano M and Takeda Y: Ferromagnetic Properties of $AFe_{1-x}Co_xO_3$ (A=Sr, Ca). *Funtai oyobi Funmatsu Yakin* **43**, 1001-1006 (1996) (in Japanese).

Kikuchi T, Kusano Y, Takada J, Ikeda Y, Takano M and Bando Y: Phases and their Relations in the $YO_{1.5}$-$BaO(BaCO_3)$-SrO-CuO System. *Funtai oyobi Funmatsu Yakin* **43**, 162-167 (1996) (in Japanese).

Takeda Y, Okazoe C, Imanishi N, Yamamoto O, Takano M and Kanno R: Electrochemical Oxidation of $Ca_{1-x}Sr_xFeO_{3-z}$ and $SrFe_{1-x}Co_xO_{3-z}$ Systems. *Funtai oyobi Funmatsu Yakin* **43**, 1095-1098 (1996) (in Japanese).

Nishiyama M, Tanaka N, Maegawa S, Oyamada A and Takano M: Magnetic Properties of Kagomé Lattice Antiferromagnets, $RFe_3(OH)_6(SO_4)_2$ [R=NH_4, Na]. *Proceedings of the 21st International Conference on Low Temperature Physics, Aug. 8-14, 1996*, 2053-2054 (1996).

Kusano Y, Kikuchi T, Takada J, Ikeda Y, Takano M and Bando Y: Phases and their Relations in the $BaO(BaCO_3)$-CaO-CuO System. *Funtai oyobi Funmatsu Yakin* **43**, 157-161 (1996) (in Japanese).

Chmaissem O, Jorgensen J D, Yamaura K, Hiroi Z, Takano M, Shimoyama J and Kishio K: Crystal Structures of Hg-Sr-Ca-Cu-O Superconductors with

Enhanced Flux Pinning: $Hg_{1-x}Re_xSr_2Ca_{n-1}Cu_nO_{2n+2+\delta}$ (n=2,3; x≈0.2-0.25). *Phys. Rev. B* **53**, 14647-14655 (1996).

Okazoe C, Takeda Y, Imanishi N, Yamamoto O, Takano M and Kanno R: Oxygen Doping in $SrFe_{1-x}Co_xO_3$ Perovskite Oxides by the Electrochemical Method. *Solid State Ionics* **86-88**, 1431-1435 (1996).

Maegawa S, Nishiyama M, Tanaka N, Oyamada A and Takano M: Observation of Successive Phase Transitions in Kagomé Lattice Antiferromagnets $RFe_3(OH)_6(SO_4)_2$ [*R*=NH_4, Na, K]. *J. Phys. Soc. Jpn.* **65**, 2776-2778 (1996).

Hiroi Z, Kobayashi N and Takano M: Synthesis, Structure, and Superconductivity of $Ca_{2-x}Na_xCuO_2C_{l2}$. *Physica C* **266**, 191-202 (1996).

Saitoh T, Mizokawa T, Fujimori A, Takeda Y and Takano M: Electronic Structure and Magnetism in Valence-Control $La_{1-x}Sr_xCoO_3$. *J. Electron Spectroscopy and Related Phenomena* **78**, 195-198 (1996).

Takada J, Ikeda Y and Takano M: Phases and their Relationships in the Bi-Pb-Sr-Ca-Cu-O System. *Bismuth-Based High-Temperature Superconductors, Applied Physics (ed. Maeda H and Togano K), Marcel Dekker, Inc., New York* **6** 93-128 (1996).

Hiroi Z, Shimoyama J and Kishio K: Microscopic Segregation in Intergrowth Layers of $(Hg,Re)Ba_2Ca_{n-1}Cu_nO_y$. *Physica C* **257**, 210-216 (1996).

Hiroi Z: New Cu Oxide Qvantum Spin Ladder Compound $La_{1-x}S_{rx}Cu\ O_{2.5}$ *Kotai Butsuri* **31**, 131-136 (1996) (in Japanese).

Ishida K, Kitaoka Y, Tokunaga Y, Matsumoto S, Asayama K, Azuma M, Hiroi Z and Takano M: Spin Correlation and Spin Gap in Quasi-One-Dimensional Spin-1/2 Cuprate Oxides: A ^{63}Cu NMR Study. *Phys. Rev. B* **53**, 2827-2834 (1996).

Sarma D D, Shanthi N, Krishnakumar S R, Saitoh T, Mizokawa T, Sekiyama A, Kobayashi K, Fujimori A, Weschke E, Meier R, Kaindl G, Takeda Y and Takano M: Temperature-Dependent Photoemission Spectral Weight in $La_{0.6}Sr_{0.4}MnO_3$. *Phys. Rev. B* **53**, 6873-6876 (1996).

Kawasaki S, Takano M and Takeda Y: Ferromagnetic Properties of $SrFe_{1-x}Co_xO_3$ Synthesized under High Pressure. *J. Solid State Chem.* **121**, 174-180 (1996).

Ishida K, Tokunaga Y, Kitaoka Y, Asayama K, Azuma M, Hiroi Z and Takano M: Antiferromagnetic Nuclear Resonance of Cu in Infinite-Layer Compounds, $SrCuO_2$ and $Ca_{0.9}Sr_{0.1}CuO_2$ -Comparison between Hyperfine Coupling Constant in a CuO_2 Plane and in a Spin-Ladder System-. J. *Phys. Soc. Jpn.* **65**, 329-330 (1996).

Eccleston R S, Azuma M and Takano M: Neutron-Scattering and Susceptibility Study of Spin Chains and Spin Ladders in $(Sr_{0.8}Ca_{0.2})_{14}Cu_{24}O_{41}$. *Phys. Rev. B* **53**, R14721-R14724 (1996).

Takano M: Spin Ladder Compounds. *Physica C* **263**, 468-474 (1996).

Hiroi Z: $La_{1-x}SrxCuO_{2.5}$ as a Doped Spin-Ladder Compound. *J. Solid State Chem.* **123**, 223-235 (1996).

Oka Y, Yao T, Yamamoto N, Ueda Y, Kawasaki S, Azuma M and Takano M: Hydrothermal Synthesis, Crystal Structure, and Magnetic Properties of $FeVO^4$II. *J. Solid State Chem.* **123**, 54-59 (1996).

Matsumoto S, Kitaoka Y, Ishida K, Asayama K, Hiroi Z, Kobayashi N and Takano M: Competition between the Singlet-Spin Liquid State and the Magnetic Ground State in a Two-Chain Spin-1/2 Antiferromagnetic Ladder Compound $LaCuO^{2.5}$: A ^{63}Cu NMR Study. *Phys. Rev. B* **53**, R11942-R11945 (1996).

Kishio K, Shimoyama J, Yamaura K, Hiroi Z, Takano M, Chmaissem O and Jorgensen J D: Chemical Stabilization and Flux Pinning in Hg-Based Superconductors. *Advances in Superconductivity VIII: Proceedigns of the 8th International Symposium on Superconductivity (ISS'95), Oct. 30-Nov. 2, 1995, Hamamatsu, Japan (ed. Hayakawa H and Enomoto Y), Springer-Verlag Tokyo, Hong Kong*, 279-284 (1996).

IV. Amorphous Materials

Zhao G, Kozuka H and Yoko T: Photoelectrochemical Properties of Dye-Sensitized TiO_2 Films Containing Dispersed Gold Metal Particles Prepared by Sol-Gel Method, *J. Ceram. Soc. Jpn.*, **104**, 164-168 (1996).

Ohyama M, Kozuka H, Yoko T and Sakka S: Preparation of ZnO Films with Preferential Orientation by Sol-Gel Method, *J. Ceram. Soc. Jpn.*, **104**, 296-300 (1996).

Sakai H, Jin JS and Yoko T: The Local Structure of Antimony Ions in Silicate Glasses, *NEW GLASS*, **11**, 27-34 (1996) (in Japanese).

Jin JS, Kozuka H, Yoko T, and Fukunaga T : Structure of Y-Ba-Si-O-N Glasses by Neutron Diffraction, *phys. stat. sol. (b)*, **193**, 295-306 (1996).

Terashima K, Kim SH and Yoko T: Nonlinear Optical Properties of B_2O_3-Based Glasses: Binay Ag_2O-B_2O_3 and Ternary AgX-Ag_2O-B_2O_3 (X=Cl, Br and I) Glasses, *Phys. Chem. Glasses*, **37**, 129-33 (1996).

Fujihara S, Kozuka H, and Yoko T: Superconducting Properties of the Li-Substituted $YBa_2Cu_4O_8$ Prepared by the Sol-Gel Method, *J. Mater. Sci.*, **31**, 2975-79 (1996).

Hashimoto T and Yoko T: Phase-Matching of Rutile Single Crystal, *Appl. Phys. Lett.*, **68**, 2478-79 (1996).

Monde T, Kamiusuki T, Nakayama N, Nemoto F, Yoko T and Konakahara T: Thermal Decomposition of Branched-Polyfluoroalkylsilane Coated on Silica-Gels, *J. Ceram. Soc. Jpn.*, **104**, 682-684 (1996).

Innocenzi P, Kozuka H and Yoko T: Dimer-to-Monomer Transformation of Rhodamine 6G in Sol-Gel Silica Films, *J. Non-Cryst. Solids*, **201**, 26-36 (1996).

Uchino T and Yoko T: Low Frequency Raman Scattering and Fast Relaxation Process in Glycerol , *Science*, **273**, 480-483 (1996).

Miyaji F, Fujimine S, Yoko T and Sakka S: Electrical

Properties of Nonconventional Bi-R-Cu-O (R = Ca, Sr, Ba) Glasses, *J. Am. Ceram. Soc*., **79**, 1815-20 (1996).

Zhao G, Kozuka H and Yoko T: Photoelectrochemical Properties of Metal Particle Doped TiO_2 Films Prepared by Sol-Gel Method, *Thin Solid Films*, **277**, 147-154 (1996).

Uchino T and Yoko T: Ab Initio Cluster Model Calculations on the Boson Peak Frequencies of B_2O_3 Glass, *J. Chem. Phys*., **105**, 4140-4151 (1996).

Hashimoto T, Yamada T and Yoko T: Third-Order Nonlinear Optical Properties of Sol-Gel Derived α-Fe_2O_3 , γ-Fe_2O_3 and Fe_3O_4 Thin Films, *J. Appl. Phys.* **80**, 3184-90 (1996).

Terashima K, Hashimoto T, Uchino T, Kim SH and Yoko T: Structure and Nonlinear Optical Properties of Sb_2O_3-B_2O_3 Binary Glasses, *J. Ceram. Soc. Jpn*., **104**, 1008-14 (1996).

Yoko T, Hu LL , Kozuka H and Sakka S: Photoelectrochemical Properties of TiO_2 Coating Films Prepared Using Different Solvents by Sol-Gel Method, *Thin Solid Films*. **283**, 188-196 (1996).

Yoko T: Preparation and Characterization of Ceramic Coating Films by Sol-Gel Method, *New Ceramics*, **9**, 39-46 (1996) (in Japanese).

Hashimoto T and Yoko T: Sol-Gel Preparation and Nonlinear Optical Properties of Transition Metal Oxide Thin Films, *Mater. Trans., JIM*, **37**, 435-441 (1996).

Yoko T: Nonlinear Optical Inorganic Materials, *ELECTRONICS COMMUNICATIONS*, **No. 11**, 2-7 (1996) (in Japanese).

Uchino T and Yoko T: Ab Initio Cluster Model Calculations on the Vibrational Frequencies of TeO_2 Glass, *J. Non-Cryst. Solids*, **204**, 243-252 (1996).

Lin H, Seo WS, Kuwabara K, Di GQ, Uchiyama S and Koumoto K: Vapor-Growth of Bismuth on Oriented Organic Films, *J. Surf. Sci. Soc. Jpn*., **17(1)**, 31-37 (1996).

Lin H, Seo WS, Kuwabara K and Koumoto K: Crystallization of Hydroxyapatite under Langmuir Monolayers, *J. Ceram. Soc. Japan*, **104(4)**, 291-295(1996).

Di GQ, Lin H, Uchida N , Kurata Y, Koumoto K and Hasegawa S: Preparation of Three-Dimensionally Oriented Polycrystalline Si Film, *Appl. Phys. Lett*., **68(1)**, 69-71 (1996).

Lin H, Ando H, Seo WS, Kuwabara K and Koumoto K: Two-Dimensionally Oriented Organic Molecules as a Substrate for Vapor-Growth of Zinc Thin Films, *Thin Solid Films*, **281-282**, 521-524 (1996).

Lin H, Yanagi T, Seo WS, Kuwabara K and Koumoto K: Crystal Growth of Hydroxyapatite under Two-Dimensionally Oriented Organic Films, *Bioceramics*, **9**, 371-374 (1996).

FUNDAMENTAL MATERIAL PROPERTIES

I. Molecular Rheology

Osaki K, Watanabe H, and Inoue T: Damping Function of the Shear Relaxation Modulus and the Chain Retraction Process of Entangled Polymers, *Macromolecules*, **29**, 3611-3614 (1996).

Watanabe H, Yao ML, and Osaki K: Comparison of Dielectric and Viscoelastic Behavior of Polyisoprene Solutions: Coherence in Subchain Motion, *Macromolecules*, **29**, 97-103 (1996).

Watanabe H, Sato T, and Osaki K: Viscoelastic Relaxation of Styrene-Butadiene Diblock Copolymer Micellar Systems. 1. Behavior in a Nonentangling, Short Polybutadiene Matrix, *Macromolecules*, **29**, 104-112 (1996).

Watanabe H, Sato T, and Osaki K: Viscoelastic Relaxation of Styrene-Butadiene Diblock Copolymer Micellar Systems. 2. Behavior in Entangling, Long Polybutadiene Matrices", *Macromolecules*, **29**, 113-118 (1996).

Watanabe H, Urakawa O, Yamada H, and Yao ML: Dielectric Relaxation of cis-Polyisoprene Chains in Oligo- and Polybutadiene Matrices: Matrix Effects on Mode Distribution and Relaxation Time, *Macromolecules*, **29**, 755-763 (1996).

Balsara NP, Dai HJ, Watanabe H, Sato T, and Osaki K: Influence of Defect Density on the Rheology of Ordered Block Copolymers, *Macromolecules*, **29**, 3507-3510 (1996).

Sato T, Watanabe H, Osaki K, and Yao ML: Relaxation of Spherical Micellar Systems of Styrene-Isoprene Diblock Copolymers. 1. Linear Viscoelastic and Dielectric Behavior", *Macromolecules*, **29**, 3881-3889 (1996).

Watanabe H, Sato T, Osaki K, and Yao ML: Relaxation of Spherical Micellar Systems of Styrene-Isoprene Diblock Copolymers. 2. Nonlinear Stress Relaxation Behavior", *Macromolecules*, **29**, 3890-3897 (1996).

Sato T, Watanabe H, and Osaki K: Rheological and Dielectric Behavior of a Styrene-Isoprene-Styrene Triblock Copolymer in n-Tetradecane: 1. Rubbery-Plastic-Viscous Transition, *Macromolecules*, **29**, 6231-6239 (1996).

Watanabe H, Yao ML, Yamagishi A, Osaki K, Shikata T, Niwa H, and Morishima Y: Nonlinear Rheological Behavior of a Concentrated Spherical Silica Suspension, *Rheol. Acta*., **35**, 433-445 (1996).

Inoue T and Osaki K: Role of polymer chain flexibilty on the viscoelasticity around the glass transition zone, *Macromolecules*, **29**, 1595-1599 (1996).

Inoue T, Okamoto H, Mizukami Y, Matsui H, Watanbe H, Kanaya T and Osaki K: Dynamic birefringence of vinyl polymers, *Macromolecules*, **29**, 6240-6245 (1996).

Inoue T and Osaki K: Viscoelastic properties and bire-

fringence of amorphous polymers around the glass transition region, *Kobunshi Ronbunshu*, **53**, 602-603 (1996))(in Japanese).

Inoue T and Osaki K: On the Strain-Induced Birefringence of Glassy Polymers, *Polymer J*., **28**, 76-79 (1996).

Inoue T and Osaki K: Viscoelastic properties of amorphous polymers, Koubunsi Kakou, **46**, 50-56 (1996) (in Japanese).

Ryu T, Inoue T and Osaki K: A Simple Evaluation Method of Stress-Optical Coefficeint of Polymers, *Nihon Reoroji Gakkaishi*, **24**, 129-132 (1996).

Ediger M D, Inoue T, Cicerone M T and Blackburn F R: Probe Rotation near and below The Glass Transition Temperature, Relationship to Viscoelasticity and Physical Aging: *Macromol. Symp*., **101**, 139 (1996).

II. Polymer Materials Science

Kanaya T, Kawaguchi T and Kaji K: Fast Process of Amorphous Polystyrene below and above the Glass Transition Temperature Tg as Studied by Quasielastic Neutron Scattering, *J. Chem. Phys*., **104**, 3841-3850 (1996).

Nagano K, Kanaya T, Fukunaga T and Mizutani U: Amorphization of PVA Powder by Mechanical Milling, *Funtai and Funmatsuyakin*, **43**, 726-730 (1996) (in Japanese).

Yamamuro O, Matsuo T, Takeda K, Kanaya T, Kawaguchi T and Kaji K: Inelastic Neutron Scattering Study of Low-energy Excitations in Glassy 1-Butene, *J. Chem. Phys*., **105**, 732-737 (1996).

Zorn R, Kanaya T, Kawaguchi T, Richter D and Kaji K: Infuluence of the Microstructure in the Incoherent Neutron Scattering of Glass-forming Polybutadienes, *J. Chem. Phys*., **105**, 1189-1197 (1996).

Kanaya T, Imai M and Kaji K: Low-energy Excitation of Amorphous and Semicrystalline Poly(ethylene terephthalate), *Physica*, **B226**, 82-85 (1996).

Kanaya T, Kawaguchi T and Kaji K: Microscopic View of Glass Transition Dynamics. A Quasielastic Neutron Scattering Study on trans-1,4-Polychloroprene, *J. Chem. Phys*., **105**, 4342-4349 (1996).

Kanaya T, Miyakawa M, Kawaguchi T and Kaji K: Annealing Effects on Low-energy Excitation of Amorphous Poly(methyl methacrylate), *Non Equilibrium Phenomena in Supercooled Fluids, Glasses and Amorphous Materials*, edited by Giordano M, Leporini D and Tosi M P (World Scientific, Singapore, 1996), p.301-302.

Fukunaga T, Nagano K, Kanaya T and Mizutani U: Formation of Amorphous Poly(vinyl alcohol) by Means of Mechanical Milling, *Kobunshi-Ronbunshu*, **53**, 665-669 (1996) (in Japanese)

Kanaya T and Kaji K: Microscopic View of Dynamics of Polymer Glasses and Glass Transition, *Kobunshi-Ronbunshu*, **53**, 648-659 (1996) (in Japanese).

Sakai Y, Imai M, Kaji K and Tsuji M: Growth Shape Observed in Two-dimensional Poly (ethylene terephthalate) Spherulites, *Macromolecules*, **29**, 8830-8834 (1996)

III. Molecular Motion Analysis

Horii F, Hu S, Deguchi K, Sugisawa H, Ohgi H and Sato T: ^{1}H CRAMPS Spectra of Poly(vinyl alcohol) Films with Different Tacticities, *Macromolecules*, **29**, 3330-3331 (1996).

Ishida M, Yoshinaga K and Horii F: Solid-State ^{13}C NMR Analyses of the Microphase-Separated Structure of Polyurethane Elastomer, *Macromolecules*, **29**, 8824-8829 (1996).

Egawa Y, Imanishi S, Matsumoto A and Horii F: Solid-State ^{13}C NMR Study on Miscibility of Polyoxymethylene/terpenephenol Blends, *Polymer*, **37**, 5569-5575 (1996).

Yamamoto H, Horii F and Hirai A: *In Situ* Crystallization of Bacterial Cellulose. II. Influences of Different Polymeric Additives on the Formation of Celluloses I_α and I_β at the Early Stage of Incubation, *Cellulose*, **3**, 229-242 (1996).

Horii F: Orientation of Polymers as Revealed by Multi-Dimentional Solid-State NMR, *Koubunshi*, **45**, 856-856 (1996) (in Japanese).

Nonaka Y and Horii F: Development of Speaker Cones Using Tunicate Cellulose, *Cellulose Commun*. **3**, 41-44 (1996) (in Japanese).

Horii F, Kaji H, Ishida H, Kuwabara K and Masuda K: Solid-State NMR Analyses of Structure and Dynamics of Polymers in the Difference States, *Proc. Soc. Solid-State NMR Mat*., **20**, 21-25 (1996).

Tsunashima Y: Dilute Solution Properties of Functional Polysaccharides, *Cellulose Commun*. **3**, 13-17 (1996) (in Japanese).

Tsunashima Y: Block Copolymer Micelles in Solution, *Koubunshi*, **45**, 482-486 (1996) (in Japanese).

Tsunashima Y, Hashimoto T and Nakano T: First and Second Concentration-Dependent Coefficients of Translational Diffusion and Sedimentation for Poly(α-methylstyrene) in a Good Solvent, *Macromolecules*, **29**, 3475-3484 (1996).

ORGANIC MATERIALS CHEMISTRY

I. Polymeric Materials

Ide N, Fukuda T and Miyamoto T: Gelation of Fully Acylated Cellobiose in n-Alkane Solution, *Bull. Chem. Soc. Jpn*., **68**, 3423-3428 (1995).

Bedekar B A, Tsujii Y, Ide N, Kita Y, Fukuda T and Miyamoto T: Dielectric Relaxation of Cyanoethylated Poly(2,3-dihydroxypropyl methacrylate), *Polymer*, **36**, 4735-4740 (1995).

Miyamoto T: Future Development of Cellulose Chem-

istry and Technology, *Ann. High Performance Paper Soc., Jpn*., **34**, 2-7 (1995) (in Japanese).

Fukuda T, Fujimoto K, Tsujii Y and Miyamoto T: Orientation-Dependent Interactions in Polymer Systems. 6. Effect of Segmental Orientation on Polymer Miscibility, *Macromolecules*, **29**, 3300-3302 (1996).

Fukuda T, Fujimoto K, Murakami M M, Kawabata K and Miyamoto T: Orientation-Dependent Interactions in Polymer Systems: Segmental Orientation, Miscibility and Self-organization, *Macromol. Symp*., **101**, 147-155 (1996).

Ide N, Tsujii Y, Fukuda T and Miyamoto T: Gelation Processes of Polymer Solutions. 1. Photodimerization of Free and Polymer-Bound Anthryl Groups, *Macromolecules*, **29**, 3851-3856 (1996).

Fukuda T and Terauchi T: Mechanism of "Living" Radical Polymerization Mediated by Stable Nitroxyl Radicals, *Chem. Lett*., 293-294 (1996).

Fukuda T, Terauchi T, Goto A, Tsujii Y and Miyamoto T: Well-Defined Block Copolymers Comprising Styrene-Acrylonitrile Random Copolymer Sequences Synthesized by "Living" Radical Polymerization, *Macromolecules*, **29**, 3050-3052 (1996).

Fukuda T, Terauchi T, Goto A, Ohno K, Tsujii Y and Miyamoto T: Mechanisms and Kinetics of Nitroxide-Controlled Free Radical Polymerization, *Macromolecules*, **29**, 6393-6398 (1996).

Yamamoto S, Tsujii Y, Yamada K, Fukuda T and Miyamoto T: Langmuir-Blodgett Films of A Glucose Residue-Carrying Amphiphilic Block Copolymer Studied by Surface Plasmons and Transmission Electron Microscopy, *Langmuir*, **12**, 3671-3674 (1996).

Okamura H, Minoda M, Komatsu K and Miyamoto T: Synthesis of Disubstituted Dihydro[60]fullerenes with Well-defined Structure by Addition of 1-Alkoxy-1-chloroethane to 2-(1-Octynyl)-1,2-dihydro[60]fulleren-1-ide Ion, *J. Org. Chem*., **61**, 8500-8502 (1996).

Matsui M, Murase Y, Ohwaki S, Iohara K and Miyamoto T: Ultra-High Speed Spinning of Poly(ethylene 2,6-naphthalenedicarboxylate) (PEN), *Koubunshi Ronbunshu*, **53**, 294-301 (1996) (in Japanese).

Gilbert R D, Buback M, Fukuda T et al.: Critically-Evaluated Propagation Rate Coefficients in Free Radical Polymerizations I. Styrene and Methyl Methacrylate, *Pure Appl. Chem*., **68**, 1491-1494 (1996).

Matsumoto M, Tsujii Y, Nakamura K and Yoshimoto T: A Trough with Radical compression for Studies of Monolayers and Fabrication of Langmuir-Blodgett Films: *Thin Solid Films*, **280**, 238-243 (1996).

Miyamoto T and Yamada K: Synthesis of Glycopolymers and Their Application to Biofunctional Materials, *Kobunshi*, **45**, 553-557 (1996) (in Japanese).

Miyamoto T, Nishimura H, Long M and Donkai N: Synthesis of New Types of Temperature-Responsive Cellulose Derivatives, *Kasen-Kouenshu*, **53**, 31-42 (1996) (in Japanese).

Fukuda T: Molecular Properties versus Thermotropicity in Cellulose Derivatives, *Cell. Commun*., **3**, 23-26 (1996) (in Japanese).

Mizutani C, Tsujii Y and Fukuda T: Effect of Fiber Structure on Heat of Wetting of Cotton and Regenerated Cellulose Fibers for Sports Underwear, *Descente Sports Science*, **17**, 77-86 (1996).

Fukuda T, Tsujii Y and Miyamoto T: Applications of Nitroxide-Controlled Free Radical Polymerization to Synthesis of New Polymer Materials, *Proceedings of ICRIS'96*, 142-146 (1996).

Tsujii Y, Minoda M, Fukuda T and Miyamoto T: Synthesis and Interfacial Properties of Amphiphilic Block Copolymer with Pendant Glucose Residues, *Proceedings of ICRIS'96*, 147-150 (1996).

Kokubo T, Miyaji F, Minoda M and Miyamoto T: Apatite Formation on Organic Polymers, *Proceedings of ICRIS'96*, 151-154 (1996).

II. High-Pressure Organic Chemistry

Kaneta N, Mitamura F, Uemura M, Murata Y and Komatsu K: Electronic Interaction of Tricarbonylchromium-Complexed Benzene with a Facing Aryl Ring in the 1,8-Diarylnaphthalene System, *Tetrahedron Lett*., **37**, 5385-5388 (1996).

Komatsu K, Takimoto N, Murata Y, Wan T S M and Wong T: Synthesis and Properties of Dialkyl Derivatives of Di[60]fullerenylbutadiene and Di[60]fullerenylacetylene: the Buckydumbbells, *Tetrahedron Lett*., **37**, 6153-6156 (1996).

Murata Y, Komatsu K and Wan T S M: The Reaction of [60]Fullerene with Lithium Fluorenide: Formation of a Novel 1,4-Adduct of [60]Fullerene, *Tetrahedron Lett*., **37**, 7061-7064 (1996).

Murata Y, Motoyama K, Komatsu K and Wan T S M: Synthesis, Properties, and Reactions of a Stable Carbanion Derived from Alkynyldihydrofullerene: 1-Octynyl-C_{60} Carbanion, *Tetrahedron*, **52**, 5077-5090 (1996).

Komatsu K, Murata Y, Wang G-W and Wan T S M: Novel Nucleophilic Addition Reactions Leading to New Derivatives of Fullerene C_{60}: *Fullerens: Recent Advances in the Chemistry and Physics of Fullerenes and Related Materials*, **3**, 1200-1211 (1996).

Wang G-W, Murata Y, Komatsu K and Wan T S M: The Solid-Phase Reaction of [60]Fullerene: Novel Addition of Organozinc Reagents, *Chem. Commun*., 2059-2060 (1996).

Okamura H, Murata Y, Minoda M, Komatsu K, Miyamoto T and Wan T S M: Synthesis of Disubstituted 1,2-Dihydro[60]fullerenes with Well-Defined Structure by Addition of 1-Alkoxy-1-chloroethanes to 2-(1-Octynyl)-1,2-dihydro[60]fulleren-1-ide Ion, *J. Org. Chem*., **61**, 8500-8502 (1996).

Komatsu K: Synthesis and Properties of Cyclic π-Conjugated Hydrocarbons Surrounded by Rigid ρ-Frameworks the Effects of C-C Hyperconjugation, *J. Synth. Chem. Jpn*., **54**, 868-878 (1996).

Kudo K, Oida Y, Mitsuhashi K, Mori S, Komatsu K and Sugita N: Hydrocarbonylation of Enol Esters Catalyzed by a Palladium(II) Complex, *Bull. Chem. Soc. Jpn*., **69**, 1337-1345 (1996).

Prassides K, Keshavarz-K M, Hummelen J C, Andreoni W, Giannozzi P, Beer E, Bellavia C, Cristofolini L, Gonzalez R, Lappas A, Murata Y, Malecki M, Srdanov V and Wudl F: Isolation, Structure, and Electronic Calculations of the Heterofullerene Salt $K_6C_{59}N$, *Science*, **271**, 1833-1835 (1996).

Komatsu K, Yoshida Z: Cyclopropenylium Salts, In *Houben-Weyl, Methods of Organic Chemistry*, G. Thieme Verlag, Stuttgart, **E17d**, 3079-3192 (1996).

SYNTHETIC ORGANIC CHEMISTRY

I. Synthetic Design

Tamao K, Nakamura K, Ishii H, Yamaguchi S, Shiro M: Axially Chiral Spirosilanes via Catalytic Asymmetric Intramolecular Hydrosilation, *J. Am. Chem. Soc*., **118**, 12469-12470 (1996).

Tamao K, Nakamura K, Yamaguchi S, Shiro M, Saito S: New Chiral Diphosphines, 2,3-Bis(siloxy)-1,4-bis(diphenylphosphino)butanes and Their Cationic Rh(I) Complexes: Synthesis and Structures, *Chem. Lett*., 1007-1008 (1996).

Tamao K, Uchida M, Izumizawa T, Furukawa K, Yamaguchi S: Silole Derivatives as Efficient Electron Transporting Materials, *J. Am. Chem. Soc*., **118**, 11974-11975 (1996).

Kawachi A, Tamao K: The Different Modes of Reaction of Monoalkoxy- and Dialkoxy-phenylchlorosilanes with Lithium Metal: Selective Formation of [2-(Alkoxy)disilanyl]lithium vs (Dialkoxysilyl)lithium, *Organometallics*, **15**, 4653-4656 (1996).

Yamaguchi S, Tamao K: Theoretical Study on the Electronic Structure of 2,2'-Bisilole in Comparison with 1,1'-Bicyclopentadiene: σ^*-π^* Conjugation and Low-Lying LUMO as the Origin of Unusual Optical Properties of 3,3',4,4'-Tetraphenyl-2,2'-bisilole, *Bull. Chem. Soc. Jpn*., **69**, 2327-2334 (1996).

Tamao K, Asahara M, Kawachi A: The Differing Modes of Reaction of 1-(8-Dimethylamino-1-naphthyl)-1-hydrodisilane and 1-(1-naphthyl)-1-hydrodisilane in nickel-catalyzed reactions with acetylene: Formation of a Pseudo-Pentacoordinate Silole via Si-Si Bond Cleavage vs. Hydrosilation without Si-Si Bond Cleavage, *J. Organomet. Chem. (Corriu issue)*, **521**, 325-334 (1996).

Tamao K, Ohno S, Yamaguchi S: Silole-Pyrrole Cooligomers: Synthesis, Structure, and UV-vis Absorption Spectra, *Chem. Commun*. 1873-1874 (1996).

Toshimitsu A, Hirosawa C, Tamao K: Chiral Friedel-Crafts Alkylation of Aromatic Compounds Using Chiral Episulfonium Ions as Carbon Electrophiles, *Synlett*, 465-467 (1996).

Yamaguchi S, Tamao K: Synthesis, Structure, and Absorption Spectra of the Well-Defined 1,1'-Bicyclopentadiene Derivatives, *Tetrahedron Lett*., **37**, 2983-2986 (1996).

Tamao K, Kawachi A, Tanaka Y, Ohtani H, Ito Y: Synthetic Applications of Functionalized Silyl Anions: Aminosilyl Anions as Hydroxy Anion Equivalent, *Tetrahdron*, **52**, 5765-5772 (1996).

Toshimitsu A, Nakano K, Mukai T, Tamao K: Steric Protection of the Selenium Atom of Episelenonium Ion Intermediate to Prevent both the Racemization of the Chiral Carbon and the Selenophilic Attack of Carbon Nucleophiles, *J. Am. Chem. Soc*., **118**, 2756-2757 (1996).

Tamao K, Hayashi T, Ito Y: Anion Complexation by Bidentate Lewis Acidic Hosts, ortho-Bis(fluorosilyl) benzenes, *J. Organomet. Chem*., **506**, 85-91 (1996).

Tamao K, Yamaguchi S: Regio-Controlled Intramolecular Reductive Cyclization of Diynes, *Pure & Appl. Chem*., **68**, 139-144 (1996).

II. Fine Organic Synthesis

K. Tanaka, K. Otsubo, and K. Fuji: Tandem Michael-Horner-Wadsworth-Emmons Reaction of a,b-Unsaturated 2,6-Di-tert-butyl-4-metylphenyl Esters as a Convenient Method for the Preparation of d-Branched Allen Carboxylates, *Tetrahedron Lett*., **36**, 9513-9514 (1995).

F. Tanaka, M. Node, K. Tanaka, M. Mizuch, S. Hosoi, M. Nakayama, T. Taga, and K. Fuji: 1,1'-Binaphthalene-2,2'-diol as a Chiral Auxiliary. Diastereoselective Alkylation of Binaphthyl Esters, Complex-Induced Proximity Effects in Enolate Formation, and One-Step Synthesis of an Optically Active b-Substituted Ketone, *J. Am. Chem. Soc*. **117**, 12159-12171 (1995)

K. Fuji, T. Kawabata, Y. Kiryu, and Y. Sugiura: Ring Opening of Optically Active cis-Disubstituted Aziridino Alcohols: An Enantiodivergent Synthesis of Functionalized Amino Alcohol Derivatives, *Heterocycles* . **42**, 701-722 (1996)

M. Node, H. Imazato, R. Kurosaki, Y. Kawano, T. Inoue, K. Nishide, and K. Fuji: Asymmetric Syntheses of (-)-Aphanorphine and (-)-Eptazocine, *Heterocycles* , **42**, 811-819 (1996).

H. Ikeda, K. Fuji, and K. Tanaka: Preparation, Characterization and DNA Photocleavage of Diazapyrene-Tethered Oligothymidylates, *Bioorg. Med. Chem. Lett*., **6**, 101-104 (1996).

M. Node, X. J. Hao, K. Nishide, and K. Fuji: A Formal Asymmetric Synthesis of Calabar Bean Alkaloids, *Chem. Pharm. Bull*.., **44**, 715-719 (1996).

K. Tanaka, K. Otsubo, and K. Fuji: Enantioselective Preparation of Allenecarboxylates by Asymmetric Horner-Wadsworth-Emmons Reaction, *Tetrahedron Lett*., **37**, 3735-3738 (1996).

T. Kawabata, A. Kuroda, E. Nakata, K. Takasu, and K. Fuji: Chirl Recogmition of Amino Acid Derivatives by 1,1'-Binaphthalene-8,8'-diol, *Tetrahedron Lett*., **37**, 4153-4156 (1996).

K. Fuji, K. Tanaka, K. Takasu, and T. Taga: Facile Synthesis of Optically Active *cis*-2,5-Diphenyl-1,4-Diazabicyclo [2.2.2] octane, *Tetrahedron: Asymmetry* , **7**, 1749-1751 (1996).
K. Tanaka, M. Ahn, Y. Watanabe, and K. Fuji: Asymmetric Synthesis of Uncommon a-Amino Acids by Diastereoselective Alkylations of a chiral Glycine Equivalent, *Tetrahedron: Asymmetry* , **7**, 1771-1782 (1996).

K. Fuji, M. Sakurai, N. Tohkai, A. Kuroda, T. Kawabata, Y. Fukazawa, T. Kinoshita, and T. Tada.Unexpedly Facile Racemization of 8-Diphenylphosphinoyl-8'-methoxy-1,1'-binaphthyl, *Chem. Commun*., 1609-1610 (1996).

K. Tanaka, K. Fuji, T.l Yokoi, T. Shingu, B. Li, and H. Sun, Structures of Taxchimins L and M, Two New Diterpenoids from Taxus chinensis var. Mairei, *Chem. Pharm. Bull*., **49**, 1770-1774 (1996).

K. Tanaka, T. Furuta, K. Fuji, Y. Miwa, and T. Taga: Preparation and Absolute Configuration of Hexahydroxy and Octahydroxyquaternaphthalene Derivatives, *Tetrahedron: Asymmetry* , **7**, 2199-2002 (1996).

K. Fuji, K. Takasu, H. Miyamoto, K. Tanaka, and T. Taga: Polyaza Macrocycles Contaiming the Piperazine Ring as a Semi-Flexible Moiety, *Tetrahedron Lett*. **37**, 7111-7114 (1996).

K. Fuji, X. Yang, K. Tanaka, N. Asakawa, X. Hao: 1,1'-Binaphthalene-8,8'-diol as an Efficient Chiral Controller: High Enantioselective Lynthesis of Optically Active Ketones, *Tetrahedron Lett*., **37**, 7373-7376 (1996).

BIOORGANIC CHEMISTRY

I. Bioorganic Reaction Theory

Okuma K, Koda G, Okumura S, Ohno A: Novel Reaction of Selenobenzophenones with Alkyllithiums Leading to Symmetrical Olefins. *Chem. Lett*., 609-610 (1996).

Ohno A, Kunitomo J, Kawai Y, Kawamoto T, Tomishima M, Yoneda F: Atropisomeric Flavoenzyme Models with a Modified Pyrimidine Ring: Syntheses, Physical Properties and Stereochemistry in the Reactions with NAD(P)H Analogs. *J. Org. Chem*., **61**, 9344-9355 (1996).

Ohno A, Tsutsumi A, Yamazaki N, Okamura M, Mikata Y, Fujii M: $NAD(P)^+$-NAD(P)H Models. 87. Nonsteric Stereochemistry Controlled by a Carbonyl Dipole. *Bull. Chem. Soc. Jpn*., **69**, 1679-1685 (1996).

Ohno A, Yamazaki N, Okamura M, Kawai Y, Tsutsumi A, Mikata Y, Fujii M: $NAD(P)^+$-NAD(P)H Models. 86. Nonsteric Stereochemistry in Hydride-Transfer to Sulfinylpyridinium Ion. *Bull. Chem. Soc. Jpn*., **69**, 1093-1098 (1996).

Tanaka K, Kitahara Y, Suzuki H, Osuga H, Kawai Y: Synthesis and Crystal Structure of Chiral Bifunctional Helicenes with π-Deficient Pyridine and π-Excessive Thiophene Units. *Tetrahedron Lett*., **37**, 5295-5298 (1996).

Kawai Y, Kunitomo J, Ohno A: Geometrical Change of a Flavoenzyme Model through Hydrogen Bonding to the Pyrimidine Ring. *Tetrahedron Lett*., **37**, 8905-8908 (1996).

Kawai Y, Saitou K, Hida K, Dao D H, Ohno A: Stereochemical control in Microbial Reduction. XXVIII. Asymmetric Reduction of α,β-Unsaturated Ketones with Bakers' Yeast. *Bull. Chem. Soc. Jpn*., **69**, 2633-2638 (1996).

Ogawa S, Ohmiya T, Kikuchi T, Kawai Y, Niizuma S, Sato R: Molecular Structure Determination and Studies on Chemical and Electrochemical Redox Reactions of a Cyclic Triselenide Compound, 4,7-Dimethoxybenzotriselenole. *Heterocycles*, **43**, 1843-1846 (1996).

Ogawa S, Nobuta S, Nakayama R, Kawai Y, Niizuma S, Sato R: Synthesis and Unique Packing Structure by X-Ray Analysis of New Types of Stable Trithioles Bound to Fused Aromatic Systems. *Chem Lett*., 757-758 (1996).

Kinoshita M, Ohno A: Factors Influencing Enantioselectivity of Lipase-Catalyzed Hydrolysis. *Tetrahedron*, **52**, 5397-5406 (1996).

Yasui S, Shioji K, Tsujimoto M, Ohno A: An Intramolecular Arbuzov Rearrangement Initiated by Anodic Oxidation. *Tetrahedron Lett*., **37**, 1625-1628 (1996).

Yasui S, Shioji K, Ohno A, Yoshihara M: Reaction of Diphenylphosphine Oxide with a 10-Methylacridinium Salt. Reversible Formation of a P-C Covalent Bond. *Heteroatom Chem*., **6**, 475-480 (1995).

Yasui S, Shioji K, Ohno A: Dediazoniation of Arenediazonium Salts with Trivalent-Phosphorus Compounds. Tool for Examination of the Reactivity of Phosphorus-Centered Radicals. *Heteroatom Chem*., **6**, 223-233 (1995).

Nakamura K, Kondo S, Kawai Y, Hida K, Kitano K, Ohno A: Enantio- and Regioselective Reduction of α-Diketones by Bakers' Yeast. *Tetrahedron: Asymm*., **7**, 409-412 (1996).

Nakamura K, Kitano K, Matsuda T, Ohno A: Asymmetric Reduction of Ketones by Acetone Powder of *Geotrichum candidum. Tetrahedron Lett*., **37**, 1629-1632 (1996).

Nakamura K, Kawasaki M, Ohno A: Lipase-Catalyzed Transesterification of Aryl-Substituted Alkanols in an Organic Solvent. *Bull. Chem. Soc. Jpn*., **69**, 1079-1085 (1996).

Nakamura K, Matsuda T, Ohno A: Asymmetric Synthesis of (*S*)-Arylalkanols by Microbial Reduction. *Tetrahedron: Asymm*., **7**, 3021-3024 (1996).

Nakamura K, Matsuda T, Itoh T, Ohno A: Different Stereochemistry for the Reduction of Trifluoromethyl Ketones and Methyl Ketones Catalyzed by Alcohol Dehydrogenase from *Geotrichum. Tetrahedron Lett*., **37**, 5727-5730 (1996).

Ishihara K, Higashi Y, Nakajima N, Utaka M, Nakamura K: Enzymatic Production of (S)-1-acetoxy-2-Alkanol with Bakers' Yeast Cell-Free Extract in a

Membrane Reactor. *J. Ferment. Bioeng*., **81**, 266-268 (1996).

Hamada H, Shiromoto M, Funahashi M, Itoh T, Nakamura K: Efficient Synthesis of Optically Pure 1,1,1-Trifluoro-2-alkanols through Lipase-catalyzed Acylation in Organic Media. *J. Org. Chem*., **61**, 2332-2336 (1996).

Itoh T, Shiromoto M, Inoue H, Hamada H, Nakamura K: Simple Preparation of Optically Pure Bis(trifluoromethyl)alkanediol through Lipase-Catalyzed Reaction. *Tetrahedron Lett*., **37**, 5001-5002 (1996).

Ishihara K, Kondo S, Nakamura K, Nakajima N: Protein Sequencs of Two Keto Ester Reductases: Possible Identity as Hypothetical Proteins.*Biosci. Biotech, Biochem*., **60**, 1538-1539 (1996).

II. Bioactive Chemistry

Fujita M, Otsuka M, and Sugiura Y: Metal-chelating inhibitors of a zinc finger protein HIV-EP1. Remarkable potentiation of inhibitory activity by introduction of SH groups, *J.Med.Chem*., **39**, 503-507 (1996).

Fuji K, Kawabata T, Kiryu Y, and Sugiura Y: Ring opening of optically active cis-disubstituted aziridino alcohols. An enantiodivergent synthesis of functionalized amino *alcohol derivatives*, *Heterocycles* , **42**, 701-722 (1996).

Okuno Y, Iwashita T, Otani T, and Sugiura Y: Interaction of C-1027 chromophore with d$(GTATAC)_2$. A binding model based on NMR experiments, *J.Am.Chem.Soc*., **118**, 4729-4730 (1996).

Nakamura E, Tokuyama H, Yamago S, Shiraki T, and Sugiura Y: Biological activity of water-soluble fullerenes. Structural dependence of DNA cleavage, cytotoxicity, and enzyme inhibitory activities including HIV-protease inhibition, *Bull.Chem.Soc.Jpn*., **69**, 2143-2151 (1996).

Guan L.L., Morii T, Otsuka M, and Sugiura Y: Specific interaction with guanine residues of z-form DNA by bleomycin-nickel(III) complex, *Biochim.Biophys.Acta*, **1308**, 169-176 (1996).

Nagaoka M and Sugiura Y: Distinct phosphate backbone contacts revealed by some mutant peptides of zinc finger protein Sp1: Effect of protein-induced bending on DNA recognition, *Biochemistry* , **35**, 8761-8768 (1996).

Otsuka M, Satake H, Murakami S, Doi M, Ishida T, Shibasaki M, and Sugiura Y: An artificial Cu^{II} complex with intriguing oxygen radical-quenching profile. X-Ray structure, cytochrome c assay, and ESR study, *Bioorg.Med.Chem*., **4**, 1703-1708 (1996).

Morii T, Yamane J, Aizawa Y, Makino K, and Sugiura Y: Cooperative oligomerization enhances sequence-selective DNA binding by a short peptide, *J. Am. Chem. Soc*., **118**, 10011-10017 (1996).

Yamamoto Y, Kimachi T, Kanaoka Y, Kato S, Bessho K, Matsumoto T, Kusakabe T, and Sugiura Y: Synthesis and DNA binding properties of amide bond-modified analogues related to distamycin, *Tetrahedron Lett*., **37**, 7801-7804 (1996).

Takahashi T, Tanka H, Yamada H, Matsumoto T, and Sugiura Y: DNA cleavage by a nine-membered masked enediyne, an analogue of the kedarcidin and C-1027 chromophores, *Angew.Chem.Int.Ed.Engl*., **35**, 1835-1837 (1996).

III. Molecular Clinical Chemistry

Ueda K, Tanaka S and Kawamata J: Correlation between Temporal Lobe Atrophy and *APOE ε4*(+) Genotype in Alzheimer's Disease: X-Ray CT and MRI Studies, *Neurobiol. Aging*, **17**, S61 (1996).

Ueda K: Gene Examination and Diagnosis, *Mol. Med*., **33**, 18-24 (1996) (in Japanese).

Ueda K: Information Control in Gene Diagnosis and Therapy, in "Gene Diagnosis and Therapy '95" (Mori T, ed), Igaku-Shoin, 98-100 (1996) (in Japanese).

Ueda: Gene-Related Laboratory Tests. 2. DNA Diagnosis Practicable in Clinical Laboratories, *Nipponrinsho*, **53** (Suppl. II), 890-893 (1995) (in Japanese).

Kido T and Ueda K: DNA Diagnosis in Clinical Laboratory Tests, *PNE (Protein-Nucleic Acid-Enzyme)*, **41**, 2484-2490 (1996) (in Japanese).

Nishikimi A and Adachi Y: Examination of Signal Transduction-Related Proteins by in vitro Kinase Assay and Phosphoamino Acid Analysis, *Radiat. Biol. Res. Commun*., **31**, 232-242 (1996) (in Japanese).

Adachi Y: *In vivo Poly*(ADP-ribosyl)ation and Apoptosis, *Nippon Nogeikagaku Kaishi*, **70**, 793-794 (1996) (in Japanese).

Nishikimi A and Adachi Y: Isolation and Biochemical Analysis of Trace Cellular Proteins by Two-cycle Immunoprecipitation, *Radiat. Biol. Res. Commun*., **31**, 150-158 (1996) (in Japanese).

Adachi Y: Retroviral Infection and Nuclear Transport: Possible Mechanism of Rev/Rex-dependent Transactivation of Viral Genes, *Exp. Med*., **14**, 62-70 (1996) (in Japanese).

Adachi Y: Possible Mechanism of Protein Transport to Nucleolus, *Seikagaku*, **68**, 35-41 (1996) (in Japanese).

MOLECULAR BIOFUNCTION

I. Functional Molecular Conversion

Hara T, Kato H, Katsube Y and Oda J: A Pseudo-Michaelis Quaternary Complex in the Reverse Reaction of a Ligase: Structure of *Escherichia coli* B Glutathione Synthetase Complexed with ADP, Glutathione, and Sulfate at 2.0 Å Resolution. *Biochemistry*, **35**, 11967-11974 (1996).

Hibi T, Nishioka T, Kato H, Tanizawa K, Fukui T, Katsube Y and Oda J: Structure of the multifunctional loops in the nonclassical ATP-binding fold of glutathione synthetase. *Nat. Struct. Biol*., **3**, 16-18 (1996).

Nakatsu T, Kato H and Oda J.: Crystallization and preliminary crystallographic study of asparagine syn-

thetase from *Escherichia coli. Acta Cryst*., **D52**, 604-606 (1996).

Katoh M, Hiratake J, Kato H and Oda J: Mechanism-Based Inactivation of *E. coli* γ-Glutamylcysteine Synthetase by Phosphinic Acid- and Sulfoximine-Based Transition-State Analogues. *Bioorg. & Med. Chem. Lett*., **6**, 1437-1442 (1996).

Kato H and Oda J: Organic Chemistry and Protein Crystallography–Probing Enzyme Mechanisms with Transition State Analogs. *Nippon Kesshou Gakkaishi*, **38**, 99-104 (1996) (in Japanese).

Oda J: Transition State Analog. *Kagaku*, **51**, 702-703 (1996) (in Japanese).

Oda J: Studies on Functional Analysis and Application of Biocatalysts. *Nippon Nôgeikagaku Kaishi*, **70**, 859-866 (1996) (in Japanese).

II. Molecular Microbial Science

Esaki N, Nakamori S, Kurihara T, Furuyoshi S and Soda K: Enzymology of Amino Acid Production, *Biotechnology*, **6**, 505-560 (1996)

Hisano T, Hata Y, Fujii T, Liu J, Kurihara T, Esaki N and Soda K: Crystallization and Preliminary X-Ray Crystallographic Studies of L-2-Haloacid Dehalogenase from *Pseudomonas* sp. YL, *PROTEINS: Structure, Function, and Genetics*, **24**, 520-522 (1996)

Hisano T, Hata Y, Fujii T, Liu J, Kurihara T, Esaki N and Soda K: Crystal Structure of L-2-Haloacid Dehalogenase from *Pseudomonas* sp. YL, *J. Biol. Chem*., **271**, 20322-20330 (1996)

Jhee K, Yoshimura T, Esaki N and Soda K: Stereospecificity of Thermostable Ornithine 5-Aminotransferase for the Hydrogen Transfer in the L- and D-Ornithine Transamination, *Biochemistry*, **35**, 9792-9796 (1996)

Yoshimura T, Jhee K and Soda K: Stereospecificity for the Hydrogen Transfer and Molecular Evolution of Pyridoxal Enzymes, *Biosci. Biotech. Biochem*., **60**, 181-187 (1996)

Esaki N and Soda K: Trace Element as an Activator of Enzyme, *Nihon-Rinsho*, **54**,17-25 (1996) (in Japanese)

Yoshimura T and Soda K: Physiological Role and Metabolism of D-Amino Acids, *Chemistry Today*, 14-19 (1996) (in Japanese)

MOLECULAR BIOLOGY AND INFORMATION

I. Biopolymer Structure

Fujii T, Hata Y, Ohzeki M, Moriyama H, Wakagi T, Tanaka N and Oshima T: Refined crystal structure of ferredoxin from thermoacidophilic archaeon, *Acta Cryst*., **A52**, C-233 (1996).

Fujii T, Hata Y, Wakagi T, Tanaka N and Oshima T: Novel zinc-binding centre in thermoacidophilic archaeal ferredoxins, *Nat. Struct. Biol*., **3**, 834-837 (1996).

Hamada K, Hata Y, Katsuya Y, Hiramatsu H, Fujiwara T and Katsube Y: Crystal Structure of *Serratia* Protease, a Zinc-Dependent Proteinase from *Serratia* sp. E-15, Containing a β-Sheet Coil Motif at 2.0 Å Resolution, *J. Biochem*., **119**, 844-851 (1996).

Hamada K, Hata Y, Miyatake H, Fujii T, Amada F, Fukuyama K: Identification of Ca^{2+} ions bound to proteins using X-ray anomalous dispersion technique, *Acta Cryst*., **A52**, C-134 (1996).

Hata Y, Hisano T, Fujii T, Liu J-Q, Kurihara T, Esaki N and Soda K: Crystal structure of L-2-haloacid dehalogenase from *Pseudomonas* sp. YL at 2.5 Å resolution, *Acta Cryst*., **A52**, C-122 (1996).

Hiragi Y: Structural Kinetics by Solution Scattering Using Synchrotron Radiation, Proc. of *the X International Conference on Small-Angle Scattering, Campinas, Brazil*, 95 (1996).

Hiragi Y, Tagawa H, Suzuki K, Miyata C, Muroga Y, Inoue H and Sano Y: Structure of Tobacco Mosaic Virus-RNA in Solution, Proc. of *the XIIth International Biophysics Congress. Amsterdam, The Netherlands*, 55 (1996).

Hisano T, Hata Y, Fujii T, Liu J-Q, Kurihara T, Esaki N and Soda K: Crystallization and Preliminary X-Ray Crystallographic Studies of L-2-Haloacid Dehalogenase From *Pseudomonas* sp. YL, *Proteins: Struct. Func. Genet.*, **24**, 520-522 (1996).

Hisano T, Hata Y, Fujii T, Liu J-Q, Kurihara T, Esaki N and Soda K: Crystal Structure of L-2-Haloacid Dehalogenase from *Pseudomonas* sp. YL. An α/β hydrolase structure that is different from the α/β hydrolase fold, *J. Biol. Chem*., **271**, 20322-20330 (1996).

Kajiwara K and Hiragi Y: Chapter 6, Structure Analysis by Small-Angle X-Ray Scattering, in "*Applications of Synchrotron Radiation to Material Analysis*" (Saisyo H and Gohshi Y, eds.), pp. 354-404, Elsevier, Amsterdam (1996).

Kojima S, Kuriki Y, Sato Y, Arisaka F, Kumagai I, Takahashi S and Miura K: Synthesis of α-helix-forming peptides by gene engineering methods and their characterization by circular dichroism spectra measurements, *Biophys. Biochem. Acta*, **1294**, 129-137 (1996).

Kokusen H, Sohrin Y, Matsui M, Hata Y and Hasegawa H: Selectivity design using interligand contact: solvent extraction and structures of first-series-transition metal-bis(pyrazol-1-yl)borate complexs, *J. Chem. Soc., Dalton Trans*., 195-201 (1996).

Sano Y, Inoue H, Hiragi Y and Kajiwara K: Difference of Reconstitution Process between Tobacco Mosaic Virus and Its Mutant by Solution X-ray Scattering Study. Proc. of *the 3rd Workshop "Principle of Protein Architecture", Kyoto*, 211 (1996).

Wakagi T, Fujii T and Oshima T: Molecular Cloning, Sequencing, and Heterologous Expression of a Novel Zinc-Containing Ferredoxin Gene from a Thermoacidophilic Arcaheon *Sulfolobus* Sp. Strain 7, *Biochem. Biophys. Res. Commun*., **225**, 489-493 (1996).

II. Molecular Biology

Nevalainen L T, Aoyama T, Ikura M, Crivici A, Yan H, Chua N-H and Nairn A C: Characterization of Novel Calmodulin-Binding Peptides with Distinct Inhibitory Effects on Calmodulin-dependent Enzymes. *Biochem. J.*, **321**, 107-115 (1997).

Aoyama T: A Glucocorticoid-mediated Transcriptional Induction System in Higher Plants. *Tanpakushitsu-Kakusan-Kouso*, **41**, 2559-2563 (1996) (in Japanese).

Aoyama T: Steroid-mediated Induction System for Protein Function. S*aibou-Kougaku, Shokubutsu-Saibou-Kougaku Series*, **4**, 125-128 (1996) (in Japanese).

Goto K: Molecular and Genetic *Analyses* of Flower Homeotic Genes of *Arabidopsis. Biosciences*, **21** (No.3), 369-378 (1996).

Goto K: Molecular Mechanisms of Floral Organ Identity. In *Ikusyugaku Saikinno-Shinpo*, **38**, 43-46 (1996) (in Japanese).

III. Biological Information Science

Bono H, Goto S, Ogata H, Kanehisa M: Systematic Prediction of Enzyme Genes by the Metabolic Pathway Database, *Recent Advance in Genome Biology of Micro-organisms*, p. 24 (1996).

Bono H, Ogata H, Goto S, Kanehisa M: Genome Scale Prediction of Enzyme Genes Utilizing the Knowledge of Metabolic Interactions, *Proc. 7th Workshop on Genome Informatics*, pp. 252-253 (1996).

Fujibuchi W, Goto S, Kanehisa M: Deductive Calculation Library for KEGG Pathway Simulation, *Proc. 7th Workshop on Genome Informatics*, pp. 250-251 (1996).

Goto S, Fukushima N, Kanehisa M: Starndard Gibbs Free Energy Changes of Enzyme Reaction in Metabolic Pathway Computation, *Proc. 7th Workshop on Genome Informatics*, pp. 248-249 (1996).

Goto S, Bono H, Ogata H, Fujibuchi W, Nishioka T, Sato K, Kanehisa, M: Organizing and Computing Metabolic Pathway Data in Terms of Binary Relations, *Proc. Pacific Symposium on Biocomputing '97*, pp. 175-186 (1996).

Kanehisa M: Toward Pathway Engineering: A New Database of Genetic and Molecular Pathways, *Science & Technology Japan*, No. 59, pp. 34-38 (1996).

Kanehisa M: Integration of Genetic Information by the Internet, *Idenshi Shinryo '96*, 101-103 (1996). (in Japanese)

Kanehisa M: Current Status and Future Prospects of Genome Informatics: From Technology Development to Functional Prediction, *Gakujutsu Geppou*, **49**, 937-942 (1996) (in Japanese).

Kanehisa M: Biological Information Network, In *Genome Biology*, Fujiyama A, Matsubara K eds. Kyoritsu Shuppan, pp. 111-130 (1996). (in Japanese)

Kanehsia M: Genome Informatics, *Jouhoushori* **37**, 908-913 (1996) (in Japanese).

Kanehisa M: Invitation to Genome Informatics, Kyoritsu Shuppan, Tokyo (1996). (in Japanese)

Kihara D, Shimizu T, Kanehisa M: A Prediction Method for Transmembrane Segments in Proteins Utilizing Multiple Discrimination Functions, *Proc. 7th Workshop on Genome Informatics*, pp. 244-245 (1996).

Kihara D: WWW Homepages for Biophysicists, *Biophysics*, **36,** 246 (1996). (in Japanese)

Nakai K, Fujibuchi W: Internet-Based System for the Analysis of Genetic Information: Current Status, *Pharmaceutical Library Bulletin*, **41**, 359-364 (1996) (in Japanese).

Ogata H, Kanehisa M: Function Analysis Using Protein Databases, *Biophysics*, **36**,152-154 (1996). (in Japanese)

Ogata H, Fujibuchi W, Kanehisa M: The Size Differences Among Mammalian Introns are Due to the Accumulation of Small Deletions, *FEBS Lett.*, **390**, 99-103 (1996).

Ogata H, Fujibuchi W, Kanehisa M: Size Distribution and Evolutionary Rate of Intron Revealed by Comparison of Different Mammalian Species, *Progress in Biophysics & Molecular Biology*, **65**, supple. 1, 75 (1996).

Ogata H, Bono H, Fujibuchi W, Goto S, Kanehisa M: Analysis of Binary Relations and Hierarchies of Enzymes in the Metabolic Pathways, *Proc. 7th Workshop on Genome Informatics*, pp. 128-136 (1996).

Ogiwara A, Uchiyama I, Takagi T, Kanehisa M: Construction and Analysis of a Profile Library Characterizing Groups of Structurally Known Proteins, *Prot. Sci.*, **5**, 1991-1999 (1996).

Sato K, Katsurada T, Kamiya T, Egoshi M, Kanehisa M: Java Applets for Handling Genome Maps in KEGG, *Proc. 7th Workshop on Genome Informatics*, pp. 254-255 (1996).

Takagi T, Kanehisa M eds.: Introduction to GenomeNet Databases, Kyoritsu Shuppan, Tokyo (1996) (in Japanese).

Tomii K, Kanehisa M: Analysis of Amino Acid Indices and Mutation Matrices for Sequence Comparison and Structure Prediction of Proteins, *Protein Engineering*, **9**, 27-36 (1996).

Tomii K, Kanehisa, M: A Statistical Analysis of Gene Arrangement Patterns in Bacterial and Yeast Genomes, *Proc. 7th Workshop on Genome Informatics*, pp. 246-247 (1996).

Tomii K, Kanehisa M: Comparison of Amino Acid Mutation Matrices: Hierarchical Clustering and Correlation to Amino Acid Indices, *Progress in Biophysics & Molecular Biology*, **65**, supple. 1, 39 (1996).

Waizumi K, Masuda H, Fukushima N: Crystallographic Investigations of Diaquatetrachloro-Cobalt (II) and Nickel (II) Complexes, *J. Coord. Chem.*, **38**, 199-206 (1996).

NUCLEAR SCIENCE RESEARCH FACILITY

I. Particle and Photon Beams
II. Beams and Fundamental Reaction

Shirai T, Kando M, Ikegami M, Iwashita Y, Okamoto H, Kakigi S, Dewa H, Fujita H, Noda A, Inoue M and Mashiko M: A 100 MeV Injector for the Electron Storage Ring at Kyoto University, *Proc. of the 1995 Particle Accelerator Conference, Dallas*, 1079-1082 (1995).

Noda A, Dewa H, Fujita H, Ikegami M, Iwashita Y, Kakigi S, Kando M, Mashiko K, Okamoto H, Shirai T and Inoue M: Electron Storage Ring, KSR for Light Source with Synchrotron Radiation, *Proc. of 1995 Particle Accelerator Conference, Dallas*, 278-280 (1995).

Iwashita Y, Noda A, Okamoto H, Shirai T, Inoue M: Cold Model Test of Biperiodic L-support Disk-and-Washer Linac Structure, *Proc. of the 1995 Particle Accelerator Conference, Dallas*, 1093-1095 (1995).

Hirota J, Hiramoto K, Nishi M, Iwashita Y, Noda A and Inoue M: A Ferrite Loaded Untuned Cavity for a Compact Proton Synchrotron, *Proc. of the 1995 Particle Accelerator Conference, Dallas*, 1770-1772 (1995).

Kando M, Ikegami M, Dewa H, Fujita H, Shirai T, Okamoto H, Iwashita Y Kakigi S, Noda A and Inoue M: Matching Section to the RFQ Using Permanent Magnet Symmetric Lens, *Proc. of the 1995 Particle Accelerator Conference*, Dallas, 1843-1845 (1995).

Kapin V, Inoue M, Iwashita Y, Noda A: Application of the Two Stable Phaes Phenomenon for Improvement of the Longitudinal Stability in RFQ-like Funneling System, *Proc. of the 12th International Conference on Laser Interaction and Related Plasma Phenomena, Osaka, Japan*, 1127-1132 (1995).

Noda A, Yoshizawa M, Watanabe T, Osuka T, Katayama T, Mizobuchi A, Emoto K: Alignment of TARNII, *Proc. of the Fourth International Workshop on Accelerator Alignment (IWAA95) KEK, Tsukuba, Japan*, I/30-I/38 (1995).

Noda K, Kanazawa M, Itano A, Takada E, Torikoshi M, Araki N, Yoshizawa J, Sato K, Yamada S, Ogawa H, Itoh H, Noda A, Tomizaa M, Yoshizawa M: Slow Beam Extraction by a Transverse RF Field with AM and FM, *Nucl. Instrum. & Meth.*, **A374**, 269-277 (1996).

Inoue M: Beam Science and Technology Now, *Beam Science and Technology* , **1**, 1-7 (1996).

Yoshimura T, Kakigi S, Okihana A, Warner R E, Chant N S, Roos P G, Samanta C, Fujiwara M, Matsuoka N, Tamura K, Koori N, Kubo E and Ushiro K: Quasifree Scattering in the (p, $p\alpha$) Reaction on Light Nuclei at E_p=296 MeV, *Beam Science and Technology*, **1**, 8-11 (1996).

Saito K, Hirota J, Katane M, Tadokoro M, Noda F, Iwashita Y, Noda A, Inoue M: RF Acceleration System of Proton Synchrotron Dedicated for Cancer Therapy, *Beam Science and Technology*, **1**, 12-16 (1996).

Matsuda K, Hiramoto K, Noda A, Inoue M: A Resonant Beam Extraction Scheme for a Compact Synchrotron, *Beam Science and Technology* , **1**, 17-20 (1996).

Kando M, Ao H, Kihara T, Sugimura T, Ikegami M, Dewa H, Tonguu H, Fujita H, Shirai T, Okamoto H, Iwashita Y, Kakigi S, Noda A, Inoue M: An Emittance Measurement System for the Low Energy Beam Transport of the ICR Proton Linac, *Beam Science and Technology* , **1**, 21-24 (1996).

Ikegami M and Okamoto H: Development of Space-Charge Codes at ICR, *Beam Science and Technology*, **1**, 25-30 (1996).

Iwashita Y: Superfast Longitudinal Kicker, Beam Science and Technology, 1, 31-36 (1996).

Noda A, Dewa H, Fujita H, Ikegami M, Inoue M, Iwashita Y, Kakigi S, Kando M, Mashiko K, Okamoto H, Shirai T, Sugimura T, Tonguu H: Electron Storage Ring, KSR, *Beam Science and Technology* , **1**, 37-40 (1996).

Kihara T, Ao H, Dewa H, Shirai T and Iwashita Y: Distribution Measurement of the Gold Strip Target for the Longitudinal Emittance Monitor, *Beam Science and Technology*, **1**, 41-44 (1996).

Watanabe T, Katayama T, Watanabe S, Yoshizawa M, Arakaki Y, Chida K, Tomizawa M, Takanaka M, Kanazawa M, Hosono K, Noda A: Beam Position Monitoring System and COD Correction at the Cooler Synchrotron TARN II, *Nucl. Instrum. & Meth.*, **A381**, 194-208 (1996).

Dewa H, Ao H, Kihara T, Tonguu H, Shirai T, Okamoto H, Iwashita Y, Fujita H, Kakigi S, Noda A, Inoue M: Longitudinal Beam Emittance Monitor for 433 MHz Proton Linac, *Review of Scientific Instruments*, **67**, No. 9, 3085-3091 (1996).

Jiang S, Gluckstern R L and Okamoto H: The Coupling Impedance of Periodic Irises in a Beam Pipe, Particle Accelerators **52**, 179-200 (1996).

Okamoto H and Wei J: Laser Cooling in a Storage Ring and Crystalline Beams, Genshikaku-Kenkyu **41**, No.2, 1-10 (1996) (in Japanese).

Matsuki S and Ogawa I: Present Status of Dark Matter Axion Search in *Kyoto, Proc. of the 30th Rencontre de Moriond Conference on the Dark Matter in Cosmology, Clocks and Tests of Fundamental Laws, Villars sur Ollon, Switzerland*, 187-194 (1995).

Ogawa I, Nakamura S, Takimoto T, Tada M, Yamamoto K, Masaike A and Matsuki S: Search for Dark Matter Axions with Rydberg Atoms in Cooled Cavities, *Proc. of the International Conference on Weak and Electromagnetic Interactions in Nuclei, Osaka*, 640-643 (1995).

Ogawa I, Matsuki S and Yamamoto K: Interactions of Cosmic Axions with Rydberg Atoms in Resonant Cavities via the Primakoff Process, *Phys. Rev.* **D53**, 1740-1744 (1996).

Matsuki S, Ogawa I, Nakamura S, Tada M, Yamamoto K and Masaike A: Rydberg-atom Cavity Detector for

Dark Matter Axion Search in Kyoto, Nucl. Phys. B (Proc. Suppl.) **51B**, 213-217 (1996).

Tonguu H, Ao H, Kihara T, Sugimura T, Kando M, Ikegami M, Dewa H, Fujita H, Okamoto H, Iwashita Y, Kakigi S, Noda A and Inoue M: Vacuum System of the Electron Storage Ring KSR, *Proc. of the 21st Linear Accelerator Meeting, Chiba,* 147-149 (1996) (in Japanese).

Dewa H, Ao H, Kihara T, Sugimura T, Kando M, Ikegami M, Kapin V, Tonguu H, Shirai T, Okamoto H, Iwashita Y, Fujita H, Kakigi S, Noda A and Inoue M: Measurement of the Beam Distribution of 433 MHz Proton Linac in Longitudinal Phase Space, *Proc. of the 1996 Linear Accelerator Conference, CERN, Geneva*, 237-239 (1996).

Shirai T, Sugimura T, Iwashita Y, Kakigi S, Fujita H, Tonguu H, Noda A and Inoue M: Performance of the 100 MeV Injector Linac for the Electron Strage Ring at Kyoto University, *Proc. of the 1996 Linear Accelerator Conference, CERN, Geneva*, 240-242 (1996).

Kapin V, Noda A,Iwashita Y and Inoue M: Multiple-beam RFE Structure with a Matrix-array of Beamlets, *Proc. of the 1996 Linear Accelerator Conference, CERN, Geneva*, 722-724 (1996).

Iwashita Y, Ao H, Noda A, Okamoto H, Shirai T, and Inoue M: Power Model of Biperiodic DAW Cavity, *Proc. of the 1996 Linear Accelerator Conference, CERN, Geneva*, 857-859 (1996).

SEMINARS

Associate Professor Tadashi Asanuma
Institute for Chemical Research, Kyoto University
"Properties of Polyolefins Synthesized Newly with Metallocene Catalysts"
Friday 12 January 1996

Professor Gerrit E W Bauer
Delft University of Technology, Delft, The Netherlands
"Magnetism and Transport of Mesoscopic Systems"
Tuesday 16 January 1996

Prof. D. H. Kim
Pohang Institute of Science & Technology, Korea,
"Weak Bondings for Bioorganic Chemists"
Thursday 1 February 1996

Professor Toshihiro Akaike
Department of Biomolecular Engineering, Tokyo Institute of Technology, Yokohama, Japan
"Biomimetic Glycotechnology and its Application to Medical Care"
Friday 23 February 1996

Dr. Mervyn.J. Miles
H.H.Wills Physics Laboratory, University of Bristol, UK
"Scanning Probe Microscopy of Organic and Biological Materials"
Tuesday 27 February 1996

Professor Stephen F. Nelsen
Department of Chemistry, University of Wisconsin, Madison, USA
"Hydrazines and Electron Transfer Reactions"
Monday 4 March 1996

Professor Barry Stoddard
Fred Hutchinson Cancer Research Center
"Stalking and Capturing Catalytic Intermediates with Mutagenesis, Kinetics, and Laue Crystallography"
Tuesday 5 March 1996

Dr. Sergei Magonov
Digital Instruments Inc., USA
"Atomic Force Microscopy of Polymers"
Tuesday 7 March 1996

Dr. Thomas Heinze
Institute of Organic and Macromolecular Chemistry, University of Jena, Jena, Germany
"Cellulose Tosylates, New View of an Old Derivative"
Monday 11 March 1996

Professor Dieter Klemm
Institute of Organic and Macromolecular Chemistry, University of Jena, Jena, Germany
"Selective Functionalization of Cellulose"
Monday 11 March 1996

Dr. Margit Schultze
Max-Planck-Institute for Polymer Research, Mainz, Germany
"Supramolecular Structures of Cellulose Derivatives"
Monday 11 March 1996

Dr. Hans-Peter Fink
Fraunhofer-Institute of Applied Polymer Research, Teltow, Germany
"Structural Changes of Cellulose at Processing"
Tuesday 12 March 1996

Dr. Yuzo Fujita
Institute for Nuclear Study, University of Tokyo, Tokyo, Japan
"Gas Counter and Beam Monitor"
Friday 15 March 1996

Professor Edgar A. Silinsh
Institute of Physical Energetics, Latvia
"Advanced Photoactive Materials and LB Molecular Assemblies for Non-linear Optics and Molecular Electronics"
Monday 18 March 1996

Professor Timothy A. Cross
Florida State University, USA
"High Resolution Dynamics in a Membrane-Bound Polypeptide by Solid-State NMR"
Tuesday 19 March 1996

Dr. Jong Heo
Department of Materials Science and Engineering, Pohang University of Science and Technology, Korea
"Rare-Earth Doped Chalcogenide Glasses: Science and Future Opportunities"
Wednesday 20 March 1996

Professor Dr. Peter Zugenmaier
Institut für Physikalische Chemie der Technischen Universität Clausthal, Clausthal, Germany
"Selected Topics on Polymer-Solvent Interactions in Lyotropic Cellulose Derivatives"
Thursday 21 March 1996

Dr. Vladimir Balek
Nuclear Research Institute Rez plc, Czech Republic
"Improvement of the Quality Control of Intermediate and Final Products of Ceramic Materials Using Emanation Thermal Analysis"
Wednesday 27 March 1996

Dr. Yurij Senichev
Institute of Nuclear Research of the RAS, Russia
"Transient Effect in High Intensity Proton Linear Accelerator and Comparison of Disk-And-Washer Structure with Side Coupled Structure"
Friday 28 March 1996

Professor Sidney Shall
Department of Biology, Sussex University, Brighton, U. K.
"Werner Syndrome/Poly(ADP-ribose)"
Tuesday 2 April 1996

Dr. Michael Richard Roberts (Senior post-doctoral Research Fellow)
Department of Biology, University of York, Heslington, York, UK
"Wound-responsive Signal Transduction in Tomato Plant"
Tuesday 2 April 1996

Dr. Martin R. Willis
University of Nottingham, U.K.

"Phthalocyanines for Device Applications"
Wednesday 3 April 1996

Professor R.Bruce Martin
Chemistry Department, University of Virginia, U.S.A.
"Aluminum: A Neurotoxic Product of Acid Rain"
Friday 5 April 1996

Prof. Akio Murai
Hokkaido University, Hokkaido, Japan
"Synthesis of Marine Cyclic Polyethers"
Thursday 11 April 1996.

Professor Ye Feng
Institute for Modern Physics, Lanzhou, China
Professor Zhang Chuang
Institute for High Energy Physics, Beijing, China
"Accelerator Projects in China, Heavy Ion and Lepton Projects"
Friday 12 April 1996

Professor Dieter Richter
Director,
Institute für Festköperforschung, Forschungszentrum, Jülich, Germany
"The Dynamic Structure Factor of Polybutadiene - Microscopic motion in the a and b relation regimes"
Monday 22 April 1996

Associate Professor Katsunobu Oide
National Laboratory for High Energy Physics (KEK), Tsukuba, Japan
"A Preliminary Design of a Muon Collider Ring"
Wednesday 24 April 1996

Professor Ronald M. Levy
Rutgers University, USA
"Solvation Thermodynamics, Hydration Shell Models, and Polarizable Models"
Friday 26 April 1996

Professor Julia S. Higgins
Imperial College of Science, Technology and Medicine, London, United Kingdom
"Rotation of Methyl Side Groups in Polymers - a Fourier transform approach to analysis of quasi-elastic neutron scattering data"
Tuesday 4 May 1996

Dr. Thomas Wirth
University of Basel, Switzeland
"Chiral Selenium Compounds in Organic Synthesis"
Monday 20 May 1996.

Professor Gert R. Strobl
Fakultät für Physik, Albert-Ludwigs-Universität Freiburg, Freiburg, Germany
"SAXS Studies on the Mechanisms of Primary and Secondary Crystallization in Polyolefins"
Tuesday 25 May 1996

Dr. Gabor
Institut de chimie des Substances Naturelles, CNRS, Gif-sur-Yvette, France
"Total Synthesis of Natural Products: Myriocin, Quadrone and Taxol"
Saturday 25 May 1996.

Professor B. Meissner
Prague Institute of Chemical Technology
"Theoretical and Experimental Studies of the Polymer-Filler Gel Formation"
Thursday 30 May 1996

Prof. R. More O'Ferrall, University of Dublin, Ireland,
"Super Acid Catalysis in Keto-Enol Tautomerism"
Monday 3 June 1996

Professor Joanna Strosznajder
Medical Research Laboratory, Polish Academy of Sciences, Warsaw, Poland
"Neurotoxic Effects of β/A4 Amyloid Peptide and Apoptosis"
Friday 7 June 1996

Professor Michael P. Doyle
Trinity University, Texas, USA
"Highly Enantioselective Catalytic Metal Carbene Transformations"
Saturday 8 June 1996

Professor Jürgen Petermann
Department of Chemical Engineering, University of Dortmund, Germany
"Polymer/Polymer and Metal/Polymer Interfaces and Their Technical Applications"
Wednesday 12, June 1996

Professor Yotaro Morishima
Department of Macromolecular Science, Faculty of science, Osaka University, Osaka, Japan
"Self-Organization of Amphiphilic Polyelectrolytes"
Wednesday 12 June 1996

Professor Saburo Nasu
Faculty of Engineering Science, Osaka University, Osaka, Japan
"Recent Advances in Mössbauer Spectroscopy"
Friday 14 June 1996

Dr. Nohara Mohara
Institute for Solid State Physics, University of Tokyo
"Specihic Heat as a Probe of the Study of Magnetism"
Thurseday 20 June 1996

Professor Tsunehisa Kimura
Tokyo Metropolitan University, Japan
"Magnetic Orientation of Polymers"
Thursday 20 June 1996

Professor Takayuki Kawashima
Department of Chemistry, University of Tokyo, Tokyo
"The Wittig Reaction, Peterson Reaction, and the Chemistry of the Corresponding Reactive Intermediates"
Tuesday 25 June 1996

Dr. Manfred Sigrist
Theoretische Physik, ETH-Hönggerberg, Zürich, Switzerland
"Thermodynamic Properties of a Class of Random Spin Systems"
Friday 28 June 1996

Professor V. Chandrasekhar
Indian Institute of Technology, Kanpur, India
"Interactions of Metals with Phosphazenes and Siloxanes : From Multisite Metal Recognition Heterocycles to Ion Conducting Macromolecules"
Thursday 4 July 1996

Professor Hideyuki Sato
Faculty of Science, Tokyo Metropolitan University, Tokyo, Japan
"Magnetism and Transport Phenomena"
Friday 12 July 1996

Prof. B. Bonini
University of Bologna, Italy,
"Synthetic Applications of Enolyzable Silyl Thioketones"
Tuesday 16 July 1996

Prof. B. Zwannenburg
University of Nijmegen, The Netherlands,
"Functionalized Small-Ring Heterocycles"
Tuesday 16 July 1996

Professor Tamas Veszpremi
Technical Univ. of Budapest, Hungary
"How to Design Stable Silylenes?"
Friday 19 July 1996

Prof. Wei - Min Dai
Hong Kong University of Science and Technology, Hong Kong
"Studies on Taxoid Synthesis Using Lewis Acid-Catalyzed Intermolecular Diels-Alder Cycloaddition"
Monday 22 July 1996.

Professor Shoroku Ohnuma
Department of Physics, University of Houston, Houston, USA
"FermiLab Main Injector Recycler Ring"
Friday 2 August 1996

Professor Mohan Srinivasarao
North Carolina State University, Raleigh, USA
"Polymer Dispersed Liquid Crystals: Phase Separation and Electro-optics"
Friday 2 August 1996

Prof. Jean d'Angelo
Centre d'Etudes Pharmacentiques, Chatenay-Malaybry, France
"The Asymmetric Michael Reaction Using Chiral Imimnes: Scope and Limitations, Mechanistric Aspects"
Monday 5 August 1996.

Prof. S. Wolfe, Saimon Fraser University, Canada,
"Methyl Transfer Reaction with Retention and Inversion of Configuration"
Tuesday 20 August 1996

Dr. Lung-Shiang Luh
Soochow University, Taipei
"Consecutive Butylation on the Cyclopentadienyl Ring"
Friday 23 August 1996

Professor Stephen Z.D. Cheng
Institute and Department of Polymer Science, The University of Akron, USA
"Crystal Structure and Morphology of Aromatic Polymers"
Friday 30 August 1996

Dr. Roberto Fernandez-Prini
CNEA, Argentine
"Thermodynamics and Structural Aspects of Aqueous Solutions of Nonpolar Gases"
Tuesday 3 September 1996

Dr. Michele Maggini
Department of Organic Chemistry, University of Padova, Padova, Italy
"Functionalization of C_{60} via Azomethine Ylides Cycloadditions: Synthesis and Properties of Fulleropyrrolidines"
Tuesday 3 September 1996

Dr. J Anthony C Bland
Cavendish Laboratory, University of Cambridge, Cambridge, UK
"Magnetic Anisotropies, Magnetic Moments and 2D Spin Switching in Ultrathin Magnetic Structures"
Tuesday 17 September 1996

Professor Seizo Miyata
Tokyo University of Agriculture and Technology Graduate School of Bio-applications and System Engineering
"Enhancement of Functional Properties of Polymers by the Control of Superstructure"
Thursday 19 September 1996

Dr. Ch. Steinbach
European Laboratory for Particle Physics (CERN), Geneva, Switzerland
"Status of the Accelerator Study for European Particle Therapy"
Friday 20 September 1996

Dr. Alexander Bürkle
Deutsches Krebsforschungszentrum, Heidelberg, Germany
"Molecular Genetic Approaches to Modulate Cellular Poly(ADP-ribosyl)ation Capacity"
Tuesday 24 September 1996

Dr. Martin A M Gijs
Philips Research Laboratories, Eindhoven, The Netherlands
"Perpendicular Magnetoresistance and Noise of Magnetic Multilayers"
Monday 30 September 1996

Professor Göran Rämme
University of Uppsala, Sweden
"Soap Films and Soap Bubbles in Education - Art and Science"
Monday 30 September 1996

Dr. Alan D. English
Central Science and Engineering Laboratories, Dupont Central Research and Development, USA
"Molecular Dynamics of Hydrogen-Bonded Polymer Crystals"
Monday 14 October 1996

Prof. Teng-Ming Chen
Department of Applied Chemistry, National Chiao-Tung University, Taiwan
"The Chemical Synthesis, Crystal Structure and Characterization of Some Ternary Metal Nitrides"
Tuesday 15 October 1996

Professor Shiquan Li
Changchun Institute of Applied Chemistry, Chinese Academy of Sciences, China

"Preparation and Characterization of Stanic Oxide Nanoparticles"
Wednesday 16 October 1996

Dr. Mafred Monkenbush
Institute for Solid State Science, Germany
"Dynamic Aspects of Self-organized Molecular System Investigated by Neutron Spin-echo Spectroscopy"
Friday 18 October 1996

Prof. Akio Murai
Hokkaido University, Hokkaido, Japan
"Synthetic Studies on Marine Toxins"
Friday 25 October 1996.

Professor Hideki Sakurai
Science University of Tokyo, Japan
"Recent Advances in the Polysilane Syntheses by Anionic Polymerization of the Masked Disilenes"
Friday 25 October 1996

Prof. Jurgen M Honig
Department of Chemistry, Purdue University, Indiana
"The Verwey Transition in Magnertite; New Thoughts on an Old Problem"
Monday 28 October 1996

Dr. David L. VanderHart
National Institute of Standards and Technology, USA
"Aspects of ^{13}C NMR of Solid Polymers: Crystallinity of Cellulose and Its Derivatives; Partitioning of Defects in Semicrystalline Polymers; and Spectral Resolution in Strongly-Coupled Systems"
Wednesday 30 October 1996

Prof. D. Tomas
Compiegne University, France
"Catalytic Antibody"
Thursday 31 October 1996

Professor Ichita Endo
Faculty of Science, Hiroshima University, Hiroshima, Japan
"Interaction Between High Energy Electrons and Crystal"
Thursday 1 November 1996

Dr. Tai-sen Wang
Los Alamos National Laboratory, New Mexico, USA
"The present Status and the Upgrade Plan of PSR"
Wednesday 6 November 1996

Professor Joel. E. Moreau
Ecole Nationale Superieure de Chimie, Montpellier, France
"The Design of Porous Materials.
Silicas from Organic-Inorganic Hybrid via Controlled Removal of Organic Templates"
Monday 11 November 1996

Dr. Masao Sakurai
Hokkaido University
"Study of Hydrophobic Hydration in the perspective of the Partial Molar Volumes and Adiabatic Compressibilities"
Tuesday 12 November 1996

Dr. Linda Britton and Dr. Fiona Rodgers
The Krebs Institute, Department of Molecular Biology and Biotechnology, University of Sheffield, UK
"Structural Studies on Enzymes of Opine Biosynthesis" and "Approaches to Purification and Crystallisation of Macromolecules for Structural Studies"
Tuesday 12 November 1996

Associate Professor Hiroshi Teraoka
Department of Pathological Biochemistry,
Medical Research Institute,
Tokyo Medical and Dental University
"DNA-PK and Apoptosis"
Wednesday 13 November 1996

Professor A. Ziya Akcasu
Department of Nuclear Engineering, The University of Michigan, USA
"The Theory of Interdiffusion in Polymer Mixtures"
Thursday 14 November 1996

Prof. Nina Berova
Columbia University at New York, U.S.A
"Exciton Couples Circular Dichroism" A Poweful Tool for Structural Studies of Bioactive Compounds"
Monday 25 November 1996.

Dr. Hirokazu Tada
Faculty of Engineering, Kyoto University
"Structural Prediction of Organic Epitaxy by Molecular Dynamics Simulation"
Tuesday 26 November 1996

Dr. Simon Butler
Imperial College, London, UK
"Neutron Reflection Studies of Polymer Interfaces: Crystalline Polymers in the Melt State"
Tuesday 26 November 1996

Prof. Shinichi Uchida
Faculty of Engineering, University of Tokyo
"Physics in Perovskite Related Oxides - BPBO, High Tc Superconductors, Spin Ladders-"
Tuesday 28 November 1996

Professor Fumio Osawa
Aichi Institute of Technology
"Molecular Function of Biological Machine"
Friday 6 December 1996

Professor Guy Bertrand
Laboratoire de Chimie de Coordination du CNRS, Toulouse, France
"New Stable Radicals, Diradicals and Carbenes"
Monday 9 December 1996

Prof. Hirokazu Tsunetsugu
Institute for Applied Physics, University of Tsukuba
"Progress in the Study of Quantum Spin Ladders I : Theory"
Tuesday 10 December 1996

Prof. Yoshio Kitaoka
Department of Material Physics, Faculty of Enginnering Science, Osaka University
"Progress in the Study of Quantum Spin Ladders II : NMR"
Tuesday 10 December 1996

Prof. Takashi Takahashi
Faculty of of Science, Tohoku University
"Progress in the Study of Quantum Spin Ladders III : Photoemission Spectroscopy"

Tuesday 10 December 1996

Professor Masataka Mori
Department of Molecular Genetics,
School of Medicine, Kumamoto University
“Molecular Genetics of the Citrulline-NO Cycle”
Tuesday 10 December 1996

Prof. Hidenori Takagi
Institute for Solid State Physics, University of Tokyo
“Progress in the Study of Quantum Spin Ladders IV: Transport Properties”
Wednesday 11 December 1996

Professor Zhu Congshan
Shanghai Institute of Optics and Fine Mechanics, Chinese Academiy of Science, P.R. China.
“Research and Development of Laser and Optical Materials”
Thursday 12 December 1996

Dr. Eugen Gheorghiu
National Institute of Biotechnology, Romania
“Nonlinear Analysis of Time Series Provided by Impedence Spectroscopy of Cell Suspensions”
Friday 13 December 1996

Professor Bernard Meunier
Laboratoire de Chimie de Coordination du CNRS, Toulous, France
“Recent Advances in Olefin Epoxidation and Pollutant Degradation Catalyzed by Biomimetic Catalysts”
Thursday 26 December 1996

Professor Bernard Meunier
Laboratoire de Chimie de Coordination du CNRS, Toulous, France
“Recent Advances in Olefin Epoxidation and Pollutant Degradation Catalyzed by Biomimetic Catalysts”
Thursday 26 December 1996

MEETINGS AND SYMPOSIUMS

ICRIS'96 (The First International Symposium Organized by Institute for Chemical Research, Kyoto University)
7-8 November 1996

I. Oral Presentations

1. Multidimensional solid state NMR studies of molecular dynamics
   H. W. Spiess

2. Polymer motion on the picosecond scale
   U. Buchenau

3. Local dynamics of amorphous polymers
   T. Kanaya and K. Kaji

4. Dynamics and structures of polymers in solution
   Y. Tsunashima

5. Dynamics of block copolymer nanostructures
   J. A. Kornfield, Z. -R. Chen,
   R. Krishnamoorti, S. Smith,
   A. Ashraf, M. Satkowski

6. Dynamics and structure of triblock copolymer systems
   H. Watanabe

7. Dynamics of volume transition in gels
   M. Doi

8. The effect of flow on binary polymer blends
   J. S. Higgins

9. Controlled organization of chiral structures in cellulose and cellulose derivatives
   D. G. Gray

10. Rigid polymer crystals
    K. Shimamura

11. Structures of peptides and polypeptides in the solid state as studied by high-resolution NMR spectroscopy
    I. Ando

12. Fine structures in crystalline polymer solids studied by high-resolution TEM
    M. Tsuji

13. Structural changes in isothermal crystallization of polyethylene as viewed from the molecular level
    K. Tashiro, S. Sasaki, and M. Kobayashi

14. Control of interface structure in block copolymer systems
    E. L. Thomas

15. Surface structures and dynamics of functionalized electroactive polymers
    Z. F. Li, T. Wang, K. G. Neoh, and
    E.-T. Kang

16. Functional polymers with controlled refractive indices for phase-matched second harmonic generation and retardation film applications
    S. Miyata

II. Posters

1. Elemental and chemical mappings by electron energy-loss spectroscopy
   T. Kobayashi, S. Isoda, H. Kurata, and
   S. Moriguchi

2. Structure analysis of thin crystals by electron crystallography
   T. Ogawa, S. Hashimoto, K. Kuwamoto,
   S. Moriguchi, S. Isoda, and T. Kobayashi

3. The first layer in epitaxy of organic molecules; point-on-line coincidence
   S. Isoda, S. Irie, and T. Kobayashi

4. Quantification of stacking faults in syndiotactic polystyrene single crystals
   M. Tosaka, M. Tsuji, and S. Kohjiya

5. Ultra-high extensibility of deswollen polydimethylsiloxane networks in supercoiled state
   K. Urayama and S. Kohjiya

6. Deformation morphology of extruded and blown polyethylene film
   S. Murakami, K. Shimamura, and S. Kohjiya

7. Molecular rheology, oops !
   K. Osaki

8. Molecular rheology of suspensions
   H. Watanabe

9. Molecular rheology of glassy polymers
   T. Inoue

10. Structure formation of polymers during the i nduction period of crystallization - crystal nucleation process -
    K. Kaji, M. Imai, G. Matsuba,
    T. Kanaya, and
    K. Nishida

11. Structure and its formation process of polymer gels
    H. Takeshita, Y. Nishikoji, T. Kanaya,
    K. Kaji, and K. Nishida

12. Salt can control electrostatic structure in polyelectrolyte solutions
    K. Nishida, K. Kaji, K. Kiriyama,
    T. Kanaya, H. Urakawa, J. S. Higgins and
    B. Gabrys

13. Dynamics of amorphous polymers near the glass transition temperature
    T. Kanaya, M. Miyakawa,
    T. Kawaguchi, and K. Kaji

14. Structure and dynamics of polymers in the different states as studied by solid state NMR spectroscopy

F. Horii, H. Kaji, H. Ishida, K. Kuwabara, and K. Masuda

15. Solid state ^{13}C NMR analyses of the medium-frequency molecular motion of solid polymers
    H. Kaji, Y. Shen, T. Tai, and F. Horii

16. Polymer chain dynamics in dilute solution under Couette flow
    Y. Tsunashima

17. *In situ* formation of organized structure of bacterial cellulose
    A. Hirai, F. Horii, M. Tsuji, J. Sugiyama, and H. Yamamoto

18. Controlling molecular/material structures for new high-performance polymeric materials
    T. Miyamoto, T. Fukuda, Y. Tsujii, M. Minoda, and N. Donkai

19. Applications of nitroxide-controlled free radical polymerization
    T. Fukuda, Y. Tsujii, and T. Miyamoto

20. Synthesis and interfacial properties of amphiphilic block copolymer with pendant glucose residues
    Y. Tsujii, M. Minoda, T. Fukuda, and T. Miyamoto

21. Apatite formation on organic polymers
    T. Kokubo, F. Miyaji, M. Minoda, and T. Miyamoto

ICR 70th Anniversary
November 29, 1996

Memorial Lecture

Metallic Multilayers
- Synthesis of New Materials -
T Shinjo

The Progress in DNA Sequencing
- Towards Deciphering Entire Genetic Information -
M Takanami

SYMPOSIUMS ORGANIZED BY RESEARCH FACILITY OF NUCLEIC ACIDS

WORKSHOP ON "A New Era in Functional Analysis of the Genome"
Tuesday, November 19, 1996

"A View of Genomic Analysis of Cyanobacteria"
Dr. Hirokazu Kotani & Dr. Satoshi Tabata
KAZUSA DNA Institute, Kisarazu, Chiba, Japan

"Mapping of Expression Patterns of the *C. elegans* Genome"
Professor Yuji Kohara
National Institute of Genetics, Mishima, Shizuoka, Japan

"The Rice Genome: From Structural Analysis to Functional Analysis"
Dr. Masahiro Yano
Rice Genome Research Program, National Institute of Agrobiological Resources, Society for Techno-innovation of Agriculture, Forestry and Fisheries, Tsukuba, Ibaraki, Japan

"Knowledge-base Approach for DNA Sequence Analysis"
Associate Professor Kenta Nakai
Institute for Molecular and Cellular Biology, Osaka University, Osaka, Osaka, Japan

"From Gene Structure to Genome Structure"
Professor Yoshio Tateno
National Institute of Genetics, Mishima, Shizuoka, Japan

ENLIGHTENMENT PROGRAM
Saturday 1 June 1996

Experiencing Course (organized by Research Facility of Nucleic Acids and Division of Molecular Biology and Information)
"The Forefront of Research on Biological Science: Instruction and Practice"

SYMPOSIUMS ORGANIZED BY NUCLEAR SCIENCE RESEARCH FACILITY

SYMPOSIUM ON "Beam Physics"
March 8 (Friday) - 9 (Saturday), 1996

"Wave and Particle Property of Beam"
Dr. Susumu Kamada
National Laboratory for High Energy Physics (KEK), Tsukuba, Japan

"Beam-Beam Simulation"
Dr. Kohji Hirata
National Laboratory for High Energy Physics (KEK), Tsukuba, Japan

"A Coherent X-ray Source Based on Resonant Transition Radiation"
Dr. N. Imanishi
Faculty of Engineering, Kyoto University, Kyoto Japan

"Production of Dense Ion Beams and the Related Physics"
Dr. Hiromi Okamoto
Institute for Chemical Research, Kyoto University, Kyoto, Japan

"RI Beam Factory Project at RIKEN"
Dr. Akira Goto
RIKEN, Saitama, Japan

"Beam Physics in MUSES Project"
Dr. Takeshi Katayama

Institute for Nuclear Study, Tokyo University, Tanashi, Japan

"On New SUBARU Project"
Dr. Ainosuke Ando
Himeji Institute of Technology, Himeji, Japan

"On Japanese Hadron Project"
Dr. Yoshiharu Mori
Institute for Nuclear Study, Tokyo University, Tanashi, Japan

"High-Power Laser and Its Application to Beam Physics"
Dr. Toshihiro Taguchi
Setsunan University, Osaka, Japan

"Personal Comments on Beam Physics"
Dr. Yukihide Kamiya
Tokyo University, Tokyo, Japan

THESES

KOKUSEN, Hisao
D Sc, Kyoto University
"Design of Novel Selective Complex Formation Systems Using Poly(pyrazolyl)borate Ligands"
Supervisor: Professor Matsui M
23 March 1995

HARA, Takane
D Agr, Kyoto University
"Active Site Architecture of *Escherichia coli* B Glutathione Synthetase Analyzed by X-Ray Crystallography and Site-Directed Mutagenesis"
Superviser: Professor ODA J
24 November 1995

MATSUO, Yo
D Sc, Kyoto University
"Protein Structure Prediction by Evaluating Sequence-Structure Compatibility"
Supervisor: Professor Kanehisa M
23 January 1996

NAKAMATSU, Hirohide
D Sc, Kyoto University
"Relation between X-Ray Absorption Near-Edge Spectra and Interatomic Distances"
Supervisor: Professor Mukoyama T
23 January 1996

OHYASU, Hitoshi
D Pharm Sc, Kyoto University
"Certain of New Thamuria Therapeutic Agent Vamicamide"
Supervisor : Professor Sugiura Y
23 January 1996

MATSUMOTO, Takuyuki
D Pharm Sc, Kyoto University
"DNA and RNA Cleavages by Chromoprotein Antitumor Antibiotic C-1027"
Supervisor : Professor Sugiura Y
23 March 1996

FUJITA, Mikako
D Pharm Sc, Kyoto University
"Molecular Design of Artificial Ligands Targeted Zinc-Finger Proteins"
Supervisor : Professor Sugiura Y
23 March 1996

GUAN, Leluo
D Pharm Sc, Kyoto University
"Specific Guanine-Binding and -Cleavage of DNA and RNA by Bleomycin-Nickel(III) Complex"
Supervisor : Professor Sugiura Y
23 March 1996

KIRYU, Yoshimitsu
D Pharm Sc, Kyoto University
"Synthesis and Application of Enantiomeric Aziridine Used Enzymatic Reaction"
Supervisor : Professor Sugiura Y
23 March 1996

OGAWA, Izumi
D Sc, Kyoto University
"Development of an Experimental System for Dark Matter Axion Search with Rydberg Atoms"
Supervisor: Professor Inoue M
23 March 1996

AOKI, Mikio
D Sci, Kyoto University
"Signal transduction pathways through reversible phosphorylation-dephosphorylation reactions in higher plants
Supervisor: Professor A. Oka
23 March 1996

ONO Teruo
D Sc, Kyoto University
"Giant Magnetoresistance Effect of Co/ Cu/ NiFe/ Cu Metallic Multilayers Prepared on Microstructured Substrates"
Supervisor: Professor Shinjo T
23 March 1996

SUMIDA, Motoo
D Agr, Kyoto University
"New Protoporphyrinogen Oxidase Inhibitors and Their Herbicidal Function"
Supervisor: Professor Soda K
23 March 1996

KAWACHI Atsushi
D Eng, Kyoto University
"The Chemistry of Functionalized Silyl Anions"
Supervisor: Professor Tamao K
23 March 1996

SUN Guang-Ri
D Eng, Kyoto University
"Synthesis, Structure and Reactivity of Polyfunctionalized Oligomeric Silanes"
Supervisor: Professor Tamao K
23 March 1996

OHTA, Yoshihisa
D Pharm Sc, Institute for Chemical Research Kyoto University
"Studies on the Asymmetric Syntheses Using Chiral Phosphonate Reagents"
Supervisor: Prof. Kaoru Fuji
23 March, 1996

ASHIUCHI, Makoto
D Agr, Kyoto University
"Structure and Function of Glutamate Racemase"
Supervisor: Professor Soda K
23 March 1996

JHEE, Kwang-Hwan
D Agr, Kyoto University
"Stereochemical Studies of Aminotransferase Reactions"
Supervisor: Professor Soda K
23 March 1996

KUROKAWA, Youichi
D Agr, Kyoto University
"Structure and Function of Thermostable Alanine Racemase"
Supervisor: Professor Soda K
23 March 1996

NAKAMURA, Takeshi
D Agr, Kyoto University
"Production and Conversion of Sulfur and Selenium-containing Amino Acids with Pyridoxal Enzymes"
Supervisor: Professor Soda K
23 March 1996

ISHIGURO, Ryo
D Sc, Kyoto University
"Spectroscopic Study about Interaction of Membrane Fusion-Active Peptides with Lipid Bilayer"
Supervisor: Professor Takahashi S
23 May 1996

MIYATAKE, Hideyuki
D Sc, Kyoto University
"Crystallographic Studies on Structure-Function Relationships of Alkaline Protease from *Pseudomonas aeruginosa* IFO3080"
Supervisor: Professor Takahashi S
23 May 1996

KAWASAKI, Masashi
D Sci, Kyoto University
"Lipase-Catalyzed Transesterification of Aryl-Substituted Alkanols in Organic Solvents"
Supervisor: Professor Ohno A
23 July 1996

TSUTSUMI, Akihiro
D Sci, Kyoto University
"Novel Atropisomeric NAD(P)H Model Compounds: Syntheses and Stereochemistry in the Reductions"
Supervisor: Professor Ohno A
23 July 1996

KINOSHITA, Masamichi
D Sci, Kyoto University
"Solvent Effect on Stereoselectivity of Lipase-Catalyzed Reaction"
Supervisor: Professor Ohno A
23 July 1996

SHIOJI, Kousei
D Sci, Kyoto University
"Studies on Reactivity of Cation Radicals Generated from Trivalent-Phosphorus Compounds"
Supervisor: Professor Ohno A
23 July 1996

KATO, Masayuki
D Pharm Sc, Kyoto University
"Synthesis and Structure-Activity Relation of Serotonin-3 Receptor Antagonist"
Supervisor : Professor Sugiura Y
23 July 1996

MATSUI, Michikage
D Eng, Kyoto University
"Structure and Properties of Polyester Fibers Produced by High-Speed Spinning"
Supervisor: Professor Miyamoto T
23 September 1996

MURAKAMI, Syozo
D Eng, Kyoto University
"Structure Development in the Uniaxial-Drawing Process of Crystalline Polymers"
Supervisor: Professor Kohjiya S
25 November 1996

ITAHANA, Koji
D Sci, Kyoto University
"Gap Junction and Oogenesis in Mammalian Ovarian Follicles"
Supervisor: Professor A. Oka
25 November 1996

DEWA, Hideki
D Sc, Kyoto University
"Measurements of the Longitudinal Beam Emittance of the Proton Linac"
Supervisor: Professor Inoue M
25 November 1996

KURODA, Akio
D Pharm Sc, Institute for Chemical Research Kyoto University
"Exploitation of Chemical Functions of Optically Active 1,1'-binaphthalene-8,8'-diol: Applications to Asymmetric Synthesis and Molecular Recognition"
Supervisor: Prof. Kaoru Fuji
25, November, 1996

TANIGUCHI, Kiyoshi
D Pharm Sc, Institute for Chemical Research Kyoto University
"Synthetic and Structure-Activity Studies on the Cyclic Amines Possessing Inhibitory Activity against Bladder Contraction"
Supervisor: Prof. Kaoru Fuji
25, November, 1996

MONDE Takashi
D Eng, Kyoto University
"Synthesis and Application of Branched-Polyfluoroalkylsilanes"
Supervisor: Professor Yoko T
12 December 1996

TERASHIMA Kentaro
D Eng, Kyoto University
"Studies on Structure and Nonlinear Optical Properties of B_2O_3-Based Glasses"
Supervisor: Professor Yoko T
24 March 1997

ORGANIZATION AND STAFF

NSTITUTE FOR CHEMICAL RESEARCH
KYOTO UNIVERSITY

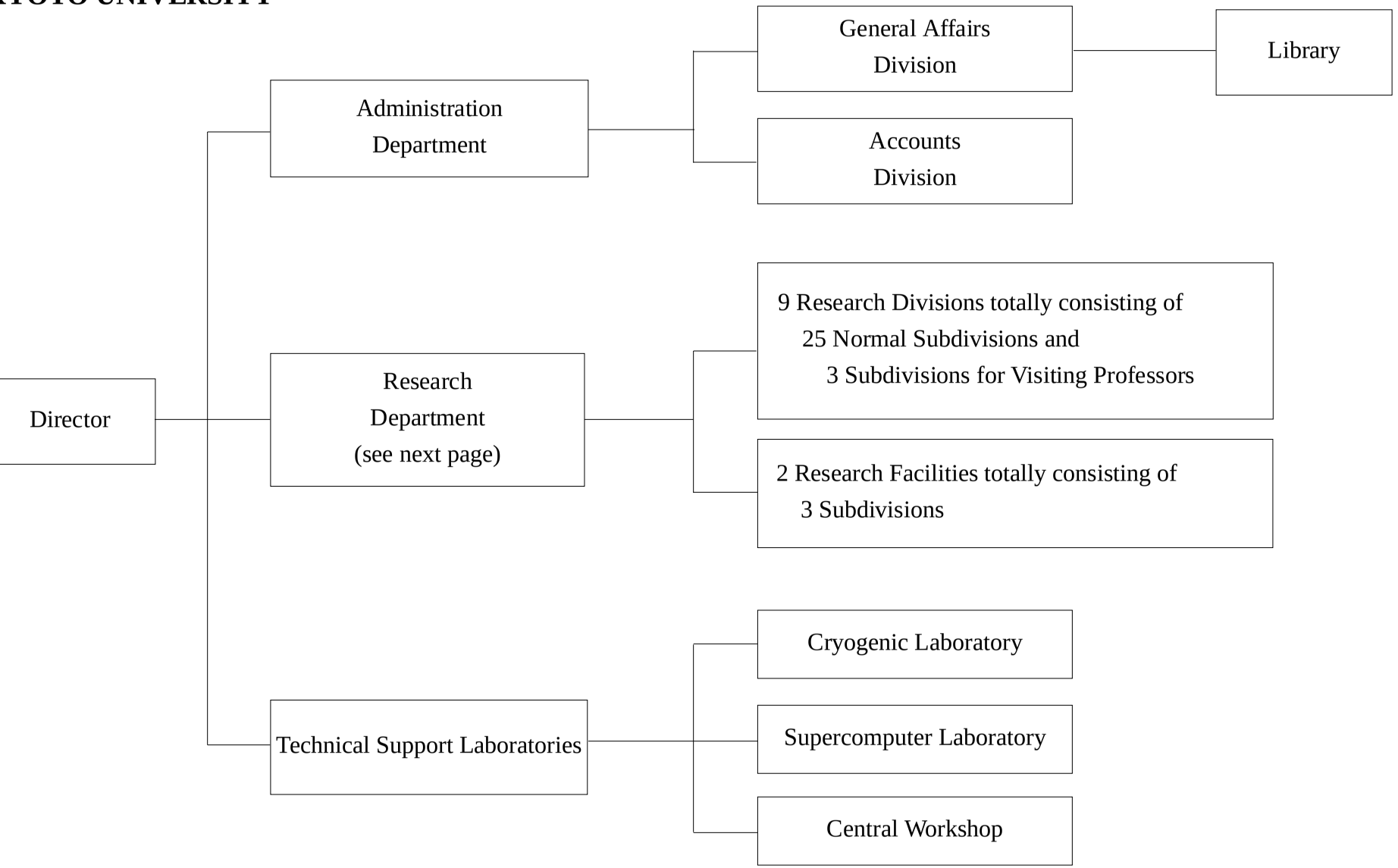

NSTITUTE FOR CHEMICAL RESEARCH, KYOTO UNIVERSITY As of 31 December 1996

ESEARCH DIVISION (G: Laboratory for Visiting Professors)

	Research Division	Subdivision (Laboratory)	Related Graduate School *Graduate School of / Division of*	Professor	Associate Professor	Instructor
Director HINJYO, eruya	States and Structure	I. Atomic and MolecularPhysics	*Science / Physics I*	MUKOYAMA, Takeshi		KATANO, Rintarou ITO, Yoshiaki NAKAMATSU, Hirohide
		II. Crystal Information Analysis	*Science / Chemistry*	KOBAYASHI, Takashi	ISODA, Seiji	OGAWA, Tetsuya
		III. Polymer Condensed States	*Engineering / Polymer Chemistry*	KOHJIYA, Shinzo	TSUJI, Masaki	URAYAMA, Kenji TOSAKA, Masatoshi
	Interface Science	I. Solutions and Interfaces	*Science / Chemistry*	NAKAHARA, Masaru	UMEMURA, Junzo	MATSUMOTO, Mutsuo KIMURA, Noriyuki MATSUBAYASI,Nobuyuki
		II. Molecular Aggregates	*Science / Chemistry*	SATO, Naoki	ASAMI, Koji	KITA, Yasuo YOSHIDA, Hiroyuki
		III. Separation Chemistry	*Science / Chemistry*	MATSUI, Masakazu	UMETANI, Shigeo	SASAKI, Yoshihiro
	Solid State Chemistry	I. Artificial Lattice Alloys	*Science / Chemistry*	SHINJO, Teruya	HOSOITO, Nobuyoshi	MIBU, Ko
		II. Artificial Lattice Compounds	*Science / Chemistry*	BANDO, Yoshichika		IKEDA, Yasunori TERASHIMA, Takahito
		III. Multicomponent Materials	*Science / Chemistry*	TAKANO, Mikio	HIROI, Zenji	AZUMA, Masaki
		IV. Amorphous Materials	*Engineering / Molecular Engineering*	YOKO, Toshinobu	KOZUKA, Hiromitsu	UCHINO, Takashi LIN, Hong
		G. Structure Analysis		TERAUCHI, Hikaru	TAKAGI, Hidenori	
	Fundamental Material Properties	I. Molecular Rheology	*Engineering / Molecular Engineering*	OSAKI, Kunihiro	WATANABE, Hiroshi	INOUE, Tadashi
		II. Polymer Materials Science	*Engineering / Polymer Chemistry*	KAJI, Keisuke	KANAYA, Toshiji	NISHIDA, Koji
		III. Molecular Dynamic Characteristics	*Engineering / Molecular Engineering*	HORII, Fumitaka	TSUNASHIMA, Yoshisuke	KAJI, Hironori
		G. Composite Material Properties		KAKUGO, Masahiro	KAWASHIMA, Takayuki	
	Organic Materials Chemistry	I. Polymeric Materials	*Engineering / Polymer Chemistry*	MIYAMOTO, Takeaki	FUKUDA, Takeshi	TSUJII, Yoshinobu MINODA, Masahiko
		II. High-Pressure Organic Chemistry	*Engineering / Energy & HC Chemistry*	KOMATSU, Koichi		MORI, Sadayuki KUDO, Kiyoshi NISHINAGA, Tohru
	Synthetic Organic Chemistry	I. Synthetic Design	*Engineering / Energy & HC Chemistry*	TAMAO, Kohei	TOSHIMITSU, Akio	KAWACHI, Atsushi YAMAGUCHI, Shigehiro
		II. Fine Organic Synthesis	*Pharmaceutical Sci. / Pharmac. Chem.*	FUJI, Kaoru	TANAKA, Kiyoshi	KAWABATA, Takeo
		G. Synthetic Theory		MURAI, Akio	INENAGA, Junji	
	Bioorganic Chemistry	I. Bioorganic Reaction Theory	*Science / Chemistry*	OHNO, Atsuyoshi	NAKAMURA, Kaoru	KAWAI, Yasushi
		I. Bioactive Chemistry	*Pharmaceutical Sci. / Drug System*	SUGIURA, Yukio	OTSUKA, Masami	MORII, Takashi
		III. Molecular Clinical Chemistry	*Medicine / Internal Medicine*	UEDA, Kunihiro	TANAKA, Seigo	ADACHI, Yoshifumi
	Molecular Biofunction	I. Functional Molecular Conversion	*Agriculture / Agricul. Chem.*	ODA, Jun'ichi	HIRATAKE, Jun	KATO, Hiroaki TANAKA, Takuji
		II. Molecular Microbial Science	*Agriculture / Agricul. Chem.*	ESAKI, Nobuyoshi	YOSHIMURA, Tohru	KURIHARA, Tatsuo
	Molecular Biology and Information	I. Biopolymer Structure	*Science / Biophysics*	TAKAHASHI, Sho	HATA, Yasuo	HIRAGI, Yuzuru FUJII, Tomomi
		II. Molecular Biology	*Science / Biophysics*	OKA, Atsuhiro	AOYAMA, Takashi	GOTO, Koji
		III. Biological Information Science	*Science / Biophysics*	KANEHISA, Minoru		GOTO, Susumu OGATA, Hiroyuki
	Nuclear Science Research Facility	I. Particle and Photon Beams	*Science / Physics II*	NODA, Akira	KAKIGI, Shigeru	SHIRAI, Toshiyuki
		II. Beams and Fundamental Reaction	*Science / Physics II*	INOUE, Makoto	MATSUKI, Seishi	IWASHITA, Yoshihisa OKAMOTO, Hiromi
	Research Facility of Nucleic Acids		*Science / Biophysics*		SUGISAKI, Hiroyuki	FUJIBUCHI, Wataru

PERSONAL

Award

Professor Emeritus Dr. Sumio Sakka

(Solid State Chemistry, Division of Amorphous Materials)

Professor Dr. Sumio Sakka, the ex-director of Institute for Chemical Research and Professor Emeritus of Kyoto University, received a Purple Ribbon Medal (Shijuhosho) on May, 1996.

Dr. Sakka was born in Osaka on the 11th of December, 1930. He graduated from the Department of Industrial Chemistry, Kyoto University in 1953. In 1953, he was appointed an instructor of the Institute for Chemical Research, Kyoto University under the supervision of Emeritus Professor Megumi Tashiro. He received a doctoral degree from Kyoto University in 1963. He was promoted to an associate professor of the Institute for Chemical Research, Kyoto University in 1963. On a leave of absence in 1965, he worked at Rensselaer Polytechnic Institute. During his 3-year stay in the USA, Dr. Sakka gained further experience on the glass science, in cooperation with Professor J.D. Mackenzie.

In 1972, Dr. Sakka moved to the Faculty of Engineering, Mie University, as a full professor of the Laboratory of Inorganic Materials Science. In 1983, he again moved back to the Institute for Chemical Research, Kyoto University, as a full professor to direct the Laboratory of Ceramic Chemistry (now, Solid State Chemistry). At the Graduate School of Molecular Engineering, Kyoto University, he gave lectures on inorganic materials science and supervised dissertation research of graduate students.

He was a visiting instructor at several Universities including Tokyo Institute of Technology, Mie University, Kobe University, Okayama University, Nagaoka University of Technology.

From the 1st of April, 1990 to the 31st of March, 1992, Dr. Sakka was appointed Director of the institute and made great contributions not only to the Institute but also to the University as a councilor.

On the 31st of March, 1994, Dr. Sumio Sakka retired from Kyoto University after 30 years of contribution to Kyoto University and was honored with the title of Emeritus Professor of Kyoto University on the following day. Now, he takes a position as a professor at Fukui University of Technology.

For almost forty years, Dr. Sakka has extensively investigated the novel synthetic processes, structure and properties of functional inorganic glasses. His most outstanding works are 1) structural studies of inorganic non-conventional glasses by various spectroscopic methods and X-ray radial distribution function analysis, 2) studies on the physical or physico-chemical properties of inorganic nonconventional glasses and 3) the development of sol-gel process for preparing new functional inorganic glasses and ceramics. Owing to these great contributions, he was awarded the Prize of the Ceramic Society of Japan for Young Scientists in 1965, the Prize of the Ceramic Society of Japan in 1979, the G.W. Morey Award of the American Ceramic Society in 1984 and the Prize of the Chemical Society of Japan in 1988. He was also honored with the title of the Fellow of the American Ceramic Society in 1983.

Dr. Sakka devoted himself to the Ceramic Society of Japan and officiated as Vice President of the Society for two years from May 1991. He was a regional editor of the international journal, Journal of Non-Crystalline Solids, from 1981 to 1992. He is now an editor-in-chief of the international journal, Journal of Sol-Gel Science and Technology, from 1992. He has also chaired a number of international conferences. Through these activities, he made a great contribution to the development of Glass Science and Sol-Gel Science in Japan and the international communication of research.

Retirement

Professor Yoshichika Bando

(Artificial Lattice Compounds Laboratory, Division of Solid State Chemistry)

On the 31st of March, 1997, Dr. Yoshichika Bando retired from Kyoto University after 36 years of service to the University and was honored with the title of Emeritus Professor by Kyoto University.

Dr. Bando was born in Tokushima on the 15th of January, 1934. After graduation from the Faculty of Science, Kyoto University in 1956, he continued his study as a graduate student at the Department of Chemistry, Faculty of Science, in Kyoto University. In 1961, he was appointed an instructor of the Department of Chemistry, Faculty of Science, Kyoto University under the supervision of Professor Sukeji Kachi. He was granted a doctoral degree for his studies on the preparation and properties of ultrafine particles of metal alloys. In 1964, he was appointed an instructor of the Laboratory of Solid State Chemistry of the Institute for Chemical Research, Kyoto University, under the supervision of Emeritus Professor Toshio Takada. In 1968, he was promoted to Associate Professor of the same laboratory. In 1976, Dr. Bando was appointed full Professor of Kyoto University and directed the Facility of Inorganic Synthesis, of the same institute.

During years his research work covered a wide range of solid state chemistry. He studied the martensitic transformation of fine particles of metal alloys, various synthesis methods of oxides and hydroxides of transition metals, growth of single crystals by the chemical transport, and also growth of epitaxial films and artificial superlattices of oxides and chalcogenides. Basic research done by him found fruitful practical applications; e.g. production of iron oxide fine particles to be used as magnetic recording materials, cosmetics and magnetic heads made of a crystal-oriented spinel ferrite. More recently, he rose into world wide notice for his outstanding work about the epitaxial films and artificial superlattices of high-T_c cuprate superconductors.

He has been awarded several prizes for his brilliant achievements by The Japan Society of Powder and Powder Metallurgy.

He gave lectures on advanced inorganic synthesis at the graduate school of science at Kyoto University and supervised dissertation works of graduate students. He was invited as a visiting professor by the University of Tokyo, Nagoya University, Kobe University, and some other institutions.

He served as a vice president of The Japan Society of Powder and Powder Metallurgy from 1984-1990, and as a director or councillor of several other societies. Since 1996 he serves as the president of The Society of Powder and Powder Metallurgy. His sincere and warm-hearted character has been admired by his friends, colleagues, and students.

Obituary

Professor Emeritus
Dr. Keinosuke KOBAYASHI (1913 - 1996)

Professor Dr. Keinosuke KOBAYASHI, Honorary Member of the Japanese Society of Electron Microscopy, Professor Emeritus of Kyoto University suddenly passed away on March 18, 1996.

He was born on May 7, 1913 in Osaka. After graduating from the Faculty of Science, Kyoto Imperial University in March, 1935 with a degree (Bachelor of Science) in zoology, he started his academic life as a research associate in the Institute for Chemical Research (ICR), Kyoto Imperial University in April, 1935. He was appointed a Lecturer of the ICR in June, 1941, a Lecturer of the Faculty of Engineering, Kyoto Imperial University in September, 1942, and then an Associate Professor of the ICR in June, 1945. He received a Ph.D. (Doctor of Engineering) from Kyoto University in March, 1962. He was promoted to a full Professor of the ICR, Kyoto University in October, 1965 to direct the Laboratory of Polymer Crystals (the present Laboratory of Polymer Condensed States, Division of States and Structures III). He gave lectures on polymer crystals in the Division of Polymer Chemistry, Graduate School of Engineering, and supervised the dissertation works of graduate students. He retired from Kyoto University and became a Professor Emeritus of Kyoto University in April, 1977. His lifework was the physical chemistry of crystalline polymers, particularly studies on formation, properties and deformation of polymer crystals. He introduced electron microscopy for structural studies on crystalline polymer solids.

Professor Kobayashi participated in the founding of the Japanese Society of Electron Microscopy in 1949, and also served as the Vice President (1970) and the President (1971) of the Society. He was awarded the Seto Prize from the Society in May, 1958 for his theoretical study on ultra-microtoming. He was again awarded the Seto Prize in May, 1962 for his continuous endeavor at developing high-voltage electron microscopes: as you know, he constructed three high-voltage transmission electron microsopes in the ICR, one 300kV machine(1957) and two 500kV machines (1963 and 1974).

He served as a visiting instructor at several universities including Kyushu University, Okayama University, Yamagata University, Fukui University and Tokyo Metropolitan University. He visited foreign countries to attend international conferences in which he always presented stimulating and attractive papers. For his such academic contribution, he was awarded the Order of the Rising Sun, Gold Rays with Neck Ribbon in April, 1986.

NAME INDEX

KEYWORD INDEX